

THIS REPORT HAS BEEN DELIMITED  
AND CLEARED FOR PUBLIC RELEASE  
UNDER DOD DIRECTIVE 5200.20 AND  
NO RESTRICTIONS ARE IMPOSED UPON  
ITS USE AND DISCLOSURE.

DISTRIBUTION STATEMENT A

APPROVED FOR PUBLIC RELEASE;  
DISTRIBUTION UNLIMITED.

# **DISCLAIMER NOTICE**

**THIS DOCUMENT IS THE BEST  
QUALITY AVAILABLE.**

**COPY FURNISHED CONTAINED  
A SIGNIFICANT NUMBER OF  
PAGES WHICH DO NOT  
REPRODUCE LEGIBLY.**

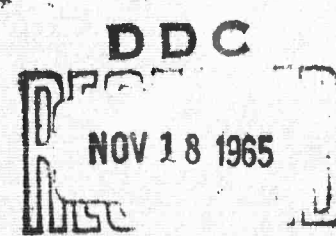
473996

ARC DISCHARGE SOURCES

Final Report  
16 October 1964 to 15 November 1965

15 November 1965

Contract Nonr-4647(00)  
ARPA Order No. 306-62, Code 4730



Westinghouse Research Laboratories  
PITTSBURGH 35, PENNSYLVANIA

Reproduction in whole or in part is  
permitted for any purpose of the  
United States Government.

This research is part of Project DEFENDER  
under the joint sponsorship of the Advanced  
Research Projects Agency, the Office of  
Naval Research and the Department of Defense.

ARC DISCHARGE SOURCES

FINAL REPORT

Covering Period from 16 October 1964 through 15 November 1965

15 November 1965

Contract Nonr-4647(00)

ARPA Order No. 306-62

Code No. 4730

Req. No. NR-012-55/6-26-64

A 12-Month Contract

Expiration Date 11/16/65

Cost \$99,552

Charles H. Church, Principal Investigator (412) 242-1500, Etx. 678 with  
Richard G. Schlecht and I. Liberman with Appendixes by B. W. Swanson,  
E. G. F. Arnott and E. Geil

R. D. Haun, Jr., Manager, Quantum Electronics Department

Westinghouse Research Laboratories  
Pittsburgh, Pennsylvania 15235

Reproduction in whole or in part is  
permitted for any purpose of the  
United States Government.

This research is part of Project DEFENDER  
under the joint sponsorship of the Advanced  
Research Projects Agency, the Office of  
Naval Research and the Department of Defense.

## TABLE OF CONTENTS

	<u>Page</u>
PREFACE .....	i
ABSTRACT.....	iii
PAPERS PRESENTED OR SUBMITTED UNDER THIS CONTRACT .....	iv
CHAPTER 1 .....	1
<u>Introduction</u> .....	1
CHAPTER 2 - THEORETICAL CALCULATION OF THE PHYSICAL PROPERTIES OF THE ARC PLASMA .....	6
2.1 <u>Theoretical Calculation of the Spectral Absorptivity</u> <u>for the Free-Free and Free Bound Processes</u> .....	6
2.2 <u>Partition Functions and Electron Densities</u> .....	9
2.3 <u>Absorption Coefficient for Lines</u> .....	12
2.4 <u>The Electrical and Thermal Conductivities for a</u> <u>Fully Ionized Plasma</u> .....	13
2.5 <u>The Thermal Conductivity in the Boundary Layer</u> .....	14
CHAPTER 3 - THE MODEL STUDIES .....	16
3.1 <u>Introduction to the Model Studies</u> .....	16
3.2 <u>Analysis</u> .....	17
3.3 <u>Plane Parallel Slab of Homogeneous Temperature</u> .....	21
3.4 <u>Cylinder of Homogeneous Temperature</u> .....	25
3.5 <u>Comparison of Model with Experiment - Spectral</u> <u>Radiance</u> .....	29
3.6 <u>Comparison of Model with Experiment - Transmissivity</u> <u>as a Function of Current Density</u> .....	29
CHAPTER 4 - EXPERIMENTAL MEASUREMENTS .....	40
4.1 <u>Experimental Measurements in the Pulsed Arc</u> .....	40
4.2 <u>Radial Distribution of the Spectral Radiance in the</u> <u>Ultraviolet</u> .....	42
4.3 <u>Time - Resolved Spectral Radiance in the Infrared -</u> <u>Temperature Measurements</u> .....	42
4.4 <u>Measurements of the Spectral Radiance and the Zeta</u> <u>(<math>\zeta</math>) Factor of Biberman &amp; Norman</u> .....	49
4.5 <u>Temperature Dependence of the Electrical Conduc-</u> <u>tivity</u> .....	57

TABLE OF CONTENTS (Con't.)

	<u>Page</u>
STATUS OF PROBLEMS & FUTURE PLANS .....	59
ACKNOWLEDGMENTS .....	61
REFERENCES .....	62
RADIATION FLUX IN A NON-ISOTHERMAL NON-GREY CYLINDRICAL ARC by B. W. Swanson .....	Appendix A
TRANSITION PROBABILITIES OF XENON by E. G. F. Arnott.....	Appendix B
COMPUTER PROGRAMS USED IN THIS WORK by Esther Geil.....	Appendix C
a. Raizer-Penner Model (SIMPLIFIED)	
b. DOUBLE - Program for spectral absorptivity and emissivities for given temperature and pressure.	
c. DICKSLAB - Calculation of radiant emittance, current density and electric field for a plane parallel slab, homogeneous temperature (with spectral absorptivity from Raizer-Penner or DOUBLE.	
d. DICKCYL - Calculation of radiant emittance, current density and electric field for an infinite cylinder of homogeneous temperature with spectral absorptivity from Raizer-Penner or DOUBLE.	
e. Radiation flux in a non-isothermal non-grey cylindrical arc.	

## PREFACE

High energy arc discharges have been used to pump lasers since the first ruby laser of Maiman, and are still the most efficient means for exciting the high energy lasers. In order to obtain larger inputs to lasers and more efficient high energy lasers, the need arose for a better understanding of the processes within the arc discharge. The literature existing on these discharges is contradictory, and the experimental evidences of such phenomena as the saturation of the discharge and dependence of efficiency upon many parameters were not readily explained.

Under these circumstances, it was felt that a more basic study of the highly radiant, high energy arc discharge was needed, in which the physical properties of these arc plasma were to be used in models for the discharges to calculate the radiant characteristics. These models for the discharge would be validated through experiment. Once the suitable models were available, the application to the specific high energy laser pumping applications would be straightforward, though not necessarily easy. The theoretical models for the pulsed arc discharge discussed in the final report possess many of the features of the actual arcs, but exhibit only semi-quantitative agreement. In part, this lack of agreement is due to deficiencies in the model, such as in not including thermal conduction power transport and such features as the Stark broadened lines which are so important in the infrared between .65 and 1.0  $\mu$ . But a large portion of the disagreement is due to insufficient quantitative knowledge of the properties of dense plasmas, in particular, the spectral absorptivities and transport properties (i.e.; electrical and thermal conductivity) of xenon. This lack of knowledge is not unique to xenon or the

other rare gases; there is a lack of quantitative data on dense plasmas of even nitrogen and oxygen. In the past five years, there has been a large amount effort devoted towards the investigation of those gases, using the cascade arc, and the shock tube. The availability of the digital computer has helped considerably -- if not made possible -- these studies.

The experimental measurements such as those discussed in this report indicate that the wall-stabilized pulsed arc or flash tube can provide valuable quantitative information in dense plasmas such as those that may be encountered in gases other than xenon.

## ABSTRACT

This report summarizes the work to date on Contract Nonr 4647(00) towards creating models for the high energy pulsed arc discharge used for high energy laser pumping. Homogeneous temperature models are discussed in which the radiant emission is balanced by the electrical power input. These models have been evaluated at various energy levels for the temperature which has been measured within the arc (assuming local thermal equilibrium). The models included the continuum spectral absorptivity calculated according to Biberman and Norman (using the Zeta factor of Schlüter). There was found to be a semi-quantitative agreement between the Zeta factor observed experimentally, and those of Biberman and Norman, and of Schlüter. The spectral transmissivity as a function of current density calculated from the models showed reasonable agreement with the experimental values of Emmett, Schawlow, and Weinberg in the visible and ultraviolet, but differ widely in the infrared (due to the strong infrared lines of xenon).

Measurements of the time-resolved profiles of lines in the infrared, of the radial distribution of the spectral radiance in the ultraviolet, and of the electrical conductivity are also discussed. These measurements provide a means for determining the temperature dependence of these quantities within these arcs. The ultraviolet radial profiles indicate that the arc is relatively homogeneous for the range of current densities and pressures studied.

Papers and Talks Resulting From This Contract

1. "A Wide Range Ultra Rapid Scan Spectrometer" by Charles H. Church and Leonard Gampel. Accepted publication by Applied Optics.
2. "Models for Pulsed Arc Discharges" by Charles H. Church and Richard G. Schlecht. Presented at October 1965 Meeting of the Optical Society of America.
3. "Arc Discharge Sources in the Infrared--Some Simple Models" by Charles H. Church and Richard G. Schlecht. Submitted to the Proceedings IRIS.
4. "Studies of Highly Radiative Plasmas Using the Wall Stabilized Pulsed Arc Discharge" by Charles H. Church, Richard G. Schlecht, Irving Liberman, and Bruce W. Swanson. Accepted for presentation at the A.P.S. PLASMA Dynamics Meeting, March 1966.
5. "Laboratory Simulation of Highly Radiative Plasmas" by Charles H. Church, Richard G. Schlecht, and Irving Liberman. Submitted for presentation at the Symposium on Interdisciplinary Aspects of Radiative Energy Transfer, February 1966.
6. "Radiation Flux in a Non-Isothermal Non-Grey Cylindrical Arc" by Bruce W. Swanson. Submitted for presentation at the Symposium on Interdisciplinary Aspects of Radiative Energy Transfer, February 1966.

## CHAPTER 1

### Introduction

Arc discharges are commonly used for exciting high energy lasers. The highly radiative arc discharges used for the high energy laser excitation has been examined experimentally by numerous groups in order to understand them more fully, but the results were in many respects contradictory. Furthermore, many of the characteristics observed were not readily explainable on any simple basis. Phenomena such as saturation of the arc, emission with increasing power input and the variation of the efficiency with size, shape, and the energy density, all required further explanation in order to apply these arc discharges to high energy laser pumping.

The radiative arc discharge consists of a core of high density plasma, in which the opacity varies widely for different spectral regions, surrounded by a cooler gas near the wall. Various disciplines, such as astrophysics, heat transfer, and reentry physics have considered various related aspects of such plasmas. The broader considerations must include, in addition to the widely varying opacity and the high density, the transport properties of the arc plasma and the energy transport due to radiation within those plasmas, which can possess a strongly varying temperature distribution from the wall to the center of the discharge.

Since the radiative arc discharge plays a major role in high energy laser pumping, it was felt by many that these arcs should be understood more thoroughly. Such an understanding would be of use not only in present laser design, but also for studies on the optimization and the maximum energy capabilities of future laser systems.

In the course of Contract Nonr 4647(00), some models for the highly radiative arc discharge were developed in which the resistive power input per unit volume is balanced by radiation and by thermal conduction from that volume. The arcs were optically thick (i.e., high absorptivity or opacity) over certain wavelength regions, particularly in the infrared and far ultraviolet, but also for many of the lines; elsewhere they were optically thin. Consequently the analyses of the energy transport within the arc included a wide range of spectral absorptivities (i.e., a non-gray radiative transport calculation). The temperature in the arc varied from being near the boiling point of quartz or less ( $\sim 2000^{\circ}\text{K}$ ) at the outer wall to a temperature in the center necessary to give electrical conductivities corresponding to those of a fully ionized gas ( $\sim 10,000^{\circ}\text{K}$ ). This inhomogeneity in temperature and the resulting gradient needed to be considered in any complete evaluation of the model for the radiative arc discharge. The First Semiannual Report<sup>1</sup> discussed many of these aspects of the considerations involved in the model studies.

In the course of the contract, models described in the First Semiannual Report were evaluated which utilized simple expressions (extended by Penner<sup>2,3</sup> from work of Raizer<sup>4,5</sup>) for the bound-free and free-free continuum absorptivities for a homogeneous temperature since the homogeneous temperature was found by experimental measurements to be a reasonable approximation for the measured temperature distribution in the arc. The calculated spectral transmission of this model was found to differ by a factor of four from experimental measurements<sup>6</sup>.

Comparison of spectral transmissivities calculated using the spectral absorptivities computed according to the methods of Biberman, Norman, and Yankov<sup>7-12</sup> and of Schlüter<sup>13</sup> with experimentally measured spectral transmissivities of Knott, Schawlow, and Weinberg<sup>6</sup>, and subsequent work of Harding<sup>14</sup>, discussed in this report, show a good correspondence at wavelengths less 0.65  $\mu$ , but wide variations for the longer wavelengths to at least 0.95  $\mu$ . Experimental measurements of the profiles of the strong of xenon lines in the infrared indicated that the broadening and the saturation of these lines in the infrared could account for a major portion of the difference in the 8000A° spectral region between the absorptivities calculated considering only free-free and free-bound transitions and the absorptivities measured.

To aid in these model studies, it was felt necessary to measure the spectral absorptivities of xenon as a function of temperature and pressure, and compare the values with theoretical calculations. The saturation of the spectral radiance at wavelengths at which the arc becomes optically thick (at the peaks of the strong lines or of the continuum, in the infrared) has allowed determination of the temperature of the core of the arc channel, (assuming the arc to be homogeneous in temperature). The temperature thus measured has been used to measure wavelength dependence of the Zeta factor (the Biberman and Norman Zeta factor<sup>7</sup>), which related the spectral absorptivity of the continuum to the particle density and temperature in the plasma. Comparison of the measured values with recently published theoretically calculated values of Schlüter<sup>13</sup> indicates a reasonable correspondence both in magnitude and variation with wavelength. The spectral radiances that we have measured at various input energy levels has been compared with theoretical calculations using the simple models for the arc plasma together with spectral absorptivities calculated using Schlüter's theoretically calculated values of the Zeta factor.

The dependence of the electrical conductivity upon temperature (and pressure) was also measured. The experimentally determined electrical conductivity was appreciably lower than the calculations made according to methods of Spitzer and his collaborators<sup>15,16</sup>.

To improve the model investigations, techniques for handling radiative transport have been developed for calculating the radiant emittance from an inhomogeneous temperature distribution, which would include the absorption in the vacuum ultraviolet by the cool gas near the walls of the tube. This work is contained in Appendix A. The iterative solutions to the differential equations, describing the energy or power balance within the arc to find the temperature distribution, were found not to have a satisfactory rate of convergence. The techniques being developed under the contract for handling radiative transport within a non-gray inhomogeneous temperature gas are generally applicable to other plasma problems. Currently the radiative transport techniques are being applied using the continuum absorptivities calculated using the theory of Biberman, Norman, and Yankov<sup>7-12</sup>, and an approximation to the transport properties which includes electron-electron, electron-ion, and neutral-neutral scattering (due to Fay<sup>17</sup>). This transport properties calculation neglects electron-neutral interactions. The theoretical calculations of the transport properties incorporating the electron-neutral scattering, which for xenon, krypton, and argon involves the Ramsauer minimum<sup>18</sup>, which were discussed in the First Semiannual Report<sup>1</sup> complex than we had originally envisioned and will be dealt with in subsequent work.

The inclusion of the lines into the models has proved to be uncertain due to the lack of data on the absolute transition probabilities and the line

broadening parameters for xenon. Since some of the lines of xenon are thought to be L-S coupled (according to Moore<sup>19</sup>), a Bates-Damgaard<sup>20</sup> calculation of the absolute transition probabilities of a number of the L-S coupled lines has been made. These calculated absolute transition probabilities were used to obtain a temperature to estimate the absolute transition probabilities for the other lines of interest in the infrared from the intensities listed in the American Institute of Physics Handbook<sup>21</sup>. This work is described in Appendix B.

The ALGOL computer programs for the Burroughs B-5500 DISK Computer that were developed in this contract are in Appendix C.

The work in Contract Nonr 4647(00) has been directed towards formulating the model for the radiative arc, and then evaluating the model by incorporating gradually more details and features of the arc plasma. Many aspects of this problem, particularly those of radiative transport in a non-gray gas and the transport properties of a partially ionized plasma, involve basic questions in plasma physics. The techniques developed on this contract, both theoretical and experimental, will be useful in solving many other problems involving radiation transport in partially ionized plasmas.

## CHAPTER 2

### Theoretical Calculations of the Physical Properties of the Arc Plasma

In order to construct models for the plasma, and as the work has progressed, to provide a basis for comparison of our experimental values with theoretical calculations, we needed to calculate the spectral absorptivities and the transport properties, electrical and thermal conductivity, as a function of temperature and pressure. The basis for our choice of the calculations for these properties is discussed fully in the Semiannual Report<sup>1</sup>. Briefly, we felt that the Biberman & Norman<sup>7</sup> method for calculating the spectral absorptivity of the continuum was the most satisfactory approach. Particle densities necessary to calculate the spectral absorptivities and the transport properties were calculated as a function of temperature and pressure using standard methods, similar to that of Drellishak<sup>22,23</sup> et al.

In the calculations to be discussed, we have used a simple method to calculate the electrical conductivity, due to Spitzer and his collaborators<sup>15,16</sup>. Work that we have in progress with the aid of Dr. R. S. De Voto of Stanford University seeks to determine experimentally and theoretically the values of conductivity that actually exist in the plasma. These measurements are briefly discussed in Section 4.5.

The portions of the sections that follow will expand on these brief descriptions.

#### 2.1 Theoretical Calculation of the Spectral Absorptivity for Free-Free and Free-Bound Processes

In order to calculate the radiative emission flux from an arc plasma, the spectral absorptivity of the plasma must be determined. If the temperature

and pressure of a gas is known, and LTE can be assumed, one can in principle determine the spectral absorptivity and emission coefficient due to free-free and free-bound transitions. The emission coefficient and spectral absorptivity of the rare gases were determined using the quantum defect calculations of Biberman and Norman<sup>7-12</sup> as originally adapted to this problem by Seaton and Burgess<sup>24</sup>.

For a plasma in LTE, Kirchhoff's law holds. The emission coefficient may be written as

$$\epsilon_v = \kappa'_v B_v \quad (2.1)$$

where  $\epsilon_v$  - emission coefficient

$\kappa'_v$  - spectral absorptivity

$B_v$  - Planck function.

The effective spectral absorptivity which includes stimulated emission is given by

$$\kappa'_v = \kappa_v (1 - e^{-hv/kT}) \quad (2.2)$$

where  $\kappa_v$  is the spectral absorptivity.  $\kappa_v$  is given by

$$\kappa_v = \sum_i \kappa_v^i \quad (2.3)$$

where  $\kappa_v^i$  is the spectral absorptivity of the atomic or ionic species i. In the Biberman and Norman technique for determining the spectral absorptivity of an atom or ion the energy levels of the system are divided into two classes (Fig. 3 - Reference 12). In the determination of the expression for the spectral absorptivity, the upper levels in the frequency region denoted by  $v_g$  are integrated over. The the low lying widely separated levels, an absorption cross section is calculated for each level. This has been done by Yankov<sup>8</sup> for the xenon atom, for the level series up to 8s. The spectral absorptivity  $\kappa_{nl}^i$  for each series of levels of the species is then obtained by

$$\kappa_{nl}^i = \sigma_{nl} N_{nl} \quad (2.4)$$

where  $\sigma_{nl}$  is the absorption cross section for the nl series of levels and  $N_{nl}$  is the number density of those levels. Assuming Boltzman statistics and relating this to the ground state we have

$$\kappa_{nl}^i = \sigma_{nl} N_g \frac{g_{nl}}{g_g} e^{-hv_{nl}/kT} \quad (2.5)$$

where  $N_g$  is the density of the ground state and  $g_{nl}$  and  $g_g$  are the statistical weights of the nl series and the ground state respectively. The spectral absorptivity for each of the nl series is then added to the spectral absorptivity due to the integrated lines and the free-free absorption. The spectral absorptivity due to the integrated lines and the free-free spectral absorptivity for species i is given by the following<sup>7</sup>:

$$\kappa_A^i = A \frac{2Q_{1+1}}{Q_1} T e^{-u_1 + u} \frac{Z_i^2}{v^3} \xi_i(v) N_i \text{ for } v \leq v_g \quad (2.6)$$

$$= A \frac{2Q_{1+1}}{Q_1} T e^{-u_1 + u_g} \frac{Z_i^2}{v^3} \xi_i(v) N_i \text{ for } v \geq v_g \quad (2.7)$$

where

$$A = \frac{16\pi^2 k e^6}{3\sqrt{3} c h^4} = .89 \times 10^{24} \text{ cm}^2 \text{ sec}^{-3} \text{ oK}^{-1} \quad (2.8)$$

$$u = \frac{hv}{kT}$$

$u_1 = \frac{hv_1}{kT}$  where  $v_1$  = threshold frequency for photo ionization from ground state

$$u_g = \frac{hv_g}{kT}$$

$Z_i$  = core charge of the residual ion

$Q_i$  = internal partition function of the  $i^{\text{th}}$  species

$Q_i = \sum_j g_j^i e^{-E_j^i/kT}$  where the sum is over all energy levels of the species and  $E_j^i$  is the energy of the  $j^{\text{th}}$  level above the ground state.

$N_i$  = number density of the  $i^{\text{th}}$  species

$\xi_i(v)$  = a correction factor for species  $i$  as calculated for the xenon atom by Biberman, Norman and Ulyanov<sup>11</sup>. (Zeta factor).

(Recent work by Schlüter<sup>13</sup> shows quite different values for  $\xi$  that agree more closely with our experimentally determined values. See Section 4.4). Then one has for the total absorption coefficient of the species  $i$  the expression

$$\kappa_v^i = \kappa_A^i + \sum_{nl} \kappa_{nl}^i \quad (2.9)$$

where the sum is over all series of levels considered independently, of course the more levels considered independently the greater the accuracy should be.

In order to calculate  $\kappa_A^i$ , one needs to know, other than the correction factor  $\xi_i(v)$ , each species partition function  $Q_i$ , each species density  $N_i$  and the temperature  $T$ . If one can experimentally determine the temperature then, under the assumptions stated earlier, one can calculate reasonable values for  $Q_i$  and  $N_i$ . This will be discussed now.

## 2.2 Partition Functions and Electron Densities

As stated earlier we have for the partition function

$$Q_i = \sum_j g_j^i e^{-E_j^i/kT} \quad (2.10)$$

The sum is over all levels and therefore diverges for a free atom or ion.

However, in a plasma, electrons tend to cluster about the ions. Thus when an ion-electron pair is produced a certain amount of energy is released. Ionization potentials are reduced by this amount of ordering energy which is dependant upon

the charge of the particle, the plasma density and the temperature. Thus the partition function summation must be truncated at an energy value of

$$E^1 = I_i - \Delta I_i \quad (2.11)$$

where  $I_i$  is the isolated ionization potential of species  $i$  and  $\Delta I_i$  is the ionization potential lowering of that species, given by<sup>25</sup>

$$\Delta I_i = 2(z_i + 1)e^3 (\pi/kT)^{1/2} (N_e + \sum_i z_i^2 N_i)^{1/2} \quad (2.12)$$

for a Debye-Hückel plasma. For the tables which have been tabulated by Charlotte Moore<sup>19</sup>,  $g_k$  is given by

$$g_k = 2 J_k + 1. \quad (2.13)$$

For those nl levels which have been approximated for xenon by McChesney and Jones<sup>26</sup>

$$g_k = \sum_n (2 J_n + 1)_k \quad (2.14)$$

where the sum is over all J states for a given nl term.

These partition functions are then used to calculate the electron density for an LTE plasma using the Saha equations<sup>22,27</sup>:

$$\frac{N_i + 1}{N_i} e = \left(\frac{2 m k}{h^2}\right)^{3/2} \frac{2^{Q_i}}{Q_i} T^{3/2} e^{-(I_i - \Delta I_i)/kT} \quad (2.15)$$

If n is the highest degree of ionization of the monatomic gas, there will be  $n + 2$  species of particles present. The set of Saha equations then gives n equations in  $n + 2$  unknowns. The other two equations necessary to solve for all the particle densities is given by

$$N_e = \sum_{i=1}^n i N_i \text{ and} \quad (2.16)$$

$$N_t = \sum_{i=0}^n (i+1) N_i \quad (2.17)$$

$N_t$  is the total particle density as is given by the equation of state. The equation of state used is the ideal gas law

$$p = N_t kT \quad (2.18)$$

The corrections to this for a Debye-Hückel interaction have been discussed by Griem<sup>25</sup>. Therefore if one is given the temperature and pressure one can solve for the electron density and the various atom and ion densities once the partition function series sum is known. However since the truncation of this sum depends on the particle densities an iteration procedure must be employed. This has been done by Drellishak, et al.<sup>22,23,28</sup> for argon\*. A computer program has been written and the partition functions, electron, atom, and ion densities and the ionization potential lowering for xenon were calculated. The program employs certain improvements over Drellishak's calculation. The cutoff of the partition function series and the ionization potential lowering are obtained as we described earlier rather than by a principal quantum number cutoff method assuming Bohr type orbits as employed by Drellishak. At very high electron densities and high temperatures the principal quantum number cutoff will introduce errors in the partition functions.

\*NOTE: An error exists in Equation (12) of reference 24. This equation should read

$$n_e^{N+1} + \sum_{i=1}^N \left[ n_e^{N+1-i} (i+1) - n_t n_e^{N-i} (i) \right] \prod_{r=1}^i K_r = 0 \quad (2.19)$$

Although this formula is incorrectly stated in references 22, 23, and 28 the correct one is used in the computer calculations so the results of those references are not affected.

### 2.3 The Absorption Coefficient of the Lines

The contribution of the bound-bound state transitions, the spectral lines, to the absorption coefficient is more difficult to calculate due to the requirements for absolute values of the transition probabilities for all of the lines that may be involved including those in the infrared or ultra-violet. The relative effect of the lines upon the radiant emittance varies with temperature and pressure tending to be greater (but not always) for the lower temperatures and high pressures--conditions similar to those in flash tubes. Our calculations of the transition probabilities are discussed in Appendix B. Work is in progress towards extending the Stark broadening theory of Griem<sup>29</sup> and other to the lines of xenon in the infrared.

### 2.4 The Electrical and Thermal Conductivities for a Fully Ionized Plasma

The electrical conductivity is taken to be that of a fully ionized plasma using the theory of Spitzer and his coworkers<sup>15,16</sup>. As the power input to the arc which is given by  $\sigma E^2$ , is probably only appreciable in the fully ionized portion of the arc discharge. The Spitzer theory for a fully ionized plasma considers only electron-electron and electron-ion scattering, which are the dominant processes for material that is more than about .1% ionized<sup>30</sup>. (We are using "fully ionized" in the sense that only those processes need be considered).

There is one major difficulty in applying the Spitzer theory to the plasmas in high energy flash tubes. This difficulty arises from the high electron density but relatively low temperature which exists in the arc discharges, for which the theory is not considered valid as the coulomb logarithm term (denoted as  $\ln \Lambda$ ) goes to zero and the errors are of the order of  $1/\ln \Lambda$ , due to the

neglect of close encounters in the Fokker-Planck equation used in the derivation.

Following Spitzer<sup>31</sup>, the electrical conductivity  $\sigma$  is given by this equation:

$$\sigma = \frac{T^{3/2} \delta T_E}{3.80 \times 10^3 Z_i \ln \Lambda_i} \quad \text{in } (\text{ohm cm})^{-1} \quad (2.20)$$

and the thermal conductivity  $K$  by

$$K = \frac{1.95 \times 10^{-11} T^{5/2} \delta T_K}{Z_i \ln \Lambda_i} \quad (2.21)$$

$\delta T_E$  and  $\delta T_K$  are correction factors dependent upon  $Z_i$ , which is the ionic charge (note:  $Z = 1$  for a singly ionized gas). From Cohen et al.<sup>16</sup>,  $\Lambda_i$  is the ratio of the Debye shielding parameter  $h$  to the impact parameter  $b_o$  ( $b_o$  is the distance for a 90° deflection of an electron by a positive ion).

$$\Lambda_i = \frac{h}{b_o} = \frac{3}{e^3 Z_i} \frac{k^3 T^3}{4 \pi N_e (1 + Z_i)} \quad (2.22)$$

When  $\Lambda_i < 12 \pi$ , Cohen et al.<sup>16</sup> and others<sup>17,32,33</sup> suggest using for  $z = 1$

$$\Lambda = \frac{3kT}{e^2 N_e^{1/2}} \text{ rather than the above value.} \quad (2.23)$$

This is equivalent to substituting the interionic distance ( $N_e^{-1/3}$ ) for the Debye shielding parameter  $h$ .

In common units, for  $Z = 1$ ,  $\ln \Lambda$  from equation 3.10 is given as

$$\ln \Lambda = 9.43 + 1/2 \ln \frac{T}{N_e} \quad (2.24)$$

for  $T$  in °K and  $N_e$  in particles/cm<sup>3</sup>. The correction factors  $\delta T_E$  and  $\delta T_K$  are given by Spitzer and Harm in terms of  $Z$  (the integral values of  $\bar{Z}$ , a value may be obtained by interpolation between the values in the following table<sup>15</sup>:

	Z = 1	Z = 2	Z = 4	Z = 16	Z = $\infty$
$\delta T_E$	.582	.683	.785	.923	1
$\delta T_K$	.225	.356	.513	.791	1

## 2.5 The Thermal Conductivity in the Boundary Layer (Used in Appendix A)

The thermal conductivity in (either the simple or complete case) is a source of great concern in this investigation. The major influence of the thermal conductivity heat transfer in the pulsed arc discharges lies in the boundary region between the arc discharge channel (where the  $\sigma E^2$  terms are dominant) and the relatively cool wall containing the arc. We say relatively cool as the temperature of the wall is assumed to be on the order of the boiling point of quartz ( $2800^{\circ}\text{K}$ ) or probably much less. In this boundary region, there can be extremely high thermal, electron density, and neutral particle density gradients (the latter being of opposite sign from the first two). Simple approaches to thermal conduction, such as that shown graphically in Fay<sup>17</sup> and in Reilly<sup>34</sup> for argon and xenon use Spitzer conductivity down to temperatures at which the neutral particle thermal conductivity becomes dominant<sup>35</sup>. This may be correct, or it may be off by an order of magnitude at one temperature or another. The neglect of the electron-neutral conductivity in gases with a Ramsauer minimum, such as argon, krypton and xenon have, may lead to large errors. There have not, as yet, been any definitive experiments, that we could find in the literature, on the measurement of the thermal conductivities of partially ionized plasmas--much less those in a high temperature and electron density gradients at the particle densities we are concerned within the flash tubes.

The thermal conductivity given in the previous section is that derived from Spitzer's theory and is probably a reasonable representation of the thermal conductivity in the arc channel proper. For the boundary layer region, for the simple representation, Fay's approach<sup>17</sup> was used calculating the values corresponding to the pressure in the flash tube.

## CHAPTER 3

### The Model Studies

#### 3.1 Introduction to the Model Studies

An arc discharge may have many different temperature distributions. If a major portion of the power put into the arc is carried away by thermal conduction, then thermal conduction power transport within the arc and external to the arc causes the variation of temperature with arc radius. This occurs when the radiative flux from the arc is small compared to the thermally conducted power; it usually occurs in low pressure arcs. If the plasma in the arc is optically very thick over a major portion of the spectral region of emission, the radiative power transport within the arc will lead to a temperature gradient similar to that of the thermal conduction. As we had mentioned in the previous report, the optically thick radiative flux is directly analogous in its effects to thermal conduction.

If the radiation emitted balances a major fraction of the input power (i.e.: thermal conduction losses are small), and the arc is optically thin over a major portion of the spectral region of interest (this case appears to be that for the pulsed flash lamp at normal energy loadings) the temperature within the arc will not change appreciably with radius except at the very edge. The temperature distribution can be taken to be constant in the arc channel.

Appendix A shows our progress towards solving the radiative transport problem for models having a non-homogeneous distribution which is necessary for solving the radiant energy balance equation discussed in the Semiannual Report<sup>1</sup> to obtain the temperature distribution.

The two new models that will be discussed in the following sections assume constant temperature in the arc channel; that is, the arc channel is homogeneous in temperature. Experimental measurements of the radial distribution of the spectral transmissivity<sup>6</sup> and of the spectral radiance in the ultraviolet (to be discussed later) support this assumption.

The arcs to be considered will be steady state arcs in which the electrical power input is balanced by the power radiated from the arc and that carried away by thermal conduction. A more complete calculation for pulsed or AC arcs would require the inclusion of the power required to ionize the gas. The calculations to be presented will also neglect thermal conduction to the arc boundaries such as the walls and the electrodes.

### 3.2 Analysis

The power is generated in the arc by resistive heating; this power is balanced by the sum of the radiated power and the power carried away by thermal processes, such as conduction and convection. In equation form, this balance is<sup>36</sup>

$$\text{div} (\bar{F} + \bar{F}_{HC}) = \sigma E^2 \quad (3.1)$$

where  $E$  is the electric field in volts/cm,  $\sigma$  is the electrical conductivity in ohm<sup>-1</sup>,  $\bar{F}$  is the radiant emittance vector in watts/cm<sup>2</sup>, and  $\bar{F}_{HC}$  is the vector representing the power carried away by the thermal processes.  $\bar{F}_{HC}$  and the convection heat transfer vector denoted by  $\bar{F}_C$ :

$$\bar{F}_{HC} = \bar{F}_H + \bar{F}_C \quad (3.2)$$

The convection term is usually small and will be considered negligible in this calculation. The thermal conduction term  $\bar{F}_H$  is usually expressed in terms of the thermal conductivity, K, by

$$\bar{F}_H = -K \operatorname{grad} T \quad (3.3)$$

where T is the temperature and  $\operatorname{grad} T$ , the temperature gradient at the point at which F is being measured. The units of K, the thermal conductivity, are watts  $\text{cm}^{-2} \text{oK}^{-1}$  cm.

Equation 3.1 can be integrated over the volume surrounding the arc.

$$\iiint_V \operatorname{div} (\bar{F} + \bar{F}_{HC}) dV = \iiint_V \sigma E^2 dV \quad (3.4)$$

The integral over the arc volume can be transformed by the Gauss Theorem to an integral of the normal component over the surface area A

$$\iint_A (\bar{F} + \bar{F}_H)_{\substack{\text{normal} \\ \text{component}}} dA = \iint_A \bar{F} \cdot \hat{n} dA + \iint_A \bar{F}_H \cdot \hat{n} dA = \iiint_V \sigma E^2 dV \quad (3.5)$$

Let us now confine our discussion to arcs of infinite length. For a volume of unit length, the power flow through the end surfaces balance so we need to consider only the power flow through the boundary surfaces. The coordinate system for the models being considered is so chosen that the x-direction is normal to the surface, and the x-component of  $\bar{F}$  and  $\bar{F}_H$  is then the normal component which is to be integrated over the surface area.

The power radiated by the arc is given by  $\bar{F}$ , the radiant emittance.  $\bar{F}$  is the integral over all frequencies (i.e., energy units) or all wavelengths of the spectral radiant emittance,  $\bar{F}_\nu$  or  $\bar{F}_\lambda$ , in frequency or wavelength units, respectively.

$$\bar{F} = \int_c^{\infty} \bar{F}_v dv = \int_0^{\infty} \bar{F}_{\lambda} d_{\lambda} \quad (3.6)$$

$\bar{F}$  may be expressed per cm or micron of wavelength;  $\bar{F}_v$  can be in  $\text{cm}^{-1}$ ,  $\text{sec}^{-1}$  or energy units.

In converting between the units, remember that

$$\lambda = \frac{1}{n} = \frac{c}{v} \text{ and } \Delta\lambda = -\frac{1}{2} \Delta n = -\frac{c}{v^2} \Delta v \quad (3.7)$$

We will use  $\text{cm}^{-1}$  units in the calculation, but refer to them as frequency units.

Let us now consider the x component of the spectral radiant emittance  $E_v_x(P)$ .  $E_v_x(P)$  is the total power per unit frequency interval flowing across a unit area perpendicular to the x-direction. It is given by the integral over all angles of the component of the spectral radiance  $I(P, \bar{s})$  in the x-direction.

$$E_v_x(P) = \int_{\omega} I_v(P, \bar{s}) \cos(\bar{s}, x) d\omega \quad (3.8)$$

Figure 1 shows this relationship. The spectral radiance,  $I_v$ , is the basic unit in radiative power transport. For a given direction  $\bar{s}$ ,  $I_v(P, \bar{s})$  is the power per unit frequency (or wavelengths), per solid angle per unit area perpendicular to the direction  $\bar{s}$  at a point P.  $I_v$  has the units watts  $\text{cm}^{-2} \text{cm steradian}^{-1}$  for frequency in  $\text{cm}^{-1}$  units. ( $I_{\lambda}$  has the units watts  $\text{cm}^{-2} \text{cm}^{-1} \text{steradian}^{-1}$  for wavelengths in cm).  $I_v$  or  $I_{\lambda}$  is also called the specific intensity of radiation. It is the radiometric unit corresponding to luminance (or brightness) in photometric units.

The spectral radiance is related to the properties of the medium through the equation of transfer which, for a medium in local thermal equilibrium<sup>39 40</sup> (LTE) can be written as

Dwg. 746A044

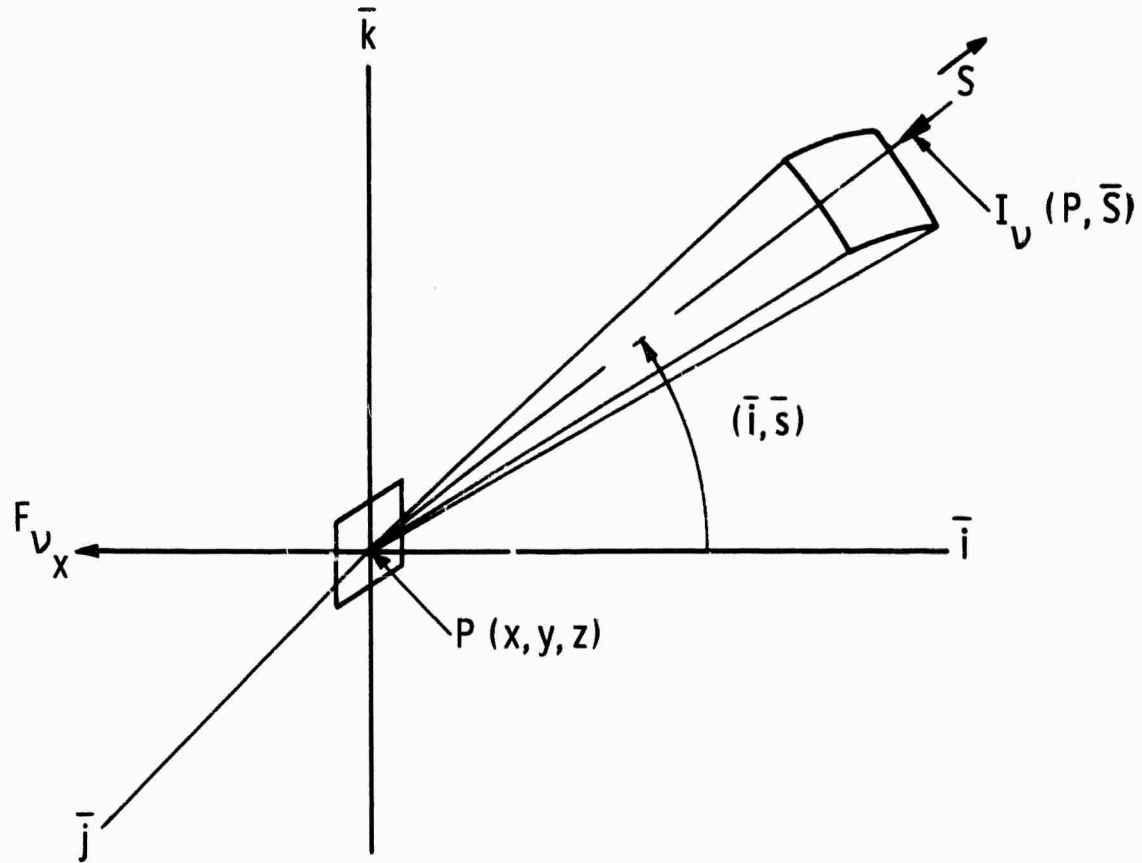


Fig. 1—The geometry of radiative transfer

$$\frac{d^2 I_\nu(P, \bar{s})}{d s^2} = \kappa'_\nu [B_\nu(T) - I_\nu(P, \bar{s})] \quad (3.9)$$

in which  $\kappa'_\nu$  is the spectral absorption coefficient including stimulated emission and  $B_\nu(T)$  the Planck function for a temperature, T.  $\kappa'_\nu$  is related to the more usual spectral absorption coefficient by the equation

$$\kappa'_\nu = \kappa_\nu (1 - e^{-h/RT}). \quad (3.10)$$

$\kappa_\nu$ , the spectral absorption, is a function of the arc medium at that temperature and pressure. It may arise from discrete transitions (lines), or from transition between bound-free or free-free states (continuum).

Following Lutz,<sup>41</sup> using standard techniques for solving a first order differential equation,<sup>42</sup> the solution can be found for equation 3.9. We assume that no radiance is incident upon the system and the temperature is homogeneous; thus, there is no variation of  $\kappa_\nu$  with  $\bar{s}$ .

$$I_\nu = B_\nu(T) [1 - e^{-\kappa'_\nu s}] \quad (3.11)$$

We will apply this to a plane parallel slab and a cylinder of homogeneous temperature.

### 3.3 Plane Parallel Slab of Homogeneous Temperature

The geometry of the plane parallel slab is shown in Figure 2.

As  $S = x \sec \theta$ , equation 3.11 becomes

$$I_\nu = B_\nu(T) [1 - e^{-\kappa'_\nu x \sec \theta}] \quad (3.12)$$

We want the radiant emittance at  $P = P(0,0,0)$  in the x-direction (actually negative x). So using 3.12 in equation 3.8 yields

$$F_x = \int_{\phi=0}^{2\pi} \int_{\theta=0}^{\pi/2} B_\nu(T) [1 - e^{-\tau_\nu \sec \theta}] \cos \theta \sin \theta d\theta d\phi \quad (3.13)$$

where  $\tau_\nu = \kappa'_\nu x$

Dwg. 746A045

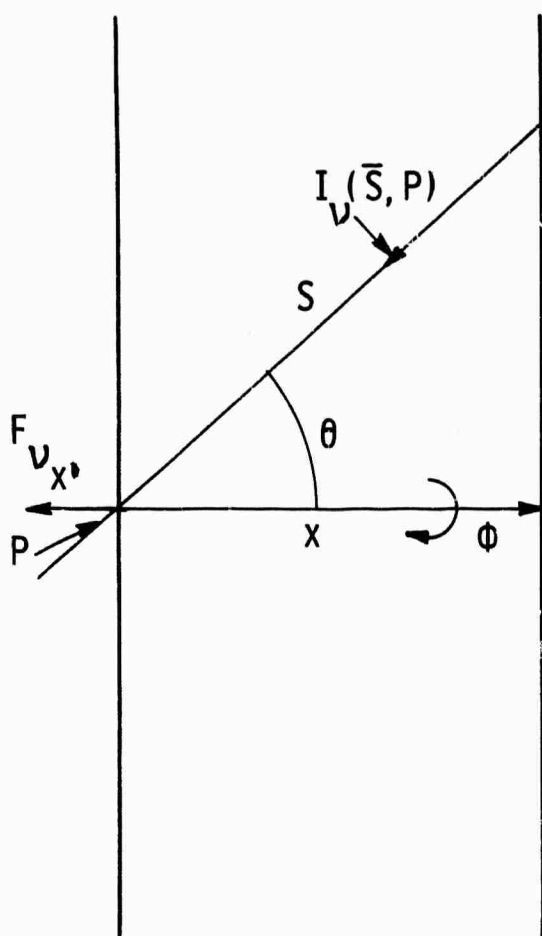


Fig. 2-A plane-parallel slab of homogeneous temperature

Integrating over  $\phi$  yields

$$F_{\nu_x} = 2\pi B_{\nu}(T) \left\{ 1/2 - \int_0^{\pi/2} e^{-\tau} \sec \theta \cos \theta \sin \theta d\theta \right\} \quad (3.14)$$

Let  $u = \sec \theta$ ,

The integral reduces to the exponential integral of the third order<sup>41, 43</sup>

$$\int_0^{\pi/2} e^{-\tau} \sec \theta \cos \theta \sin \theta d\theta = \int_1^{\infty} \frac{e^{-\tau u}}{u^3} du = E_3(\tau) \quad (3.15)$$

The exponential integral of third order<sup>43</sup> may be integrated twice by parts to the first exponential integral denoted by  $E_1(\tau)$

$$E_3(\tau) = \frac{e^{-\tau}(-\tau) + \tau^2 E_1(\tau)}{2} \quad (3.16)$$

$$\text{where } E_1(\tau) = \int_1^{\infty} \frac{e^{-\tau u}}{u} du, \text{ the first exponential integral.} \quad (3.17)$$

The properties of the first exponential integral are discussed and the values tabulated in a number of places (for example references (43) and (44)). For calculations on a computer, there are two useful expansions:<sup>44</sup>

For  $0 \leq \tau \leq 1$

$$E_1(\tau) = \ln \tau + a_0 + a_1 \tau + a_2 \tau^2 + a_3 \tau^3 + a_4 \tau^4 + a_5 \tau^5 + \epsilon(\tau) \quad (3.18)$$

$a_0$	- .57721566	$a_3$	.05519968
$a_1$	.99999193	$a_4$	.00976004
$a_2$	.24991055	$a_5$	.00107857

where  $|\epsilon(\tau)| < 5 \times 10^{-5}$

For  $1 \leq \tau \leq \infty$

$$E_1(\tau) = \frac{e^{-\tau}}{\tau} \left( \frac{\tau^2 + a_1 \tau + a_2}{\tau^2 + b_1 \tau + b_2} \right) + \epsilon(\tau) \quad (3.19)$$

$$a_1 = 2.33473$$

$$b_1 = 3.330657$$

$$a_2 = 0.250621$$

$$b_2 = 1.681534$$

where  $|\epsilon(\tau)| < 5 \times 10^{-5}$

The spectral radiant emittance in the x-direction is given by

$$F_{\nu_x} = \pi B_\nu(T) [1 + (\tau_\nu - 1)e^{-\tau_\nu} \tau_\nu^2 E_1(\tau_\nu)] \quad (3.20)$$

The radiant emittance  $F_x$  may be considered as the sum of the integrals over the optically thick and optically thin spectral regions

$$F_x = \int_0^\infty F_{\nu_x} d\nu \quad (3.21)$$

$$= \sum_{TK} \int_{\nu_{TK}}^{\infty} F_{\nu_x}(TK) d\nu + \sum_{TN} \int_{\nu_{TN}}^{\infty} F_{\nu_x}(TN) d\nu \quad (3.22)$$

Each of the separate integrals over the various thick and thin spectral regions may be calculated to allow an estimate of the energy transfer within the plasma, which of course, is neglected in this model of homogeneous temperature.

The electrical field  $E$  was calculated to be that necessary to create twice the radiant emittance in the x direction to account for both sides radiating. The radiant emittance in the y and z directions were balanced by that from adjacent sections in the infinite extent plane parallel slab.

This balance of radiant emittance and electrical power is expressed as

$$\sigma E^2 d = 2 F_x \quad (3.23)$$

where  $d$  is the plasma thickness

$$E = \sqrt{\frac{2F_x}{\sigma d}} \quad (3.24)$$

The current density  $J$  in the plane parallel slab was calculated from

$$J = \sigma E \quad (3.25)$$

The pressure in the model was

$$p = (N_e + N_c)kT \quad (3.26)$$

where  $N_e$  is the electron density and  $N_c$  is the heavy particle density.

### 3.4 Cylinder of Homogeneous Temperature

The cylinder of homogeneous temperature represents another simple model for describing an arc discharge. The cylinder problem is more difficult to handle than the plane parallel slab due to the boundaries existing in two coordinates rather than only one, thereby making the integral over  $F$  more complex.

Figure 3 shows the geometry we are considering in a fashion similar to the parallel slab model; we can write the spectral radiance  $I_v(\theta, \phi)$  at the point P (0,0,0) on the edge of the cylinder as:

$$I_v(\theta, \phi) = B_v [1 - e^{-\kappa_v S(\theta, \phi)}] \quad (3.27)$$

where  $S(\theta, \phi)$  is the distance through which the radiation travels in the cylinder of homogeneous temperature, and diameter  $d$ . Referring to Figure 4,  $S$  is expressed as

$$S(\theta, \phi) = \frac{d}{\cos \theta + \tan \theta \sin \theta \sin^2 \phi} \quad (3.28)$$

and the spectral radiance  $I_v(\theta, \phi)$  is

$$I_v = B_v \left(1 - \exp \frac{-\kappa_v d}{\cos \theta \tan \theta \sin \theta \sin^2 \phi}\right) \quad (3.29)$$

The spectral radiant emittance in the radial direction,  $F_{v_r}$ , is given by

$$F_{v_r} = \int_0^{2\pi} \int_0^{\pi/2} I_v \cos \theta \sin \theta d\theta d\phi \quad (3.30)$$

Substituting the value of  $I_v$  in this equation, the spectral radiant emittance is as follows:

Dwg. 746A019

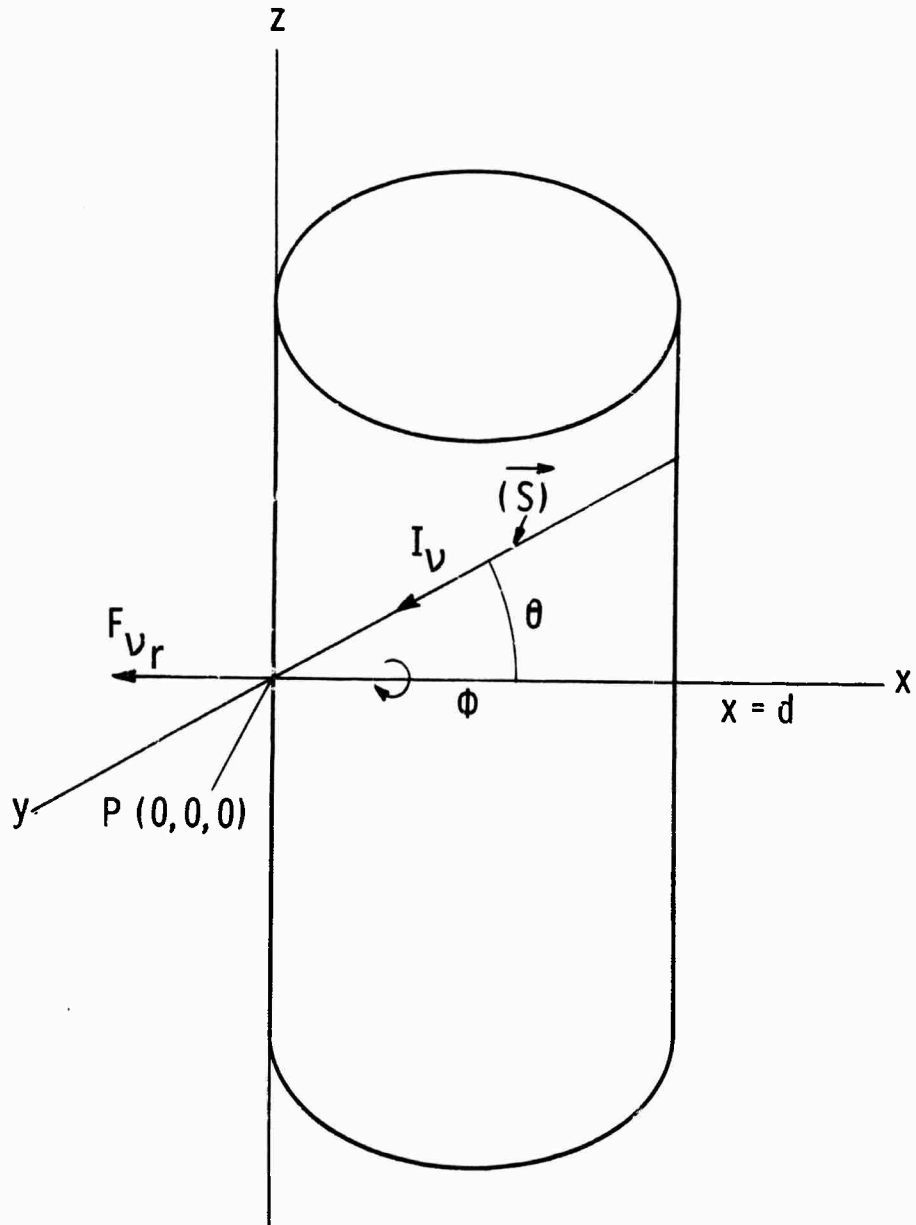
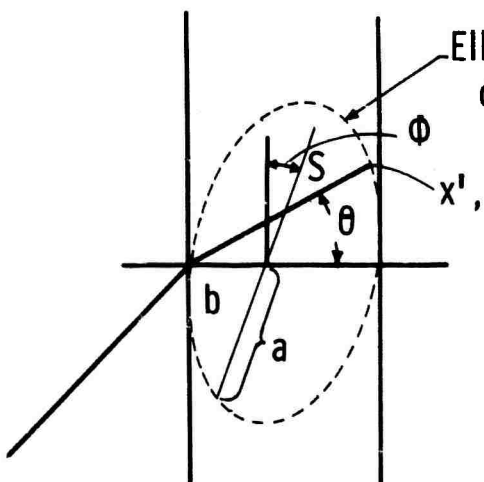


Fig. 3 - An infinite cylinder showing coordinate system

Dwg. 746A033



Ellipse in  $x'y'$  plane  
containing  $S(\theta)$

Equation of ellipse is:

$$x'^2 - x'd + y'^2 \sin^2 \phi = 0$$

where  $0 \leq \phi \leq 2\pi$ ,  $0 \leq \theta \leq \pi/2$

and  $x' = S \cos \theta$ ;  $y' = S \sin \theta$

$$\therefore S = d / \cos \theta + \tan \theta \sin \theta \sin^2 \phi$$

Fig. 4—Radiation traveling through a cylinder of homogeneous absorption

$$F_v = B_v(T) \int_0^{2\pi} \int_0^{\pi/2} (1 - \exp \frac{-\kappa' d}{\cos \theta + \tan \theta \sin \theta \sin^2 \phi}) \cos \theta \sin \theta d\theta d\phi \quad (3.31)$$

The first term within the integral may be integrated to yield

$$F_v = B_v(T) \pi/4 \int_0^{\pi/2} \int_0^{\pi/2} (\exp - \frac{\kappa' d}{\cos \theta + \tan \theta \sin \theta \sin^2 \phi}) \cos \theta \sin \theta d\theta d\phi \quad (3.32)$$

Letting  $\mu = \cos \theta$  allows this equation to be rewritten as:

$$F_v = B_r(\tau) \pi/4 \int_0^{\pi/2} \int_0^1 \exp \frac{-\kappa' v d\mu}{\mu^2 + (1-\mu^2) \sin^2 \phi} \mu d\mu d\phi \quad (3.33)$$

This integral is well-behaved so it can be readily integrated numerically.  $F_v$  when integrated over all  $v$  yields the radian<sup>+</sup> emittance in the radial direction.

$$F_r = \int_0^\infty F_v r dv \quad (3.34)$$

Neglecting thermal conduction heat transfer, the radiant emittance per unit length integrated over the radiating surface can be equated to the power input to the arc plasma per unit length.

$$\int_S F_r dA = \int_V \sigma E^2 dv \quad (3.35)$$

As  $F_r$  is independent of direction and  $\sigma E^2$  is invariant over the volume

$$F_r = \sigma E^2 \frac{d}{4} \quad (3.36)$$

Solving for  $E$ , the electric field intensity for the cylinder of homogeneous temperature is

$$E = \sqrt{\frac{4F_r}{\sigma d}} \quad (3.37)$$

### 3.5 Comparison of Models with Experiment - Spectral Radiance

To evaluate these models, we needed theoretical expression for the spectral absorptivity and the electrical and thermal conductives as a function of temperature and pressure. The spectral absorptivity calculation was discussed in Chapter 2 together with the particle density calculation. Calculation of the electrical conductivity using Spitzer was in Section 2.4.

The results calculated using this cylindrical model together with the experimentally measured values are shown in Tables I, II and III for three temperatures and pressures.

The three temperatures and pressures 10,000 K, 7.6 ATM; 11,500 K, 11ATM correspond to the three temperatures (and the pressures resulting from the homogeneous temperature assumption) measured at the peak of the arc discharge cycle. These measurements are discussed in Section 4.3 Figure 5, 6, and 7 (and Figures 19, 20, and 21 on a linear scale) show the wavelength dependence of the spectral radiances on Tables I, II, and III and the measured radiances. These results are discussed further in Section 4.4.

### 3.6 Comparison of Models with Experiment: Transmissivity as a Function of Current Density

In order to obtain an estimate of the validity of these homogeneous temperature models, a number of comparisons were made with experimental measurements, both by other workers and in our own Laboratory. These measurements included those of spectral transmissivity, and of the radial distribution of the spectral radiance. These measurements

LN LAMBDA = 5.4934400  
 ELECTRICAL CONDUCTIVITY SIGMA = 5.5759401 INVERSE OHMS INVERSE CM  
 THERMAL CONDUCTIVITY K = 1.5729402 WATTS/CM DEGREES

FROM NNU=24,794 TO NNU=12,327 THE VALUE OF THE INTEGRAL OF FNU IS 1.8699401 WATTS/CM<sup>2</sup> THICK  
 FROM NNU=11,807 TO NNU= 0,208 THE VALUE OF THE INTEGRAL OF FNU IS 3.2522403 WATTS/CM<sup>2</sup> THIN  
 FROM NNU= 0,124 TO NNU= 0,012 THE VALUE OF THE INTEGRAL OF FNU IS 1.3949401 WATTS/CM<sup>2</sup> THICK

RADIANT EMISSANCE F = 3.2854403 WATTS/CM<sup>2</sup>  
 ELECTRIC FIELD E = 1.3629401 VOLTS/CM  
 CURRENT DENSITY J = 7.5958402 AMP/CM<sup>2</sup>

THETA=0.95 EV NTOTAL=5.6150+18 NNU=5.2000+19 PARTICLES/CM<sup>3</sup>  
 T= 10000.0 DEGREES K. P= 7.65 ATU

MNU	WAVELLENGTH	KAPPA=H'IME	TAU	(-TAU)	NNU	TNU	FNU
EV	MICRONS	1/CM		1/F	WATTS/CM STER		WATTS/CM
24,794	5.0000E-02	5.2130E+01	6.6210E+01	1.0000E+00	3.0440E-09	3.0440E-09	7.7120E-05
22,540	5.5000E-02	1.2200E+02	1.5540E+02	1.0000E+00	1.1280E-08	3.1280E-08	7.9260E-04
20,662	6.0000E-02	1.8090E+02	2.2970E+02	1.0000E+00	2.1310E-07	2.1310E-07	5.4050E-03
19,072	6.5000E-02	2.3040E+02	2.9260E+02	1.0000E+00	1.0400E-06	1.0400E-06	2.6650E-02
17,710	7.0000E-02	2.7290E+02	3.4650E+02	1.0000E+00	4.1250E-06	4.1250E-06	1.0450E-01
16,529	7.5000E-02	3.0960E+02	3.9370E+02	1.0000E+00	1.3200E-05	1.3200E-05	3.3450E-01
15,496	8.0000E-02	3.4150E+02	4.3410E+02	1.0000E+00	3.6070E-05	3.6070E-05	9.1400E-01
13,774	9.0000E-02	3.9550E+02	5.0230E+02	1.0000E+00	1.8680E-04	1.8680E-04	4.7340E+00
12,397	1.0000E-01	4.9840E+02	5.5680E+02	1.0000E+00	6.7360E-04	6.7360E-04	1.7070E+01
11,807	1.0500E-01	3.3930E+03	4.3090E+03	4.2990E-03	1.1540E-03	4.9630E-06	1.2510E+01
8,265	1.5000E-01	6.9540E+03	8.8320E+03	8.7930E-03	2.4150E+02	2.1230E+04	5.3480E+00
6,199	2.0000E-01	1.2450E+02	1.5840E+02	1.5720E-02	1.1210E-01	1.7620E-03	4.4370E+01
4,959	2.5000E-01	1.9740E+02	2.5000E+02	2.4760E-02	2.4240E+01	6.0070E-03	1.5110E+02
4,132	3.0000E-01	2.4410E+02	3.4590E+02	3.5930E-02	3.6820E-01	1.3230E-02	3.3250E+02
3,542	3.5000E-01	3.9580E+02	5.0270E+02	4.9020E-02	4.6380E-01	2.2740E-02	5.7100E+02
3,099	4.0000E-01	5.3240E+02	6.7840E+02	6.5400E-02	5.2520E-01	3.4350E-02	8.4100E+02
2,755	4.5000E-01	6.7390E+02	8.5580E+02	8.2020E-02	5.5740E-01	4.5760E-02	1.1460E+03
2,479	5.0000E-01	8.4580E+02	1.0740E+03	1.0190E-01	5.4900E-01	5.7960E-02	1.4500E+03
2,254	5.5000E-01	6.3710E+02	8.0920E+02	7.7730E-02	5.4540E-01	4.1950E-02	1.1020E+03
2,066	6.0000E-01	7.5860E+02	9.6340E+02	9.1850E-02	5.5220E-01	5.0720E-02	1.2700E+03
1,907	6.5000E-01	3.1680E+02	4.0210E+02	3.9430E-02	5.3310E-01	2.1020E-02	5.2830E+02
1,771	7.0000E-01	2.4830E+02	3.1530E+02	3.1040E-02	5.1060E-01	1.5850E-02	1.9560E+02
1,653	1.5000E-01	2.9020E+02	3.6580E+02	3.6190E-02	4.8660E-01	1.7610E-02	4.4270E+02

1.550	8.0000E-01	3.3570E+02	4.2630E+02	4.1730E-02	4.6220E-01	1.9290E-02	4.8470E+02
1.458	8.5000E-01	3.8450E+02	4.8830E+02	4.7660E-02	4.3800E+01	2.0880E-02	5.2440E+02
1.377	9.0000E-01	4.6160E+02	5.8420E+02	5.6930E-02	4.1460E+01	2.3600E-02	5.9250E+02
1.305	9.5000E-01	5.2100E+02	6.6170E+02	6.4030E-02	3.9220E+01	2.5110E-02	6.3000E+02
1.240	1.0000E+00	5.8440E+02	7.4200E+02	7.1510E-02	3.7090E+01	2.6530E-02	6.6520E+02
1.181	1.0500E+00	6.5120E+02	8.2700E+02	7.9370E-02	3.5090E+01	2.7850E-02	6.9800E+02
1.127	1.1000E+00	6.4360E+02	8.1740E+02	7.8480E-02	3.3210E+01	2.4060E-02	6.5320E+02
1.078	1.1500E+00	5.4100E+02	7.1240E+02	6.8760E-02	3.1440E+01	2.1620E-02	5.4230E+02
1.033	1.2000E+00	6.2370E+02	7.9210E+02	7.4150E-02	2.9700E+01	2.2690E-02	4.6870E+02
0.992	1.2500E+00	6.7260E+02	1.1040E+01	1.0490E-01	2.8250E+01	2.9640E-02	7.4140E+02
0.954	1.3000E+00	9.6110E+02	1.2210E+01	1.1490E+01	2.6820E+01	3.0810E-02	7.7020E+02
0.918	1.3500E+00	1.0540E+01	1.3390E+01	1.2530E+01	2.5470E+01	3.1920E-02	7.9720E+02
0.886	1.4000E+00	1.1520E+01	1.4630E+01	1.3610E+01	2.4220E+01	3.2050E-02	8.2250E+02
0.855	1.4500E+00	1.2540E+01	1.5990E+01	1.4720E+01	2.3050E+01	3.3030E-02	8.4620E+02
0.826	1.5000E+00	1.3600E+01	1.7280E+01	1.5870E+01	2.1960E+01	3.4840E-02	8.6820E+02
0.800	1.5500E+00	1.4150E+01	1.7960E+01	1.6440E+01	2.0930E+01	3.4420E-02	8.5750E+02
0.775	1.6000E+00	1.5370E+01	1.9510E+01	1.7730E+01	1.9980E+01	3.5410E-02	8.8130E+02
0.751	1.6500E+00	1.6630E+01	2.1110E+01	1.9040E+01	1.9040E+01	3.6330E-02	9.0340E+02
0.729	1.7000E+00	1.7950E+01	2.2610E+01	2.0390E+01	1.8240E+01	3.7160E-02	9.2340E+02
0.708	1.7500E+00	1.9310E+01	2.4520E+01	2.1750E+01	1.7450E+01	3.7050E-02	9.4150E+02
0.689	1.8000E+00	2.0710E+01	2.6310E+01	2.3130E+01	1.6710E+01	3.8650E-02	9.5820E+02
0.670	1.8500E+00	2.2160E+01	2.8140E+01	2.4530E+01	1.6010E+01	3.9270E-02	9.7270E+02
0.652	1.9000E+00	2.3640E+01	3.0020E+01	2.5930E+01	1.5360E+01	3.9820E-02	9.8540E+02
0.634	1.9500E+00	2.5160E+01	3.1950E+01	2.7350E+01	1.4740E+01	4.0300E-02	9.9450E+02
0.620	2.0000E+00	2.6710E+01	3.3920E+01	2.8770E+01	1.4160E+01	4.0720E-02	1.0040E+03
0.624	5.0000E+00	1.7540E+00	2.2280E+00	8.9220E+01	2.8620E+02	2.5530E+02	6.1250E+02
0.124	1.0000E+01	6.4910E+00	8.2419E+00	9.9970E+01	7.7070E+03	7.7050E+03	1.9310E+02
0.062	2.0000E+01	2.4360E+01	3.0093E+01	1.0000E+00	1.0990E+01	1.0990E+01	5.0610E+01
0.025	5.0000E+01	1.4510E+02	1.8430E+02	1.0000E+00	3.2680E+04	3.2680E+04	8.2820E+00
0.012	1.0000E+02	5.7010E+02	7.2800E+02	1.0000E+00	8.2300E+05	8.2300E+05	2.0850E+00

Table I

LN L4M4D4 = 4.416E+01  
 ELECTRICAL CONDUCTIVITY SIGMA = 7.695E+01 INVERSE OHMS INVERSE CM  
 THERMAL CONDUCTIVITY K = 2.542E+02 WATTS/CM DEGREES

FROM NUE=24.794 TO NUE=12.407 THE VALUE OF THE INTEGRAL OF FNU IS 1.416E+02 WATTS/CM<sup>2</sup> THICK  
 FROM NUE=11.807 TO NUE= 8.620 THE VALUE OF THE INTEGRAL OF FNU IS 1.779E+02 WATTS/CM<sup>2</sup> THIN  
 FROM NUE= 8.248 TO NUE= 6.012 THE VALUE OF THE INTEGRAL OF FNU IS 1.213E+02 WATTS/CM<sup>2</sup> THICK

RADIANT EMITTANCE F = 1.805E+02 WATTS/CM<sup>2</sup>  
 ELECTRIC FIELD E = 2.718E+01 VOLTS/CM  
 CURRENT DENSITY J = 2.092E+03 AMP/CM<sup>2</sup>

THETA=0.99 EV      NUE=6.127E+01  
 I = 11500.0 DEGREES K,      PE = 9.61 AT

NNU	WAVELENGTH	KAMPA/PRIME	TAU	(-1/TAU)	BNU	INU	FNU
EV	MICRONS	1/CM		1-E	WATTS/CM STER	WATTS/CM	
24.794	5.000E+02	4.574E+01	5.809E+01	1.000E+00	1.298E+07	1.298E+07	1.289E+03
22.540	5.500E+02	1.073E+02	1.367E+02	1.000E+00	9.485E+07	9.485E+07	2.403E+02
20.662	6.000E+02	1.587E+02	2.015E+02	1.000E+00	4.862E+06	4.862E+06	1.237E+01
19.072	6.500E+02	2.021E+02	2.567E+02	1.000E+00	1.902E+05	1.902E+05	4.819E+01
17.710	7.000E+02	2.394E+02	3.040E+02	1.000E+00	4.020E+05	6.020E+05	1.526E+00
16.529	7.500E+02	2.714E+02	3.450E+02	1.000E+00	1.611E+04	1.611E+04	4.083E+00
15.436	8.000E+02	2.999E+02	3.809E+02	1.000E+00	3.766E+04	3.766E+04	9.542E+00
13.774	9.000E+02	3.469E+02	4.406E+02	1.000E+00	1.503E+03	1.503E+03	3.809E+01
12.397	1.000E+01	3.844E+02	4.881E+02	1.000E+00	4.399E+03	4.399E+03	1.115E+02
11.807	1.050E+01	1.363E+02	1.731E+02	1.716E+02	4.895E+03	1.183E+04	2.975E+00
8.265	1.500E+01	2.798E+02	3.551E+02	3.491E+02	8.434E+02	2.945E+03	7.406E+01
6.199	2.000E+01	5.034E+02	6.394E+02	6.193E+02	2.869E+01	1.777E+02	4.458E+02
4.959	2.500E+01	7.997E+02	1.016E+01	9.657E+02	5.154E+01	4.980E+02	1.246E+03
4.132	3.000E+01	1.171E+01	1.447E+01	1.382E+01	4.932E+01	9.578E+02	2.390E+03
3.542	3.500E+01	1.612E+01	2.047E+01	1.851E+01	8.023E+01	1.485E+01	3.694E+03
3.099	4.000E+01	2.191E+01	2.782E+01	2.429E+01	8.541E+01	2.074E+01	5.139E+03
2.755	4.500E+01	2.771E+01	3.519E+01	2.966E+01	8.456E+01	2.567E+01	6.338E+03
2.479	5.000E+01	3.494E+01	4.447E+01	3.567E+01	8.513E+01	3.054E+01	7.505E+03
2.254	5.500E+01	2.752E+01	3.495E+01	2.950E+01	8.217E+01	2.424E+01	5.984E+03
2.066	6.000E+01	3.279E+01	3.164E+01	3.406E+01	7.837E+01	2.469E+01	6.570E+03
1.907	6.500E+01	1.633E+01	2.073E+01	1.872E+01	7.420E+01	1.389E+01	3.455E+03
1.771	7.000E+01	1.242E+01	1.577E+01	1.459E+01	6.992E+01	1.020E+01	2.545E+03
1.653	7.500E+01	1.451E+01	1.843E+01	1.663E+01	6.571E+01	1.106E+01	2.754E+03

1.550	8.000E+01	1.677E+01	2.129E+01	1.918E+01	6.167E+01	1.183E+01	2.941E+03
1.458	8.500E+01	1.919E+01	2.438E+01	2.163E+01	5.745E+01	1.251E+01	3.106E+03
1.377	9.000E+01	2.311E+01	2.935E+01	2.544E+01	5.426E+01	1.380E+01	3.817E+03
1.305	9.500E+01	2.607E+01	3.111E+01	2.519E+01	5.092E+01	1.435E+01	3.547E+03
1.240	1.000E+00	2.922E+01	3.711E+01	3.100E+01	4.742E+01	1.482E+01	3.456E+03
1.181	1.050E+00	3.255E+01	4.133E+01	3.386E+01	4.495E+01	1.522E+01	3.746E+03
1.127	1.100E+00	3.269E+01	4.152E+01	3.398E+01	4.230E+01	1.437E+01	3.538E+03
1.074	1.150E+00	2.958E+01	3.758E+01	3.131E+01	3.945E+01	1.248E+01	3.077E+03
1.033	1.200E+00	3.281E+01	4.167E+01	3.408E+01	3.758E+01	1.281E+01	3.153E+03
0.992	1.250E+00	4.582E+01	5.819E+01	4.412E+01	3.549E+01	1.566E+01	3.829E+03
0.954	1.300E+00	5.037E+01	6.395E+01	4.725E+01	3.355E+01	1.585E+01	3.871E+03
0.914	1.350E+00	5.914E+01	7.003E+01	5.035E+01	3.176E+01	1.599E+01	3.898E+03
0.886	1.400E+00	6.014E+01	7.638E+01	5.341E+01	3.010E+01	1.608E+01	3.911E+03
0.855	1.450E+00	6.537E+01	8.302E+01	5.640E+01	2.856E+01	1.611E+01	3.913E+03
0.826	1.500E+00	7.083E+01	8.995E+01	5.932E+01	2.713E+01	1.609E+01	3.904E+03
0.800	1.550E+00	7.429E+01	9.435E+01	6.107E+01	2.580E+01	1.575E+01	3.819E+03
0.775	1.600E+00	8.049E+01	1.027E+00	6.420E+01	2.456E+01	1.577E+01	3.817E+03
0.751	1.650E+00	8.777E+01	1.115E+00	6.720E+01	2.340E+01	1.573E+01	3.803E+03
0.729	1.700E+00	9.491E+01	1.205E+00	7.004E+01	2.232E+01	1.564E+01	3.774E+03
0.708	1.750E+00	1.023E+00	1.299E+00	7.273E+01	2.132E+01	1.550E+01	3.743E+03
0.689	1.800E+00	1.099E+00	1.394E+00	7.525E+01	2.037E+01	1.533E+01	3.700E+03
0.670	1.850E+00	1.178E+00	1.494E+00	7.760E+01	1.949E+01	1.512E+01	3.650E+03
0.652	1.900E+00	1.259E+00	1.599E+00	7.979E+01	1.866E+01	1.489E+01	3.593E+03
0.636	1.950E+00	1.342E+00	1.704E+00	8.181E+01	1.788E+01	1.463E+01	3.531E+03
0.620	2.000E+00	1.427E+00	1.812E+00	8.367E+01	1.715E+01	1.435E+01	3.465E+03
0.604	5.000E+00	9.780E+00	1.229E+01	1.000E+00	3.356E+02	3.356E+02	8.462E+02
0.124	1.000E+01	3.618E+01	4.595E+01	1.000E+00	8.949E+03	8.949E+03	2.267E+02
0.062	2.000E+01	1.364E+02	1.733E+02	1.000E+00	2.309E+03	2.309E+03	5.852E+01
0.025	5.000E+01	3.151E+02	1.035E+03	1.000E+00	3.766E+04	3.766E+04	9.542E+00
0.012	1.000E+02	3.206E+03	4.071E+03	1.000E+00	9.473E+05	9.473E+05	2.401E+00

Table II

LN LAMBDA = 4.7014e00  
 ELECTRICAL CONDUCTIVITY SIGMAE = 8.4908e01 INVERSE OHMS INVERSE CM  
 THERMAL CONDUCTIVITY K = 3.142e02 WATTS/CM DEGREES

FROM NU=24.794 TO NU= 12.397 THE VALUE OF THE INTEGRAL OF FNU IS 3.450e+02 WATTS/CM<sup>2</sup>  
 FROM NU=11.407 TO NU= 6.670 THE VALUE OF THE INTEGRAL OF FNU IS 3.189e+04 WATTS/CM<sup>2</sup>  
 FROM NU= 6.652 TO NU= 6.012 THE VALUE OF THE INTEGRAL OF FNU IS 1.931e+03 WATTS/CM<sup>2</sup>

RADIANT EMITTANCE F = 3.416e+04 WATTS/CM<sup>2</sup>  
 ELECTRIC FIELD E = 3.479e+01 VOLTS/CM  
 CURRENT DENSITY J = 3.093e+03 AMP/CM<sup>2</sup>

THETA=1.06 EV      NTOTAL=6.5644e1H  
 T = 12300.0 DEGREES K,      P = 11.01 ATM

HNU	WAVELENGTH	KAPPA=PRIME	T4U	(-TAU)	HNU	INU	FNU
EV	MICRONS	1/CM		1-E	WATTS/CM STER	WATTS/CM	
24.794	5.000e+02	4.982e+01	5.185e+01	1.000e+00	6.609e-07	6.609e-07	1.674e+02
22.540	5.500e+02	9.581e+01	1.217e+02	1.000e+00	4.164e-06	4.164e-06	1.055e+01
20.462	6.000e+02	1.416e+02	1.759e+02	1.000e+00	1.887e-05	1.887e-05	4.782e+01
19.072	6.500e+02	1.804e+02	2.291e+02	1.000e+00	6.649e-05	6.649e-05	1.685e+00
17.710	7.000e+02	2.134e+02	2.713e+02	1.000e+00	1.925e-04	1.925e-04	4.478e+00
16.529	7.500e+02	2.424e+02	3.079e+02	1.000e+00	4.745e-04	4.745e-04	1.208e+01
15.496	8.000e+02	2.677e+02	3.399e+02	1.000e+00	1.041e-03	1.041e-03	2.438e+01
13.774	9.000e+02	3.097e+02	3.933e+02	1.000e+00	3.712e-03	3.712e-03	9.406e+01
12.397	1.000e+03	3.433e+02	4.359e+02	1.000e+00	9.926e-03	9.926e-03	2.515e+02
11.807	1.050e+03	2.354e+02	2.999e+02	2.948e-02	1.497e-02	4.411e-04	1.110e+01
8.265	1.500e+01	4.841e-02	6.149e-02	5.963e-02	1.652e-01	8.658e-03	2.173e+02
6.199	2.000e+01	8.725e-02	1.104e-01	1.049e-01	4.313e-01	4.524e-02	1.132e+03
4.959	2.500e+01	1.389e-01	1.763e-01	1.417e-01	9.157e-01	2.483e+03	
4.132	3.000e+01	2.037e-01	2.586e-01	2.279e-01	9.136e-01	2.082e-01	5.164e+03
3.542	3.500e+01	2.807e-01	3.564e-01	2.998e-01	1.020e+00	3.058e-01	7.547e+03
3.099	4.000e+01	3.835e-01	4.871e-01	3.856e-01	1.058e+00	4.078e-01	1.001e+04
2.755	4.500e+01	4.849e-01	6.159e-01	4.598e-01	1.051e+00	4.832e-01	1.181e+04
2.479	5.000e+01	6.144e-01	7.803e-01	5.417e-01	1.018e+00	5.513e-01	1.341e+04
2.254	5.500e+01	4.928e-01	6.259e-01	4.652e-01	9.704e-01	4.518e-01	1.103e+04
2.066	6.000e+01	5.473e-01	7.454e-01	5.257e-01	9.164e-01	4.817e-01	1.173e+04
1.907	6.500e+01	3.151e-01	4.002e-01	3.298e-01	8.605e-01	2.838e-01	6.990e+03
1.771	7.000e+01	2.365e-01	3.003e-01	2.594e-01	8.054e-01	2.089e-01	5.171e+03
1.653	7.500e+01	2.762e-01	3.507e-01	2.958e-01	7.525e-01	2.226e-01	5.495e+03

1.550	8.000e-01	3.190e-01	4.052e-01	3.331e-01	7.027e-01	2.341e-01	5.764e+03
1.458	8.500e-01	3.651e-01	4.637e-01	3.710e-01	6.562e-01	2.435e-01	5.981e+03
1.377	9.000e-01	4.402e-01	5.591e-01	4.283e-01	6.132e-01	2.428e-01	4.425e+03
1.305	9.500e-01	4.965e-01	6.305e-01	4.677e-01	5.735e-01	2.682e-01	4.550e+03
1.240	1.000e+00	5.561e-01	7.061e-01	5.065e-01	5.370e-01	2.720e-01	6.628e+03
1.181	1.050e+00	6.193e-01	7.865e-01	5.446e-01	5.034e-01	2.741e-01	4.666e+03
1.127	1.100e+00	6.264e-01	7.955e-01	5.487e-01	4.726e-01	2.593e-01	4.304e+03
1.075	1.150e+00	5.757e-01	7.311e-01	5.186e-01	4.442e-01	2.304e-01	5.610e+03
1.033	1.200e+00	6.381e-01	8.103e-01	5.553e-01	4.182e-01	2.322e-01	5.443e+03
0.992	1.250e+00	8.901e-01	1.130e+00	6.771e-01	3.942e-01	2.469e-01	4.453e+03
0.954	1.300e+00	9.776e-01	1.242e+00	7.111e-01	3.721e-01	2.646e-01	4.390e+03
0.918	1.350e+00	1.069e+00	1.350e+00	7.428e-01	3.517e-01	2.612e-01	4.306e+03
0.886	1.400e+00	1.165e+00	1.480e+00	7.724e-01	3.328e-01	2.571e-01	4.203e+03
0.855	1.450e+00	1.266e+00	1.608e+00	7.996e-01	3.154e-01	2.522e-01	4.086e+03
0.826	1.500e+00	1.371e+00	1.741e+00	8.246e-01	2.992e-01	2.447e-01	3.956e+03
0.800	1.550e+00	1.443e+00	1.833e+00	8.400e-01	2.842e-01	2.387e-01	3.764e+03
0.775	1.600e+00	1.573e+00	1.998e+00	8.643e-01	2.723e-01	2.336e-01	3.408e+03
0.751	1.650e+00	1.708e+00	2.160e+00	8.858e-01	2.573e-01	2.279e-01	3.458e+03
0.729	1.700e+00	1.849e+00	2.349e+00	9.045e-01	2.452e-01	2.218e-01	3.228e+03
0.708	1.750e+00	1.995e+00	2.533e+00	9.206e-01	2.340e-01	2.154e-01	3.184e+03
0.689	1.800e+00	2.145e+00	2.724e+00	9.344e-01	2.234e-01	2.088e-01	3.034e+03
0.670	1.850e+00	2.300e+00	2.921e+00	9.461e-01	2.136e-01	2.021e-01	4.886e+03
0.652	1.900e+00	2.460e+00	3.121e+00	9.560e-01	2.041e-01	1.954e-01	4.735e+03
0.634	1.950e+00	2.424e+00	3.339e+00	9.643e-01	1.957e-01	1.887e-01	4.585e+03
0.620	2.000e+00	2.792e+00	3.546e+00	9.712e-01	1.873e-01	1.822e-01	4.431e+03
0.244	5.000e+00	1.921e+01	2.439e+01	1.000e+00	3.620e-02	3.620e-02	9.162e+02
0.124	1.000e+01	7.210e+01	9.154e+01	1.000e+00	9.611e-03	9.611e-03	2.436e+02
0.062	2.000e+01	2.725e+02	3.460e+02	1.000e+00	2.475e-03	2.475e-03	6.272e+01
0.025	5.000e+01	1.430e+03	2.070e+03	1.000e+00	4.031e-04	4.031e-04	1.021e+01
0.012	1.000e+02	6.411e+03	8.142e+03	1.000e+00	1.014e-04	1.014e-04	2.549e+00

Table III

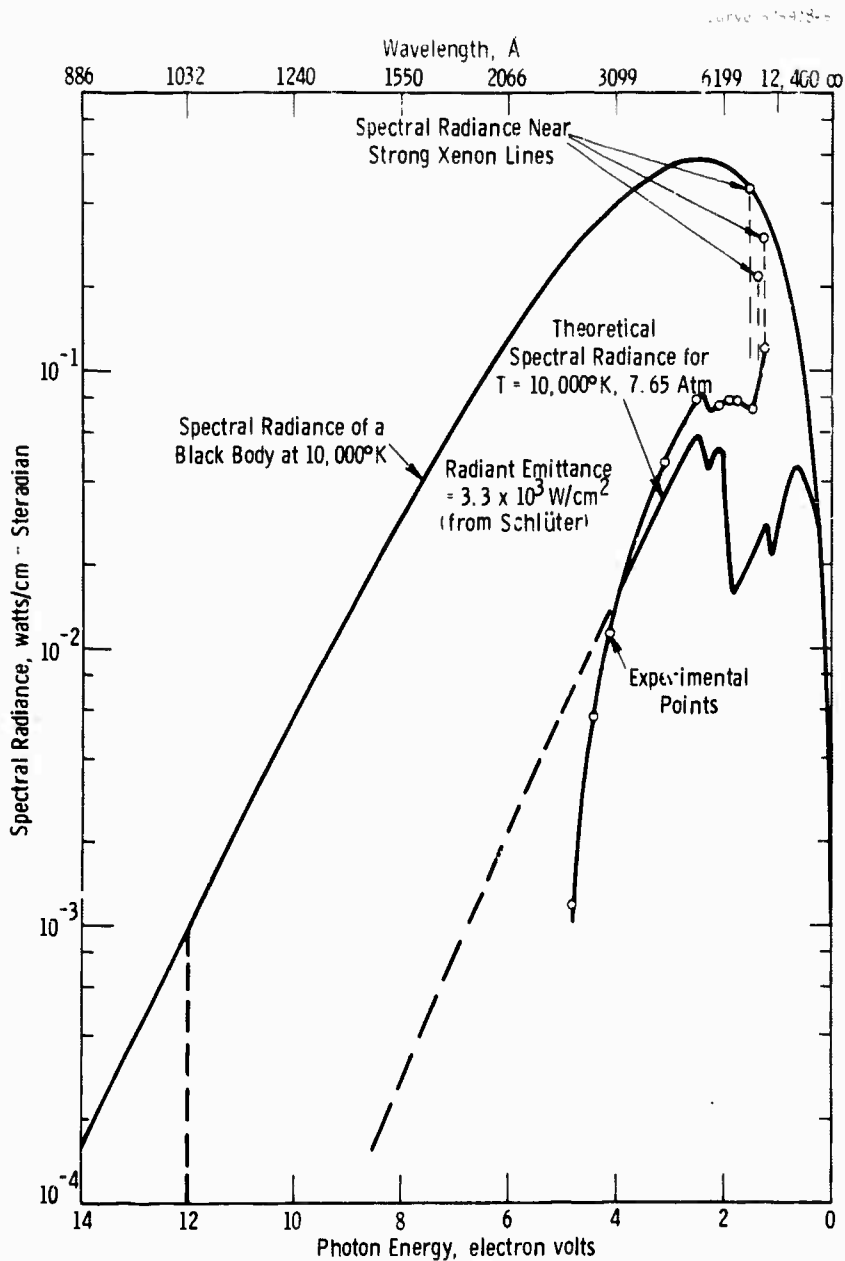


Fig. 5—Experimental & theoretically determined peak spectral radiance of a 1.27 cm thick xenon plasma; theoretical calculation used Schlüter's value of  $\xi$  (dotted portion was extrapolated). Experimental conditions: Energy: 780J,  $V_B = 1.4$  KV,  $C = 800 \mu\text{F}$ ,  $L = 100 \mu\text{H}$   
Flash Tube: 1.27 cm inside diameter, 30 cm arc length, 150 torr initial pressure  
Peak Current Density:  $1000 \text{ A/cm}^2$ ; Peak Electric Field: 32V/cm

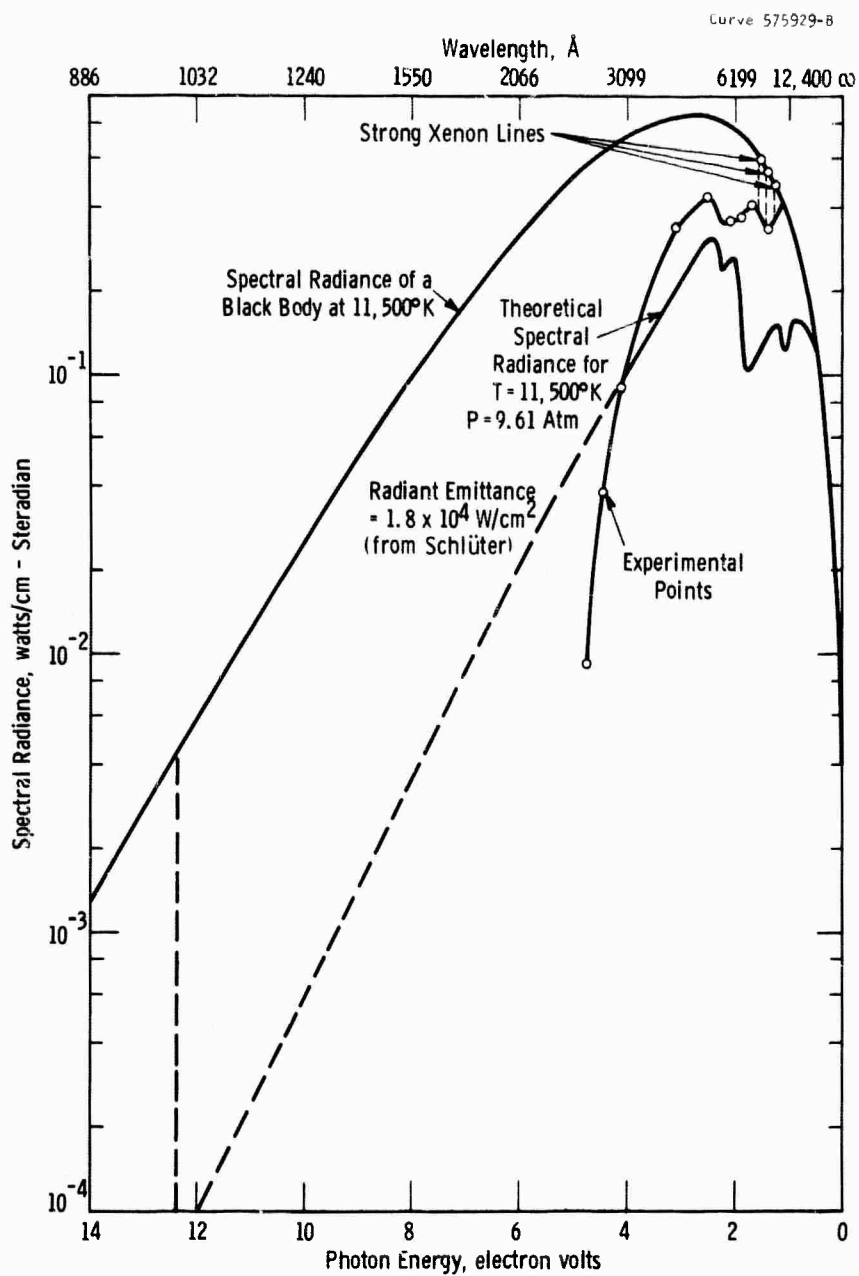


Fig. 6— Experimental & theoretically determined peak spectral radiance of a 1.27 cm thick xenon plasma; theoretical calculation used Schlüter's values for  $\xi$  (dotted portion was extrapolated). Experimental conditions: Energy: 3140J,  $V_B$  = 2.8 KV,  $C$  = 800  $\mu$ F,  $L$  = 100  $\mu$ H  
Flash Tube: 1.27 cm inside diameter, 30 cm arc length, 150 torr initial pressure  
Peak Current Density: 2580 A/cm<sup>2</sup>; Peak Electric Field: 54.3 V/cm

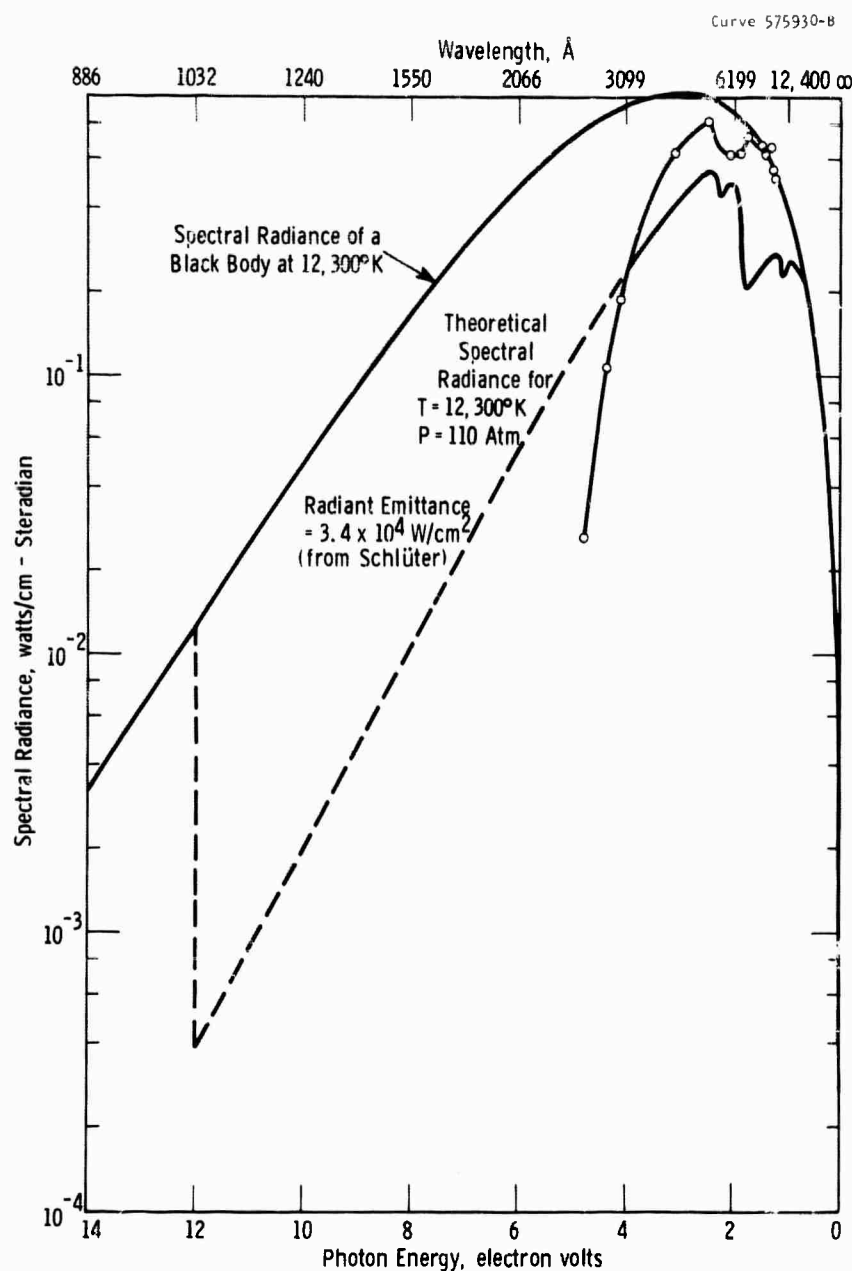


Fig. 7-Experimental and theoretically determined peak spectral radiance of a 1.27 cm thick xenon plasma; theoretical calculation used Schliuter's values for  $\xi$  (dotted portion was extrapolated). Experimental conditions: Energy: 6400J,  $V_B$  = 4.0 KV,  $C$  = 800  $\mu$ F,  $L$  = 100  $\mu$ H  
Flash tube: 1.27 cm inside diameter, 30 cm arc length, 150 torr initial pressure  
Peak Current Density: 4480 A/cm<sup>2</sup>; Peak Electric Field: 69.1 V/cm

led to a means to measure the temperature within the discharge, and thus in turn means to measure various properties of the arc plasma as a function of temperature.

Emmett, Schawlow, and Weinberg<sup>6</sup> had measured the transmissivity at various wavelengths in the ultraviolet, in the visible and in the near infrared as a function of current density. By plotting  $e^{-\tau}$  from the model versus the current density predicted by the balance with the radiated power, we could calculate similar plots for the slab and cylindrical geometries. Figures 8, 9, and 10 show the comparison of the calculated and observed values for  $3000A^{\circ}$ ,  $5000A^{\circ}$ , and  $8000A^{\circ}$ . The former two plots are within the error of the measurements. The latter results, in Figure 10, at  $8000A^{\circ}$ , differed strongly between theory and experiment. This high, measured value for the opacity was caused (as we shall show later in Section 4.3) by the broadened and saturated strong infrared lines of xenon.

The results in this section utilized purely theoretical calculations for the special absorptivity and electrical conductivities which are not truly representative of the values in the arc plasma. As better theoretical calculations are developed for the continuum, lines, and conductivities, through these studies and others, the agreement at all wavelength measured by Emmett, Schawlow, and Weinberg<sup>6</sup> should improve.

Curve 575491-A

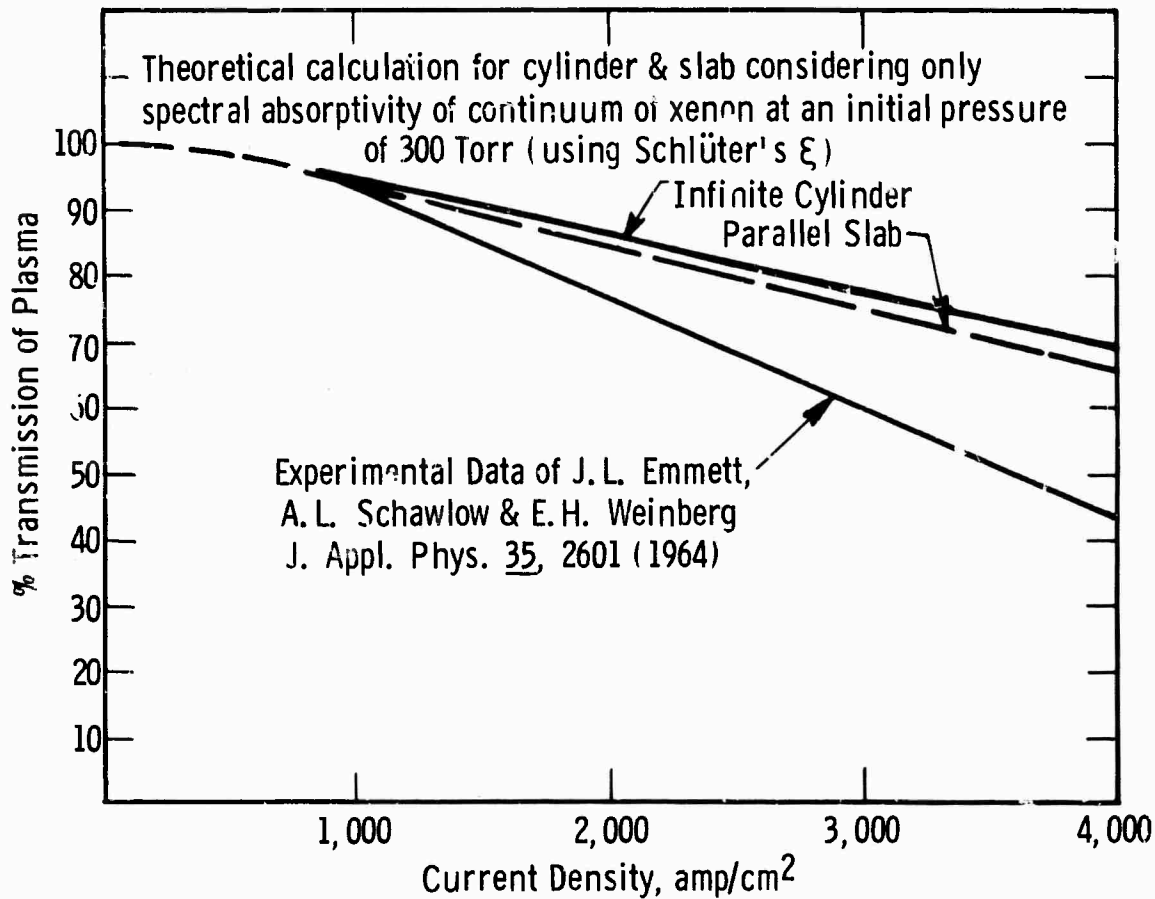


Fig. 8—Transmission of a 1 cm thick layer of xenon of homogeneous temperature at 3000 Å

Curve 575493-A

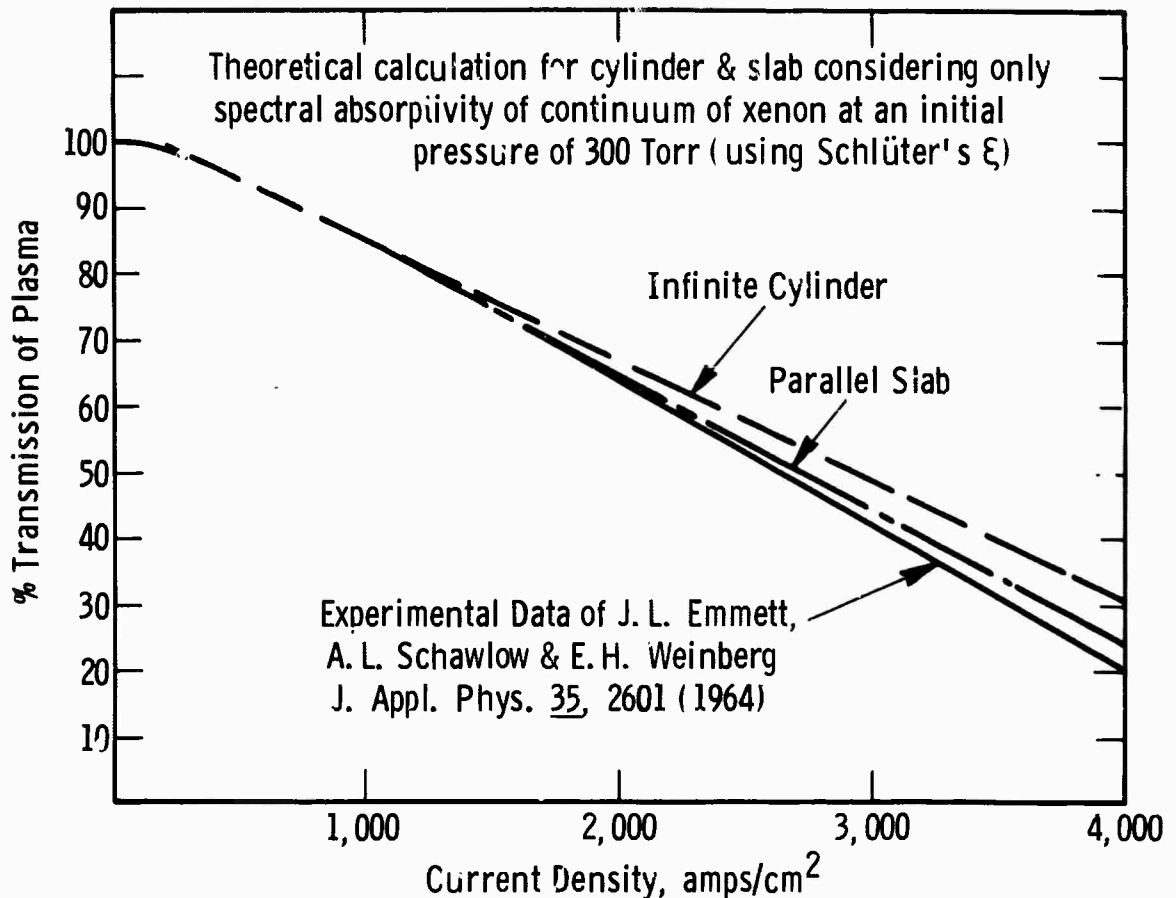


Fig. 9—Transmission of a 1 cm thick layer of xenon of homogeneous temperature at 5000 Å

Curve 575492-A

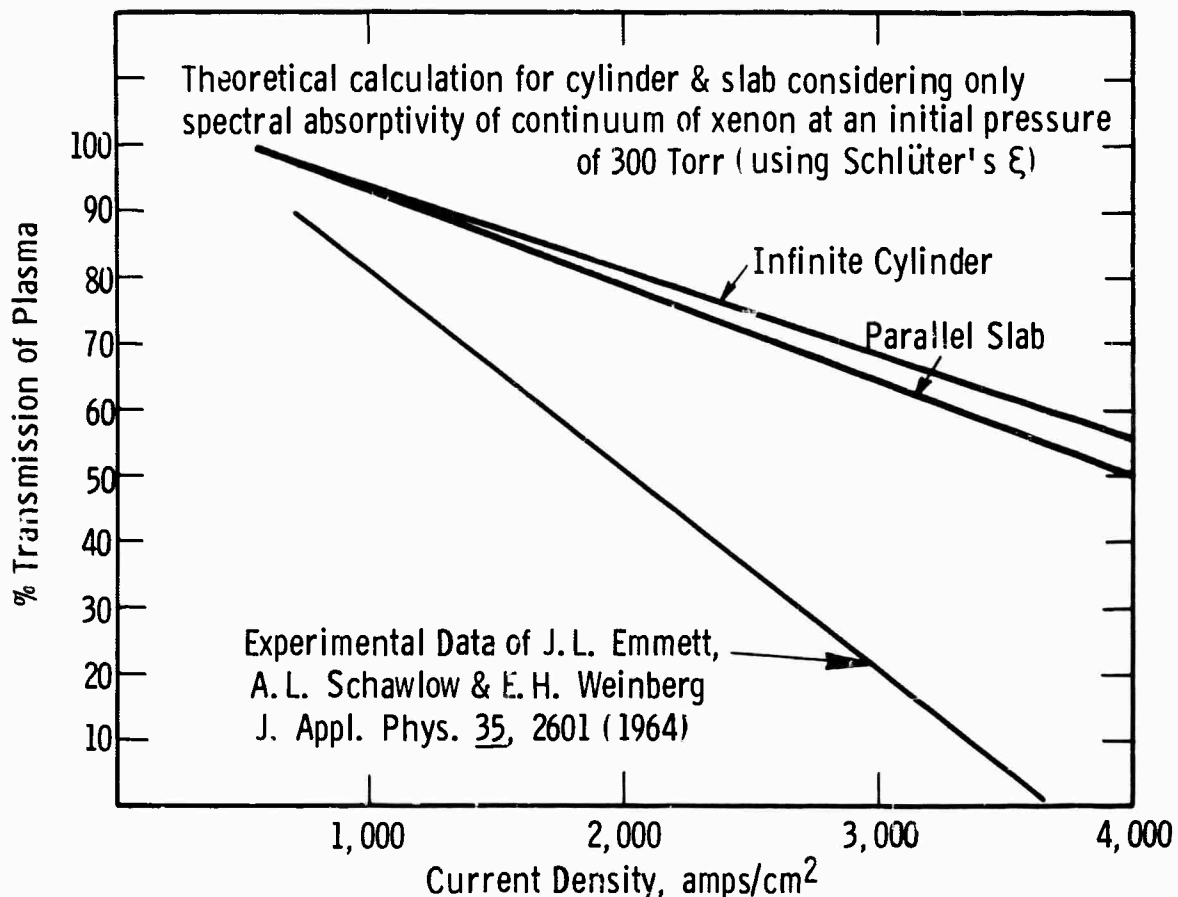


Fig. 10—Transmission of a 1 cm thick layer of xenon of homogeneous temperature at 8000 Å

## CHAPTER 4

### Experiment 1 Measurements

#### 4.1 Experimental Measurements Measured on the Pulsed Arc

The spectral radiance in a high current pulsed arc was measured at a number of wavelengths and positions within the arc. The voltage and the currents through the arc were also measured simultaneously with the time varying spectral radiance. These measurements were first used to determine the temperature and then the temperature dependence of the spectral absorptivity and electrical conductivity of the xenon arc.

The experimental arrangement for these measurements is shown in Figure 11. A 12.7 mm bore tube filled to a pressure of 150 torr of xenon was used. Two off-axis paraboloidal mirrors of 1 meter focal length imaged the arc discharge upon the entrance slit. The various radial portions of the discharge were studied by traversing the monochromator across the image between firings of the bank, with the monochromator set for the wavelength at which the spectral radiance was to be measured. The power input and electrical conductivity of the discharge was monitored through recording the voltage and current for each shot (with the capacitance .800  $\mu$ F and the inductance .100  $\mu$ H held constant for the whole series). The energy input was varied by charging the capacitor bank voltage. The current was measured with a T&M coaxial current shunt (.001 r), the voltage with a Tektronix voltage divider. The entire optical system, including the mirrors, monochromator and photomultiplier detector was calibrated for spectral radiance by the substitution method, using a synchronous detector recorder with a tungsten strip filament lamp (GE 30A/T24/17) being used as the standard. This lamp in turn had been calibrated by Eppley Laboratories.

Dwg. 746A035

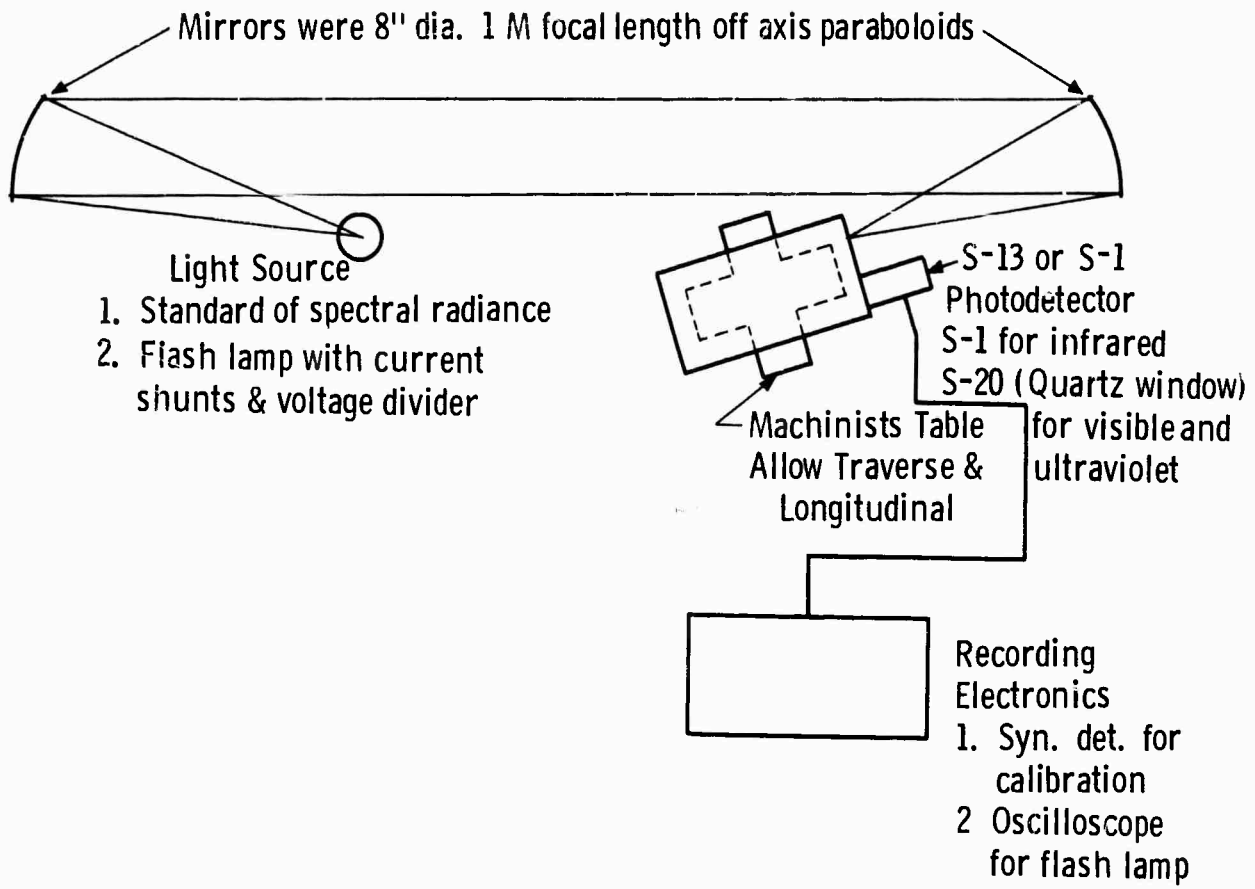


Fig. 11—Monochromator arrangement for studies on flash lamps

#### 4.2 Radial Distribution of Spectral Radiance

The spectral radiance was measured on the central axis for a number of wavelengths in the ultraviolet where the plasma should be optically thin<sup>6</sup>. There were no emission lines noted in this spectral region in the xenon short arc spectra discussed in section 5.5 of the First Semiannual Report.

The radial distribution of the spectral radiance was measured at 2600, 2800 and 3000 $\text{\AA}$  at a number of different radial positions on each side of the center line. The results of these measurements are shown in Figures 12 and 13 for two different energy levels and thus current densities.

The spectral radiance at 3000 $\text{\AA}$  near the tube wall was measured to ascertain, if possible, the boundary layer thickness. The values shown are the raw values of spectra radiance at various diameters, not as yet corrected to the radial dependence by means of the Abel inversion using techniques described in Freeman and Katz<sup>45</sup> and many other papers. These values indicate roughly that the homogeneous temperature model is reasonable as a rough approximation.

The homogeneous temperature distribution is shown in dashed lines. The walls of the tube were at  $\pm .25$  inches (i.e.:  $\pm .635$  cm). The high radiance in the wall region is not readily explicable, but is probably due to reflections from the quartz wall interfaces. Frost<sup>46</sup> and Maecker<sup>47</sup> have shown that no lens effect exists in the region inside the walls (i.e.: a distance from the centerline outside the tube corresponds to the spectral radiance that distance from the centerline. Figure 14 shows a simple proof of this.

#### 4.3 Time-Resolved Spectral Radiance in the Infrared - Temperature Measurements

The spectral radiance in the center of the arc was measured as a function of time in the immediate vicinity of some strong lines of xenon in the

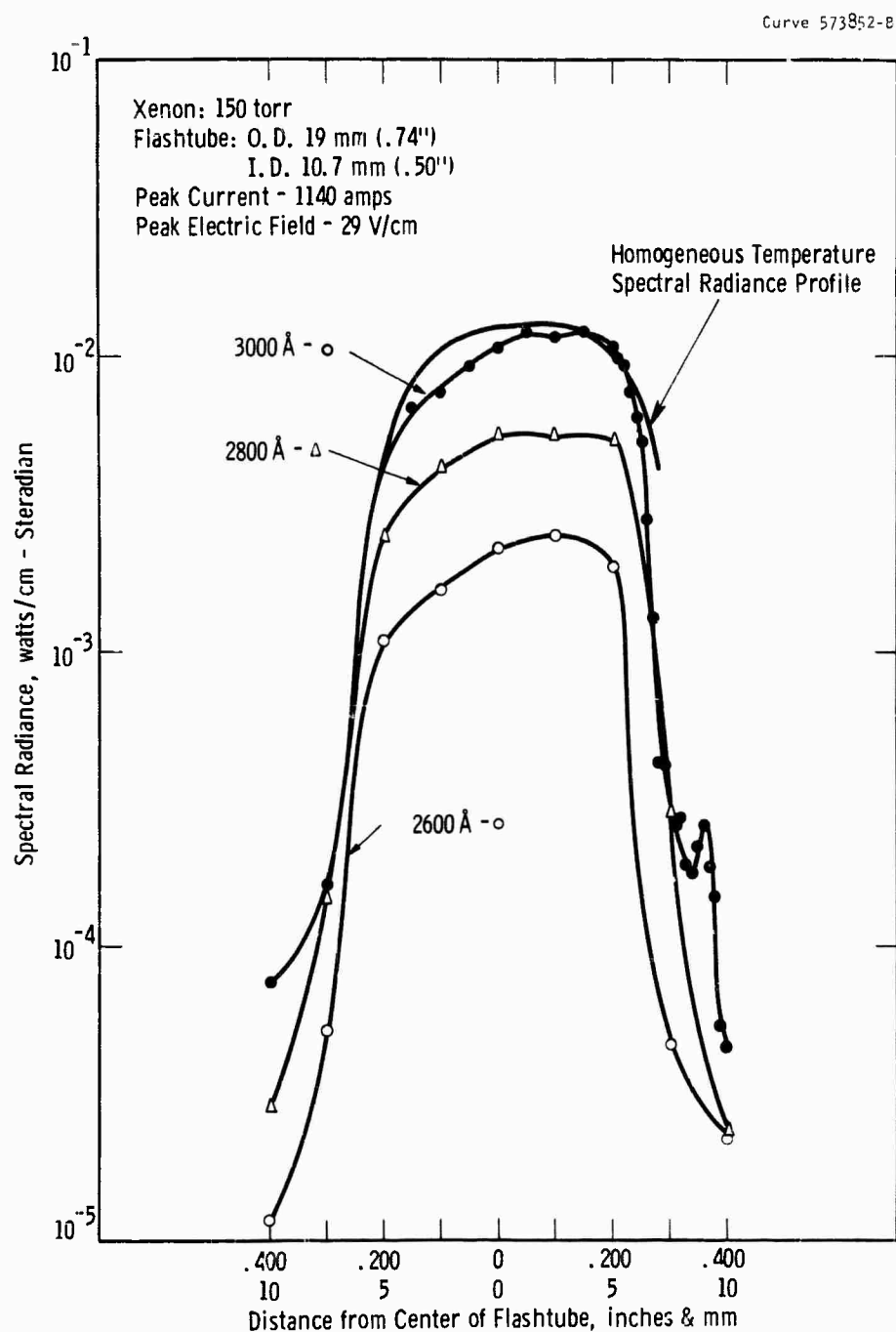


Fig. 12 - Peak spectral radiance at different distances from flashtube center at three wavelengths for 780 J input. (not corrected Abel inversion). Homogeneous temperature profile indicated

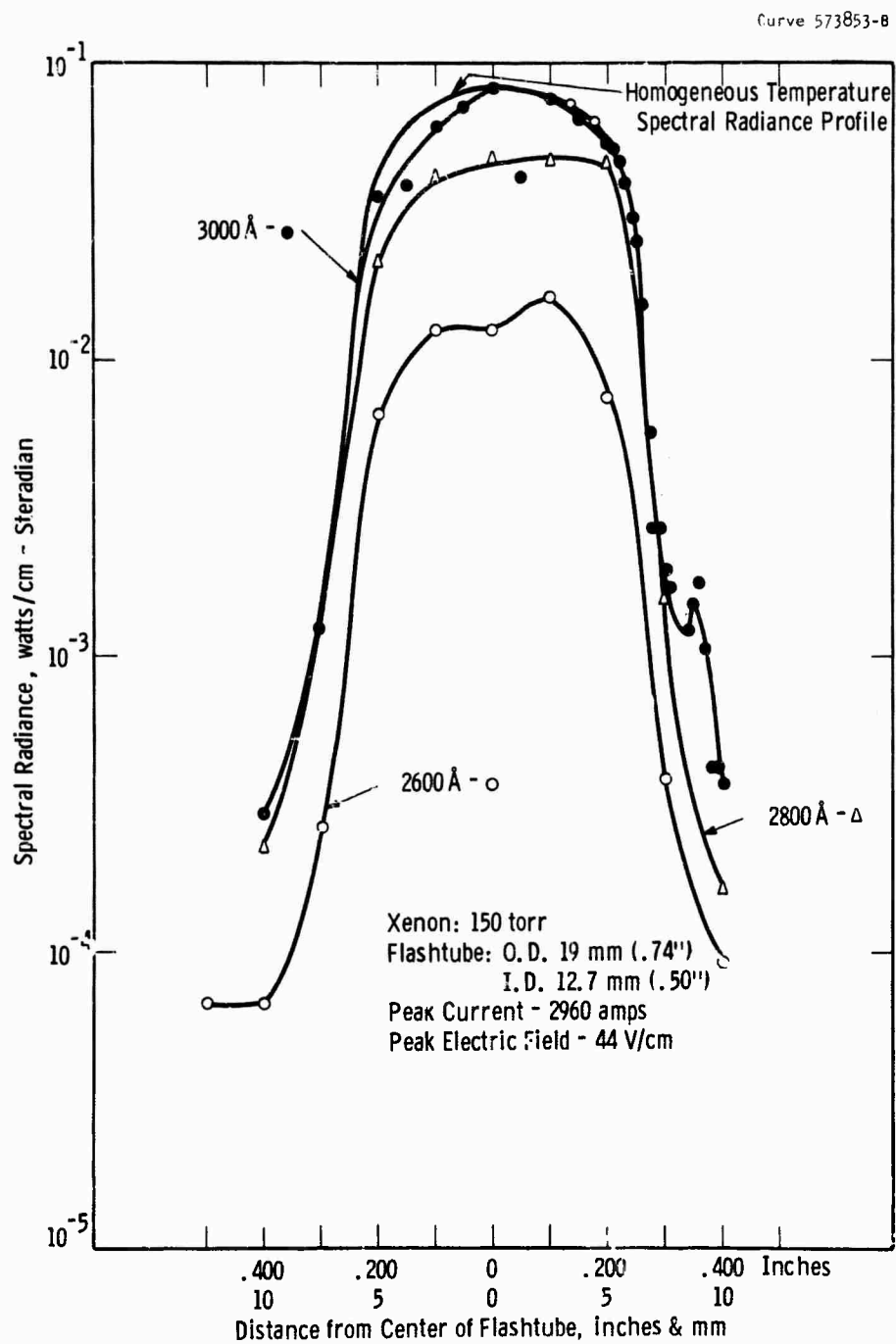
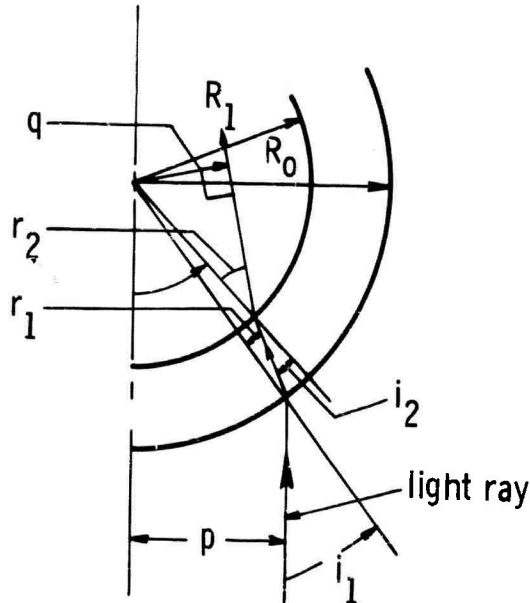


Fig. 13—Peak spectral radiance at different distances from flashtube center at three wavelengths for 3140 J input. (not corrected Abel inversion). Homogeneous temperature profile indicated

Curve 575937-A



Let  $i_1$  = angle of incidence with respect to axis

$$\sin i_1 = \frac{p}{R_0} \text{ where } R_0 \text{ is the outer radius of the tube}$$

$$\sin r_1 = \frac{\sin i_1}{n}; n = \text{index of refraction of cylinder}$$

$i_2$  = angle of incidence from cylinder to plasma

$$\sin i_2 = \frac{R_0}{R_1} \sin r_1$$

$$\sin r_2 = n \sin i_2$$

Tracing whole route of the ray through cylinder yields:

$$\sin r_2 = n \sin i_2 = nR_0/R_1, \sin r_1 = R_0/R_1 \sin i_1$$

$$\sin r_2 = p/R_0 \times R_0/R_1 = p/R_1$$

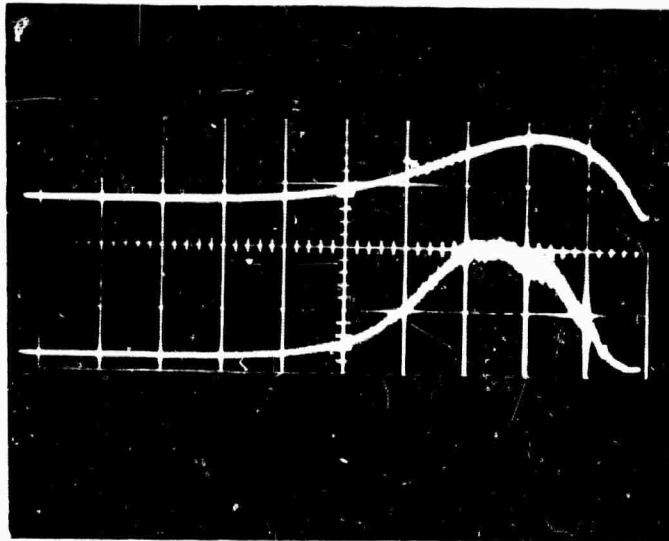
$q/R_1 = \sin r_2 = p/R_1 : q = p$  where  $q$  is the perpendicular distance of the ray in the cylinder to the center of the cylinder

Fig. 14—Derivation of Frost's and Maecher's center line distance relation

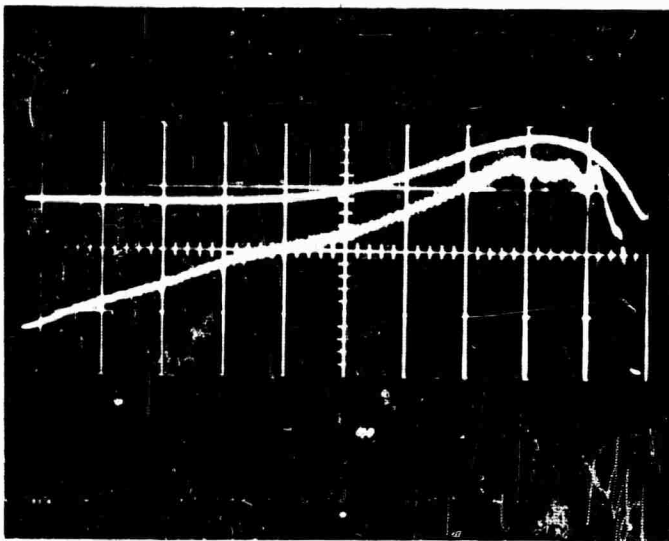
infrared. The slit width of the monochromator was set for a spectral resolution of just under  $1\text{A}^{\circ}$  to avoid over lapping of the spectral radiance determinations. Figure 15 shows two oscilloscope traces, the upper with twice the gain of the lower. The lower trace was taken at the unshifted center of the  $8231.6\text{A}^{\circ}$  line of xenon; the upper trace was taken at  $8198\text{A}^{\circ}$ , approximately  $34\text{A}^{\circ}$  away towards the shorter wavelength. The current trace is the upper curve on both pictures. The energy input to the 12.7 mm diameter, 30 cm arc length tube was 780J. To be noted on these traces is the saturation and long persistance of the line at  $8231.6\text{A}^{\circ}$  particularly in comparison with the current or the  $8198\text{A}^{\circ}$  trace. Figure 16 is a cross section in wavelength of the spectral radiance about the line for different time intervals. Each wavelength setting was a separate shot (note the reproducibility at the peak). To be noted is the shift and broadening of the line with increasing current. The wings of the line contribute strongly to the spectral absorptivity of the continuum away from the line center.

The saturation of the spectral radiance of the line provides a means to determine the temperature within the arc. If the arc is homogeneous, this temperature so determined is that of the arc core. If the arc is not homogeneous, further measurements would be required of the radial distribution of the saturated radiance. The units were converted to temperatures using Walker's tables<sup>48</sup> which list spectral radiances for black bodies.

Temperature measurements by means of spectral radiance measurements in the infrared require high precision in the measurement of the spectral radiance and the other quantities for which the temperature dependence being measured. Source of error in the methods for measured temperature, particularly



a) 8198 Å (Continuum) Gain 100 mv/cm  
(2 x (b))



b) 8231.6 Å (Line) (Gain 200 mv/cm)

Fig. 15—Oscilloscope traces of the voltage representing the spectral radiance at the center of the 8231.6 Å line and at 8198 Å (in the continuum). The 8198 Å trace has twice the gain of the other trace. The upper curve in both cases is the current. The time scale is 100  $\mu$  sec/scale division

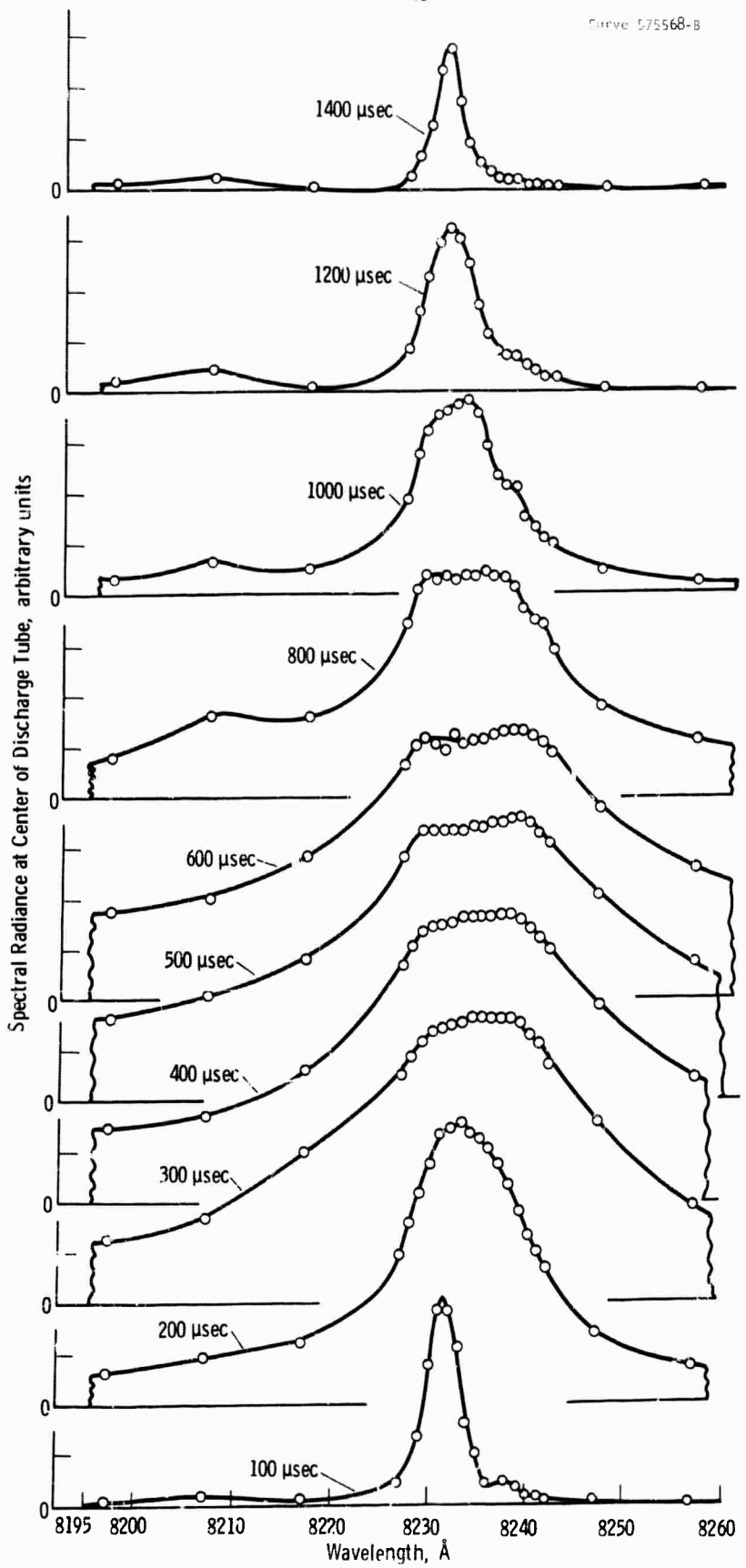


Fig. 16—Time history of 8231.6 Å line of xenon  
780J input, 12.7 mm dia. tube, 150 torr initial pressure  
Peak current 1140 amps  
Peak electric field, 29 v/cm

with the pulsed discharge, are the shot to shot variations (simultaneous measurements are to be preferred) and the difficulties in reading oscilloscope deflections accurately, in addition to the more usual problems of accurate measurements of spectral radiance (i.e.: those of the standard lamp and of the same viewing geometry, etc.). The technique has the supreme virtue of yielding a temperature without assumptions on the detailed properties of the plasma.

The temperatures obtained by this method were used to measure the temperature dependence of the spectral radiance and of the electrical conductivity of the arc to be discussed in subsequent sections.

#### 4.4 Measurements of the Spectral Absorptivity and the $\xi$ Factor of Biberman & Norman

Earlier measurements of the radial distribution of the spectral radiance in the ultraviolet in the First Semiannual Report<sup>1</sup>, and analyzed more thoroughly in this report, and spectral transmissivity measurements<sup>6</sup> indicated that the arc plasma at current densities to at least 3000 amp ( $\text{cm}^2$ ) was nearly homogeneous in spectral absorptivity, and therefore in temperature. During the development of the models, the need for some confirmation of the values of the spectral absorptivity used in the models was required.

Measurements of the spectral radiance at wavelengths for the arc was thick (at the peak of a strong line or the continuum in the infrared) had led to the determination of the temperature of this homogeneous plasma. Using the values of temperature thus determined, the pressure was calculated assuming that the entire volume of the tube was of homogeneous temperature. Figure 17 is a chart derived from the particle density versus pressure calculations to aid this computation. By comparing the spectral radiance observed on the flash

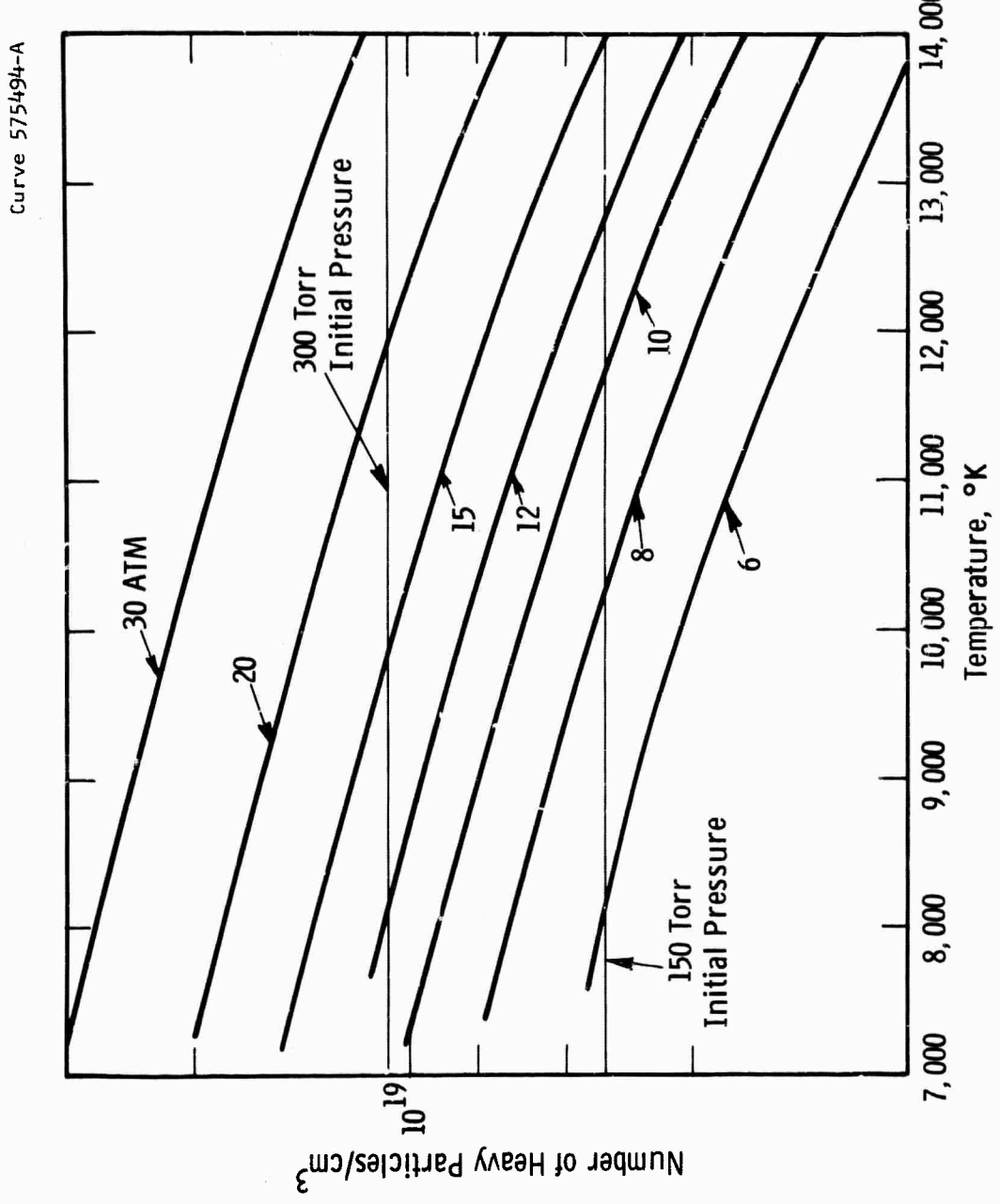


Fig. 17—Heavy particle (atoms + ions) density as function of temperature for various pressures.  
For homogeneous temperature model, dynamic pressure is given by horizontal line  
representing initial pressure and thus particle density

tube with that calculated using the Biberman & Norman continuum theory<sup>7</sup> using Schlüter's values for the  $\xi$  factor for the same pressure and temperature, an experimental value of the variation of  $\xi$  with wavelength was obtained. The experimentally determined values are shown in Figure 18 together with the theoretically calculated values of Biberman & Norman<sup>7</sup>, and of Schlüter<sup>13</sup>. The measured values have a semi-quantitative agreement with the wavelength variation and the magnitude of Schlüter's values but still differ widely in the infrared between .7 and 1.0  $\mu$ . The large values of  $\xi$  measured between  $1000\text{A}^{\circ}$  and  $10000\text{A}^{\circ}$  is probably due to the effects of the wings of the strong lines of xenon in the infrared (as shown in Section 4.3). Furthermore, accurate measurements of  $\xi$  particularly in the ultraviolet below  $2600\text{A}^{\circ}$ , and in the infrared beyond  $10000\text{A}^{\circ}$ , would provide further insight into the actual values of  $\xi$  for further theoretical calculations and would be the extension of his theory to the shorter wavelengths where the slope of Schlüter's values of  $\xi$  differ widely from our experimental values shown in Figure 18. Figure 19 is a plot of the spectral radiance at  $3000\text{A}^{\circ}$  with temperature for various pressures. The arc discharge in the flash tube which may be considered to be a constant heavy particle processes follows the heavy lines indicated.

Figures 20, 21, and 22 present on a linear scale for clarity the experimentally measured values of the spectral radiance together with the black body radiance and the spectral radiance calculated using Schlüter's values for  $\xi$  corresponding to the temperatures measured in the arc in Section 4.3. These figures are linear plots of Figures 5, 6, 7 which are semi-log. The linear plot shows the detailed correspondence and theoretical distribution more

Curve 575927-A

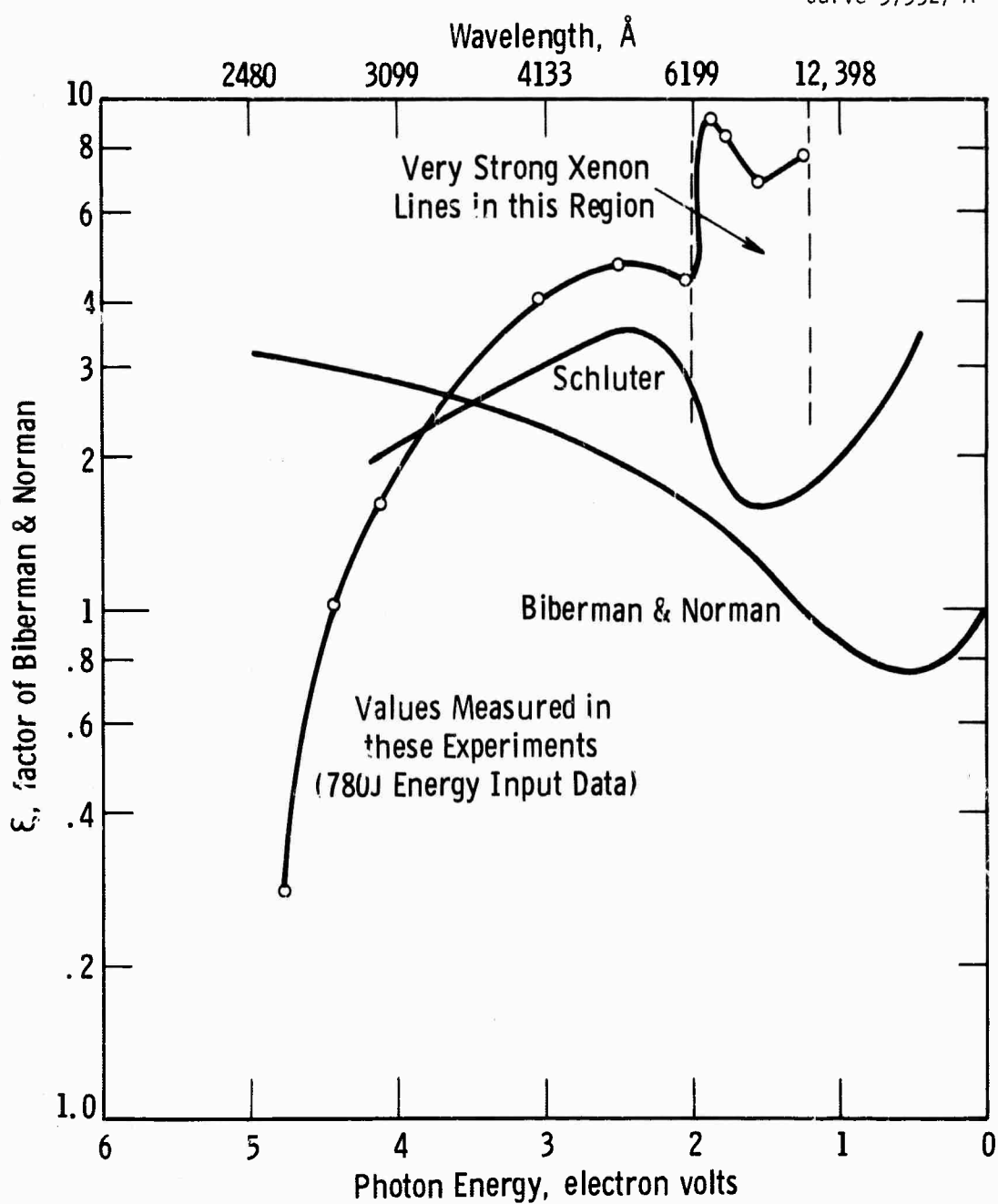


Fig. 1 - Comparison of experimentally measured values of Biberman & Norman  $\xi$  Factor with theoretical calculated values of Schluter (Z. Astrophys. 61, 67 (1965) and of Biberman & Norman (J. Quant. Spectr. Rad. Transfer 3, 221 (1963)

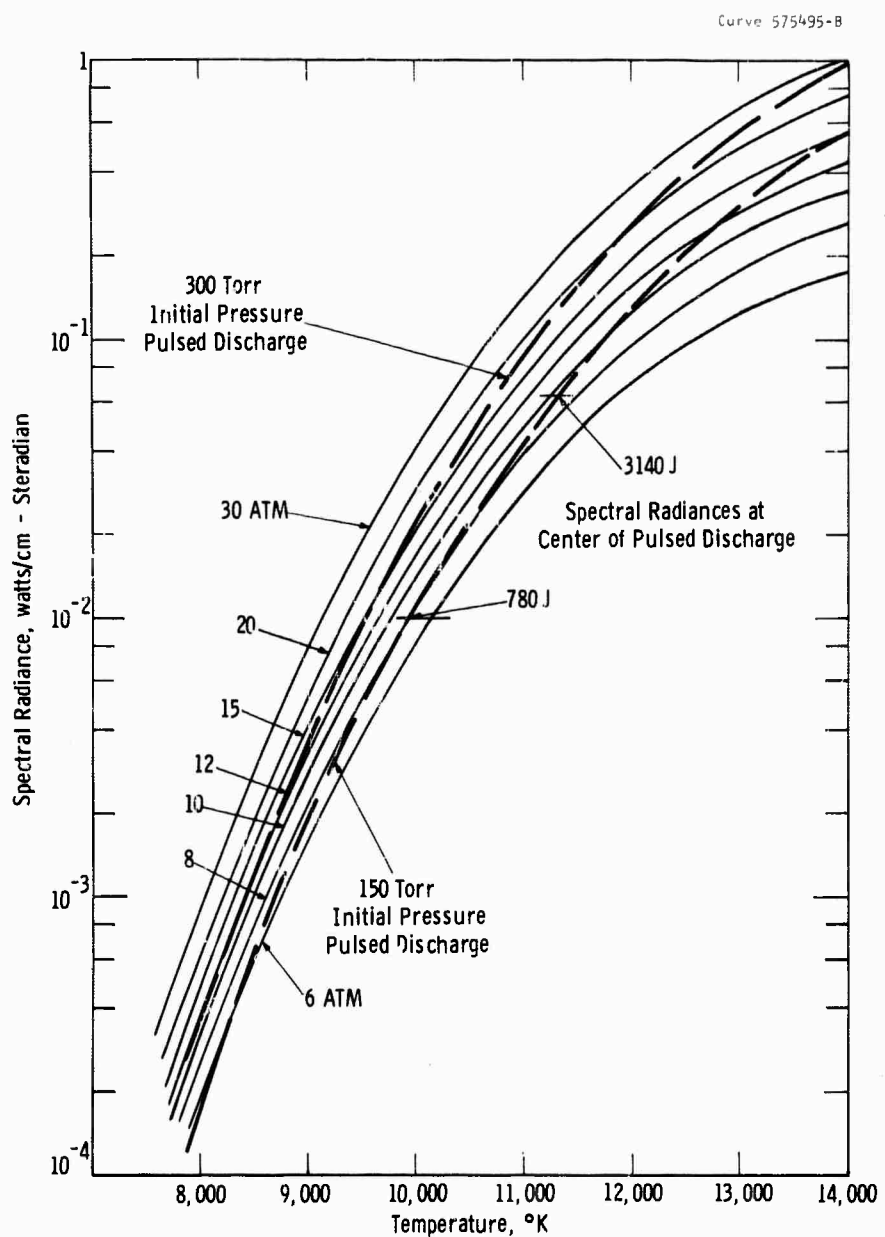


Fig. 19-Spectral radiance at 3000 Å at a constant pressure of a 1 cm thick layer of xenon.  
The pulsed discharge curves are for a homogeneous temperature plasma with a  
constant heavy particle concentration derived from the initial pressure

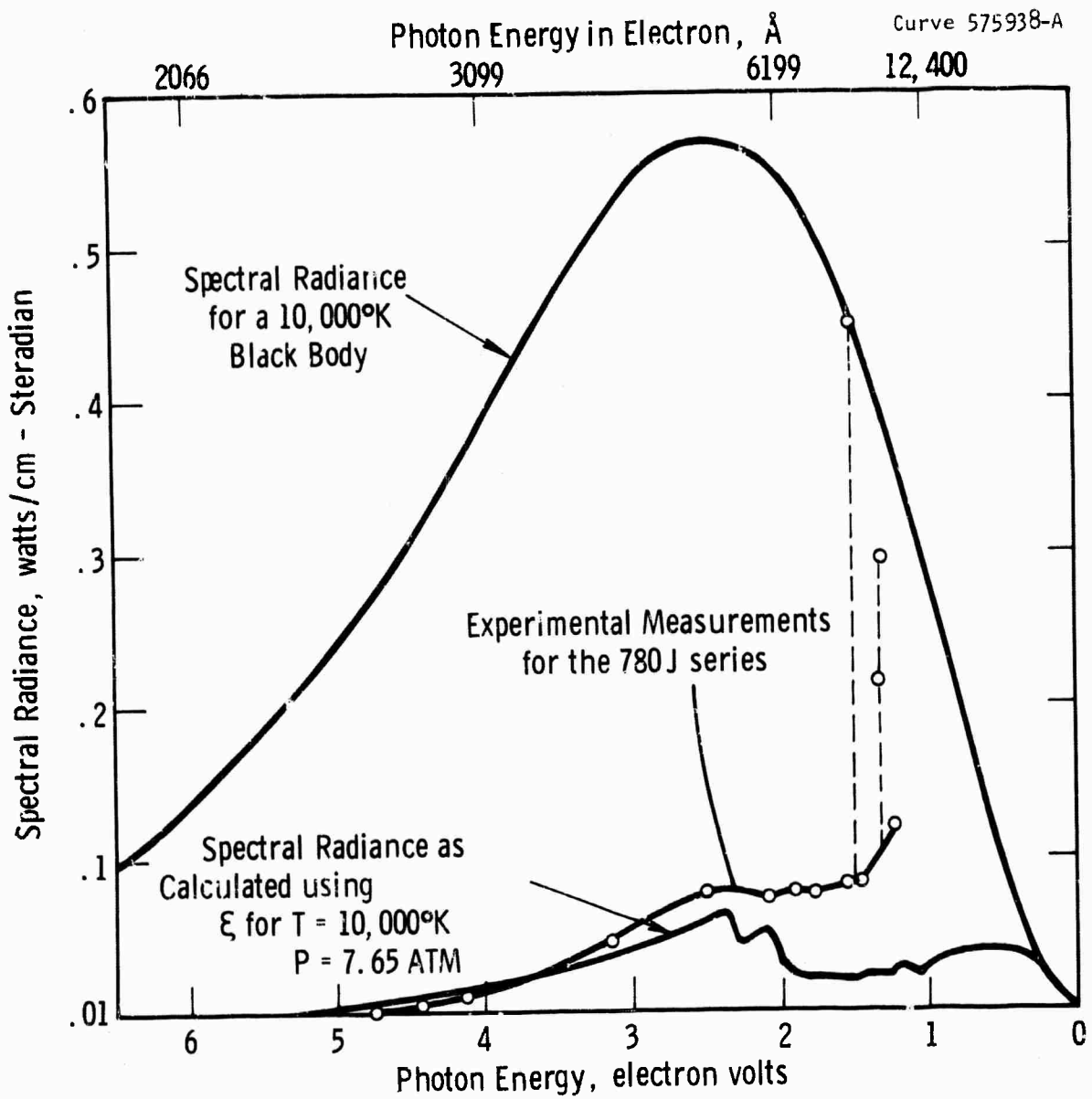


Fig. 20 -Linear plot of the experimental and theoretical values for the spectral radiance of a 1.27 cm thick xenon plasma of homogeneous temperature corresponding to the 780 J -  $1000 \text{ A/cm}^2$  peak current density series  
Flashtube: 1.27 cm inside dia. 30 cm long filled to 150 torr xenon

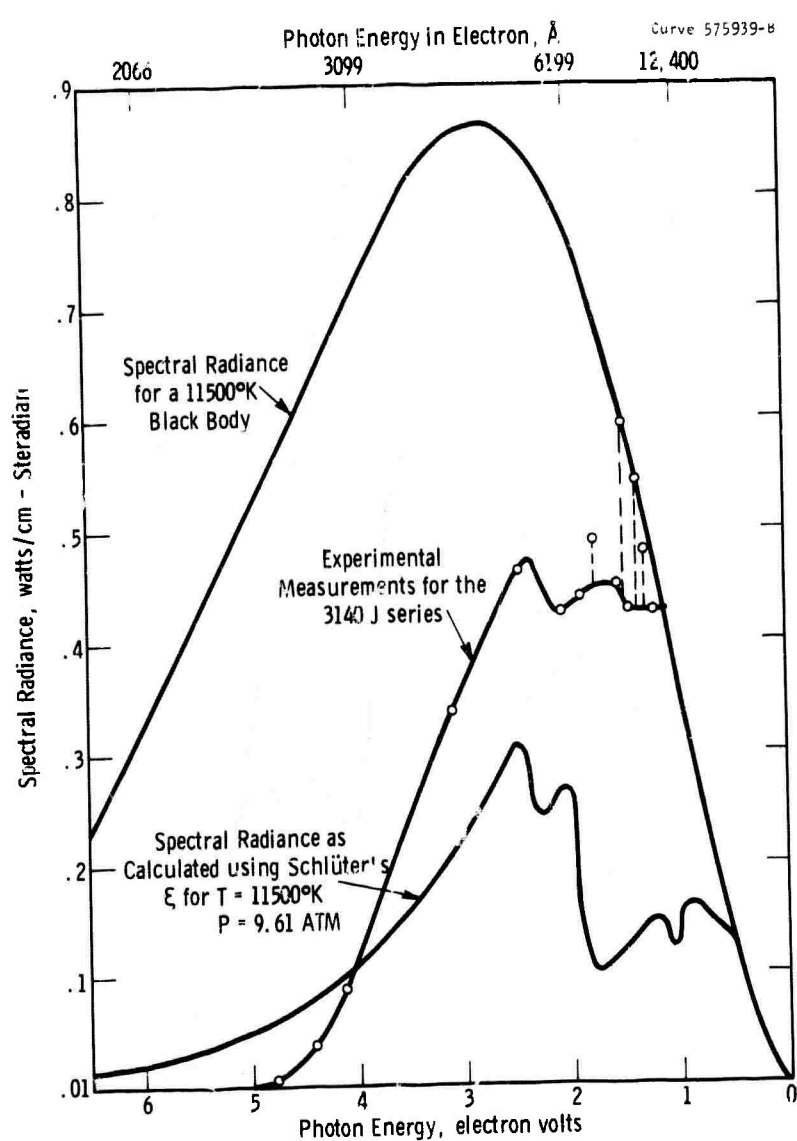


Fig. 21—Linear plot of the experimental and theoretical values for the spectral radiance of a 1.27 cm thick xenon plasma of homogeneous temperature corresponding to the 3140 J - 2580 A/cm<sup>2</sup> peak current density series  
Flashtube: 1.27 cm inside dia, 30 cm long filled to 150 torr xenon

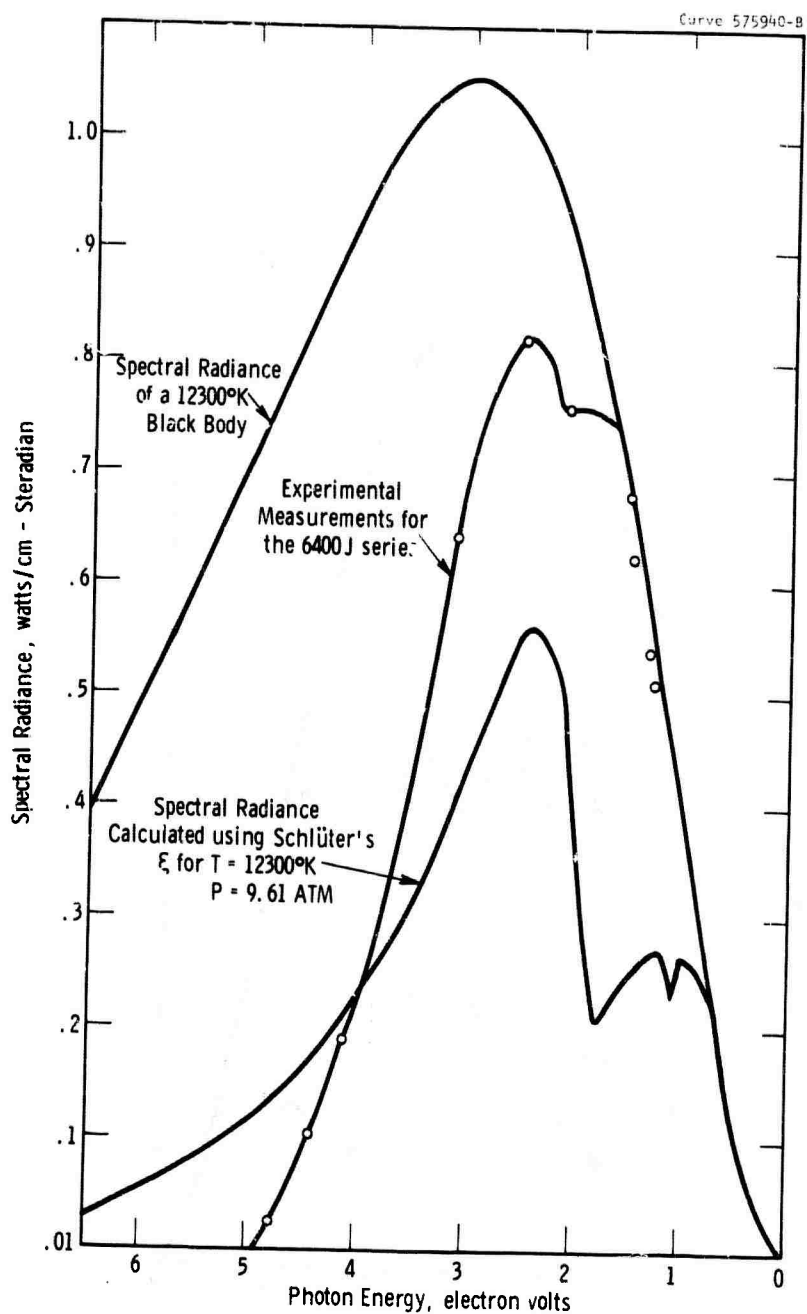


Fig. 22 -Linear plot of the experimental and theoretical values for the spectral radiance of a 1.27 cm thick xenon plasma of homogeneous temperature corresponding to the 6400 J -  $4480 \text{ A/cm}^2$  peak current density series  
Flashtube: 1.27 cm inside dia 30 cm long filled to 150 torr xenon

clearly while the semi-log plot shows well the wide variation with wavelength of the spectral radiance and in optical thickness.

#### 4.5 Temperature Dependence of the Electrical Conductivity

The electrical conductivity in the xenon plasma was measured as a function of temperature using the temperature as determined in Section 4.3. The temperature dependence (for the same number of heavy particles) is shown in Figure 23. The voltage drop at the electrodes was considered to be negligible (Gonz<sup>49</sup> estimated the voltage drop to be 10 to 20 volts in similar flash tubes). The electrical conductivity measured is the average value over the cross section of the tube. The average value will equal the actual value if the flash tube is completely filled with a homogeneous plasma. The correction factor necessary to allow for the boundary layer has not yet been determined; though the radial spectral radiance profiles (Section 4.2) indicated the boundary layer should be small.

The measured electrical conductivity is considerably smaller than that calculated using Spitzer's theory<sup>15,16</sup> for the same temperature and pressure also shown in Figure 22. This is not wholly unexpected as the electron-neutral scattering could be important at 1000°K, (and 7.6 atm.) even though the gas is about 10% ionized. As the electron density was calculated to be about  $1 \times 10^{18}$  for these conditions, Spitzer's theory and in particular the Coulomb term may be beyond its limits of validity. Both areas (i.e.: electron neutral effects and high density corrections) need further investigation.

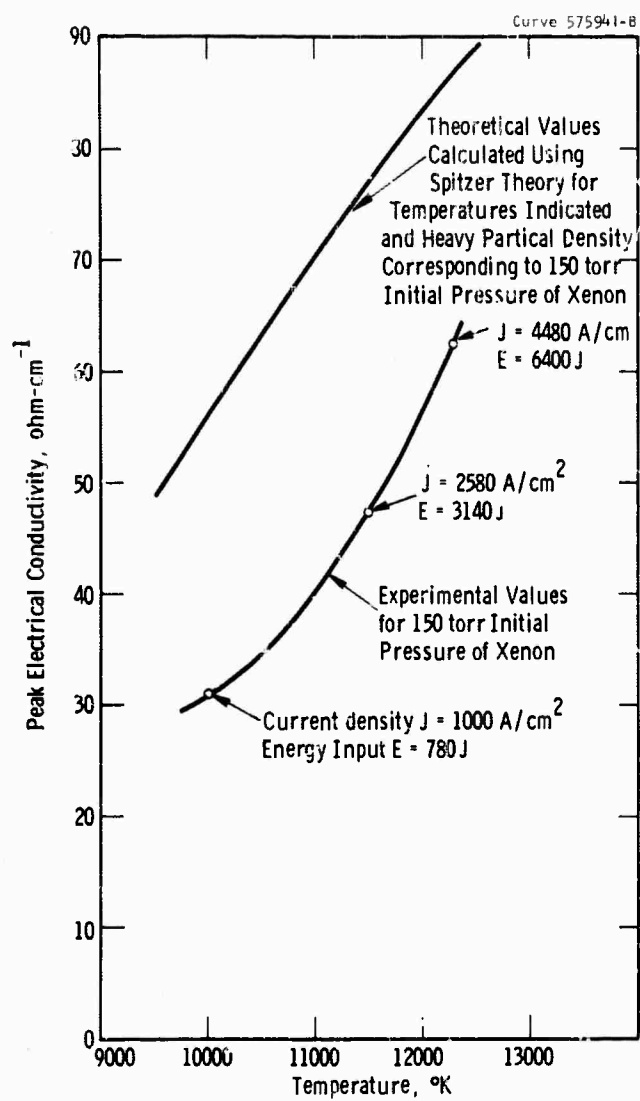


Fig. 23 -Experimental and theoretical dependence of electrical conductivity of xenon upon temperature at a constant heavy particle density

#### STATUS OF THE PROBLEM AND FUTURE WORK

In this report, we have presented some simple models for the arc discharge. The models have many features that agree in a semi-quantitative fashion with the actual arc. These areas of agreement include 1) the arc is thick in the infrared and visible, and thin in the ultraviolet, 2) large changes in input power can lead to relatively small changes in spectral radiance in the infrared where the arc is thick, but very large changes of the spectral radiance in the ultraviolet where the arc is thin. To utilize these models and to develop more complete models that include energy transport within the arc and to the walls the physical properties of the arc need to be better known. Future work on these arcs should include experimental and theoretical studies to improve the quantitative agreement between the theory of the spectral absorptivity of the continuum (Section 4.4) and the actual experimental values. Inclusion of the pressure broadened lines in the infrared would probably improve the agreement, particularly for arcs of moderate current densities ( $\sim 1000 \text{ A/cm}^2$ ) which are becoming of more interest due to the advances in laser efficiency.

We have neglected thermal conductivity and have used a simple representation for electrical conductivity in these model calculations. Quantitative models particularly in the current density range ( $\sim 1000 \text{ A/cm}^2$ ) should include thermal conduction and better values of electrical conductivities to allow calculation of the power balance as the energy transfer by thermal conduction and the heating away from the central core becomes more important in the lower power-lower pressure arcs.

The extension of these models to more complex arc systems in which the power balance between radiation and thermal conduction is a factor that requires an extension of radiative transport theory beyond that of Appendix A. As the techniques improve, we must see what simplifications are warranted and how and when to include the walls, be they transparent or reflective. It should also be possible to apply these theories and the model calculations to actual laser pumping situations such as is found in a coaxial laser pump closely coupled to the laser rod.

The techniques devised in this work, both experimental and theoretical, can be applied to other problems of radiative plasma such as those occurring in lightning arcs, in light sources, and in simulating plasmas of astrophysical interest.

ACKNOWLEDGMENTS

We wish to thank Dr. Elliot Weinburg of ONR-London and Dr. R. D. Haun, Jr. of Westinghouse for their aid and counsel in our pursuit of these models. We also wish to thank many of the personnel of Westinghouse Research Laboratories who have assisted in this work, particularly J. Lesnick, M. Uman, J. Lowke, C. Chen, W. A. Stewart, E. Somers, A. Sletten, A. Phelps, L. Frost, and E. Corinaldesi. Many people in the Quantum Electronics Department have contributed through advice or through loan of equipment. We also wish to thank R. Grassell, J. Humphreys, Jr., and L. Criscella for their good services gathering the experimental data.

The contributions of Ethel Marko and Martha Fischer to the typing; J. Getsko, M. Bowman, and others in Drafting to the figures; K. Moelk, H. Payne, and others in Graphic Arts for the reproduction are also appreciated.

REFERENCES

1. C. H. Church and R. G. Schlecht, "Arc Discharge Sources, Semi-Annual Technical Report in Contract Nonr 4647(00), Westinghouse Research Laboratories, Pittsburgh, Pa. (May 15, 1965).
2. S. S. Penner and M. Thomas, "Approximate Theoretical Calculation of Continuum Opacities," A.I.A.A.J., 2, 1572-1575 (1964).
3. R. A. Pappert and S. S. Penner, "Approximate Opacity Calculations for Polyelectronic Atoms at High Temperatures," J. Quant. Spect. Rad. Transfer, 1; 259-268 (1961).
4. Yu. P. Raizer, "A Simple Method of Calculating the Degree of Ionization and Thermodynamic Functions of a Multiply Ionized Ideal Gas," Sov. Phys.-J.E.T.P., 9, 1124-1125 (1959).
5. Yu. P. Raizer, "Simple Method for Computing the Mean Range of Radiation in Ionized Gases at High Temperatures," Sov. Phys.-J.E.T.P., 10, 769 (1960).
6. J. E. Emmett, A. L. Schawlow, and E. H. Weinberg, "Direct Measurement of Flashtube Opacity," J. Appl. Phys., 35, 2601-2604 (1964).
7. L. M. Biberman and G. E. Norman, "Plasma Radiation due to Recombination and Bremsstrahlung Processes," J. Quant. Spect. Rad. Transfer, 3, 221-245 (1963) General Atomics-San Diego Translation GA tr 4943.
8. V. V. Yankov, "On the Distribution of Energy in the Continuous Absorption Spectrum of Xenon," Optics and Spectroscopy, 14, 14-17 (1963).
9. L. M. Biberman and G. E. Norman, "On the Calculation of Photoionization Absorption," Optics and Spectroscopy, 8, 230-232 (1960).
10. L. M. Biberman, G. E. Norman, and K. N. Ulyanov, "The Photoionization of Excited Complex Atoms and Ions," Sov. Astronomy - AJ 6, 77-83 (1962).

11. L. M. Biberman, G. E. Norman, and K. N. Ulyanov, "On the Calculation of Photoionization Absorption in Atomic Gases," Optics and Spectroscopy, 10, 297-299 (1961).
12. L. M. Biberman, Yu. N. Toropkin, and K. N. Ulyanov, "The Theory of Multi-stage Ionization and Recombination," Soc. Phys. - Tech. Phys. 7, 605-609 (1963).
13. D. Schlüter, "Die Berechnung der Übergangswahrscheinlichkeiten von Seriengrenzkontinua mit Anwendung auf die schweren Edelgase," Z. Astrophys. 61, 67-76 (1965).
14. G. O. Harding, "Laser Flashlamp Final Report," Contract Nonr-4122(00), PEK Labs. Inc., Sunnyvale, California.
15. L. Spitzer, Jr. and R. HArm, "Transport Phenomena in a Completely Ionized Gas," Phys. Rev., 89, 977-981 (1953).
16. R. S. Cohen, L. Spitzer, Jr. and P. Routly, "The Electrical Conductivity of an Ionized Gas," Phys. Rev., 80, 230-238 (1950).
17. J. Fay, "High Temperature Aspects of Hypersonic Flow," Ed. by W. C. Nelson, Pergamon Press Inc., New York (1964).
18. L. S. Frost and A. V. Phelps, "Momentum Transfer Cross Sections for Slow Electrons in He, Av, Kr, and Xe from Transport Coefficients," Phys. Rev. 136, A1538-A1545 (1964).
19. C. E. Moore, "Atomic Energy Levels," National Bureau of Standards Circular 467, Government Printing Office, Washington, D.C. (Vol. I, 1949; Vol. II, 1952; Vol. III, 1958).
20. D. R. Dates and A. Damgaard, "The Calculation of the Absolute Strengths of Spectral Lines," Phil. Trans. Roy. Soc. (London), 242A, 101-120 (1949).

21. "American Institute of Physics Handbook," 2nd Edition, edited by D. E. Gray, McGraw Hill Book Company, Inc., New York (1963).
22. K. Drellishak, C. Knopp, and A. B. Cambel, "Partition Functions and Thermodynamic Properties of Argon Plasma", Phys. Fluids 6, 1280-1283 (1963).
23. K. S. Drellishak, C. F. Knopp, and A. B. Cambel, "Partition Functions and Thermodynamic Properties of Argon Plasma" AEDC-TDR-63-146, Northwestern University, Evanston, Illinois (August 1963).
24. A. Burgess and M. J. Seaton, "A General Formula for the Calculation of Atomic Photo-Ionization Cross Sections," Mon. Not. Roy. Astron. Soc. 120, 121-151. (1960).
25. H. Griem, "High Density Corrections in Plasma Spectroscopy," Phys. Rev. 128, 997-1003 (1962).
26. M. McChesney and N. R. Jones, "Equilibrium Properties of Shock Ionized Xenon," Proc. Phys. Soc. 84, 983-1000 (1964).
27. H. Griem, Plasma Spectroscopy, McGraw-Hill Book Co., New York (1964).
28. K. S. Drellishak, "Partition Functions and Thermodynamic Properties of High Temperature Gases," AEDC-TDR-64-22, Northwestern University, Evanston, Illinois (January 1964).
29. H. R. Griem, "Stark Broadening of Isolated Spectral Lines in a Plasma," U.S. Naval Research Laboratory, NRL Report 6084 (June 1964), AD 443 76Z.
30. I. P. Shkarofsky, "The A.C. Conductivity of Air at Temperatures of 300-12,000°K in the Presence of a Static Magnetic Field", Can. J. Phys.
31. L. Spitzer, Jr., Physics of Fully Ionized Gases, 2nd Edition, Interscience Publishers, John Wiley and Sons, Inc., New York (1962).

32. J. A. Fay and N. H. Kemp, "Theory of End Wall Heat Transfer in a Monatomic Gas, Including Ionization Effects," BSD-TDR-63-47, AVOC-Everett Research Laboratory (March 1963) AD 425461.
33. M. Camac, J. A. Fay, R. M. Feinberg, and N. H. Kemp, "Heat Transfer from High Temperature Argon," Proceedings of the 1963 Heat Transfer and Fluid Mechanics Institute, Stanford University Press (1963).
34. J. P. Reilly, "Stagnation-Point Heating in Ionized Monatomic Gases," Phys. Fluids 7, 1905-1912 (1964).
35. I. Amdur and E. A. Mason, "Properties of Gases at Very High Temperatures," Phys. Fluids 1, 370-383 (1959).
36. Private communication from Dr. E. Caproitti.
37. See for example J. C. Slater and N. H. Frank, "Electromagnetism," McGraw Hill Book Co., New York, p. 200-201, (1947).
38. S. Chandrasekar, "An Introduction to the Study of Stellar Structure," Dover, New York (1939).
39. R. M. Goody, Atmospheric Radiation, Vol. I, Theoretical Basis, Oxford Univ. Press, London (1964).
40. H. Mayer, "Opacity Calculations, Past and Future," J. Quant. Spectr. Rad. Transfer 4, 585-95 (1964).
41. M. A. Lutz, "Radiant Energy Loss from a Cesium-Argon Plasma to an Infinite Plane Parallel Enclosure", BSD-TDR-64-6, AVOC Everett Research Laboratory (Sept. 1963). AD 431640.
42. W. Kaplan, "Advanced Calculus", Addison-Wesley Press Inc., Cambridge, Mass. (1952).
43. S. Chandrasekar, Radiative Transfer, Dover Publications, Inc., New York (1960).

44. M. Abramowitz and I. Stegun, Editors, "Handbook of Mathematical Functions with Formulas, Graphs, and Mathematical Tables," National Bureau of Standards Applied Mathematical Series 55. U.S. Government Printing Office, Washington 20402 (June 1964).

**APPENDIX A**

**RADIATION FLUX IN A NON-ISOTHERMAL NON-GREY CYLINDRICAL ARC**

**by**

**B. W. Swanson**

Nomenclature

$\Delta A$	element of area	$\text{cm}^2$
$B_\lambda$	Planck function	(watt/ $\text{cm}^3$ )
	$B_\lambda = \frac{2 c^2 h}{\lambda^5 \left[ \exp \left( \frac{ch}{\lambda k T} \right) - 1 \right]}$	
$B[T]$	$B[T] = \int_0^\infty B_\lambda(T) d\lambda = \sigma^1 T^4 / \pi$	(watt/ $\text{cm}^2$ )
$B[s]$	$B[s] = B[T(s)]$	(watt/ $\text{cm}^2$ )
$b$	constant in equation 44	
$C_1$	integration constant in equation 20	
$c$	velocity of light	
	$c = 3.0 \times 10^{10} \text{ cm/sec}$	
$d\omega$	differential element of solid angle	
$d\lambda$	differential element of wavelength	(cm)
$ds$	differential element of length along a ray	(cm)
$E$	electric field	(volts/cm)
$F(r)$	radiation flux; equation 16	(watts/ $\text{cm}^2$ )
$\hat{F}(r)$	approximate radiation flux; equation 42	(watts/ $\text{cm}^2$ )
$f_1$	$f_1 = -\sin\theta \cos\phi \cos\theta' - \sin\theta \sin\phi \sin\theta'$	
$f_2$	$f_2 = \sin\theta \cos\phi \sin\theta' - \sin\theta \sin\phi \cos\theta'$	
$f_3$	$f_3 = -\cos\theta$	
$G_n(x)$	$G_n(x) = \int_0^{\frac{\pi}{2}} e^{-\frac{x}{\sin\theta}} (\sin\theta)^n d\theta$	

Nomenclature (cont'd)

$h$	Planck's constant	
	$h = 6.625 \times 10^{-34}$ watt sec <sup>2</sup>	
$I_\lambda(r, \omega)$	intensity of radiation at $r$ in direction $\vec{\omega}$ ; equation 5	(watts/cm <sup>3</sup> )
$\vec{i}_x$	unit vector along $x$ axis	
$\vec{j}_y$	unit vector along $y$ axis	
$\vec{k}_z$	unit vector along $z$ axis	
$K$	constant absorption coefficient	(cm <sup>-1</sup> )
$\bar{K}$	Boltzmann constant	
	$\bar{K} = 1.380 \times 10^{-23}$	(watt sec/deg)
$K_P$	Planck mean absorption coefficient	
	$K_P(T) = \frac{\int_0^\infty k_\lambda(T) B_\lambda(T) d\lambda}{B(T)}$	(cm <sup>-1</sup> )
$K$	thermal conductivity	(watt/cm deg)
$K_R$	Rosseland mean absorption coefficient; equation 48	(cm <sup>-1</sup> )
$K_a$	mean absorption coefficient; equation 44	(cm <sup>-1</sup> )
$M$	projection of point $Q$ into $x$ - $y$ plane; Figure 1	
$\vec{n}$	unit vector normal to $\Delta A$	
$Q$	intersection of ray with arc boundary; Figure 1	
$R$	point internal to arc; Figure 1	
$r$	radial coordinate	(cm)
$R_A$	arc radius	(cm)

Nomenclature (cont'd)

$\vec{R}_{OM}$	radial vector from origin to point M	
$\vec{R}_{OR}$	radial vector from origin to point R	
$\vec{R}_{OS}$	radial vector from origin to point s on ray R-M; Figure 1	
$R_o$	$R_o =  \vec{R}_{or} $	(cm)
$\vec{R}_{RM}$	vector from point R to point M along ray R-M; Figure 1	
$\vec{R}_{RS}$	vector from point R to point s along ray R-M; Figure 1	
$R_M$	$R_M =  \vec{R}_{RM} $	(cm)
$R_Q$	length of ray Q-R	(cm)
$\vec{r}$	cylindrical coordinate unit vector; Figure 1	
$s^{\prime \prime}$	variable of integration	
$s'$	point on ray Q-R; Figure 1	
$s$	distance along ray R-M; Figure 1	(cm)
$\Delta t$	differential time increment; equat. on 5	(sec)
T	arc temperature	(°K)
$T(s)$	temperature at point s on ray R-M	(°K)
$T_c$	constant temperature	(°K)
$\alpha$	angle between vectors $\vec{R}_{OR}$ and $\vec{R}_{OM}$ ; Figure 1	
$\theta'$	cylindrical coordinate; Figure 1	(radian)
$\theta$	spherical coordinate; Figure 1	(radian)
$\vec{e}$	cylindrical coordinate unit vector; Figure 1	
$\kappa_\lambda$	absorption coefficient	(cm <sup>-1</sup> )

Nomenclature (cont'd)

$\bar{\chi}_\lambda$	average absorption coefficient	(cm <sup>-1</sup> )
$\lambda$	wavelength of radiation	(cm)
$\lambda_{\min}$	minimum wavelength for numerical integration	(cm)
$\lambda_{\max}$	maximum wavelength for numerical integration	(cm)
$s$	variable of integration	
$\sigma$	electrical conductivity	(ohm-cm) <sup>-1</sup>
$\sigma'$	Stefan Boltzmann constant	
	$\sigma' = 5.6686 \times 10^{-12}$ watts/cm <sup>2</sup> deg <sup>-4</sup>	
$\tau_p(s)$	Planck optical length along ray M-R; equation 46	
$\tau_\lambda$	optical thickness	
$\tau_R(s)$	Rossmeland optical length along ray M-R; equation 45	
$\phi$	spherical coordinate; Figure 1	(radian)
$\vec{\omega}$	unit direction vector along ray Q-R; Figure 1	
$\gamma$	angle between vectors $\vec{n}$ and $\vec{\omega}$	

Scientific Paper 65-8D8-GASDY-P1  
PROPRIETARY CLASS 3 M.G.S.

November 1, 1965

RADIATION FLUX IN A NON-ISOTHERMAL NON-GREY CYLINDRICAL ARC\*

B. W. Swanson

Abstract

In a study of highly radiative arc discharges, an analysis has been made for determining the radiation flux (i.e., radiant emittance) throughout the interior of a non-grey cylindrical arc. These flux calculations are necessary to determine the divergence of the flux which is needed to obtain a solution of the integro-differential arc energy equation. The flux is expressed as a triple integral where the integrand is the product of absorption coefficient, Planck function and an attenuation factor which involves a line integral of the absorptivity. A computer program performs the integration with respect to wavelength, a spherical coordinate and the distance along a radiation vector. Separate programs calculate the spectral absorptivities and transport properties for use in the flux program. The cases to be discussed include only the free-free and bound-free continuum. Radial flux distributions are presented for xenon at pressures of 15 and 20 atmospheres for the following temperature distributions: (a) isothermal arcs at 20,000°K and 15,000°K; (b) linear arcs from 15,000°K to 12,000°K and 2000°K; (c) a non-linear "parabolic" arc from 15,000°K to 5000°K.

\* This research is part of Project DEFENDER under joint sponsorship of the Advanced Research Projects Agency, the Office of Naval Research, and the Department of Defense.

## Introduction

Neglecting convection, the steady state energy equation for an arc is given by

$$\vec{\nabla} \cdot (K \vec{\nabla} T) - \vec{\nabla} \cdot \vec{F} + \sigma(P, T) E^2 = 0 \quad (1)$$

where  $\vec{F}$  is the radiation flux vector,  $K(T)$  the thermal conductivity,  $T$  the arc temperature,  $\sigma$  the electrical conductivity,  $P$  the arc pressure and  $E$  the electric field. In addition the arc temperature must satisfy certain boundary conditions which depend upon the application. In turn the divergence of  $F$  is given by\*

$$\begin{aligned} \vec{\nabla} \cdot \vec{F} &= 4\pi \int_0^\infty K_\lambda(T) B_\lambda(T) d\lambda \\ &- \int_0^\infty K_\lambda \int_{\omega=4\pi} I_\lambda d\omega d\lambda + \frac{F}{r} \end{aligned} \quad (2)$$

where  $K_\lambda$  is the non-grey absorption coefficient,  $B_\lambda$  the Planck function,  $I_\lambda$  the intensity of radiation and  $F$  the radiation flux. Equation 1 is an integro-differential equation which can be solved using an iteration technique. In the iteration process, a temperature distribution is assumed, and the flux  $F$  and the second integral in equation 2 are evaluated as functions of  $r$ . Equation 1 is then solved for a new temperature distribution and this process repeated until the temperature solutions converge. If the axis temperature is held constant, a value of  $E$  is associated with each temperature solution and the values of  $E$  also converge. To obtain an arc temperature distribution, it is therefore necessary to calculate the flux as a function of radial position. This paper is concerned with making

\* Appendix

flux calculations for a non-grey cylindrical xenon arc for several assumed temperature distributions. Future work will employ the flux program to solve the arc energy equation.

#### Radiation Flux Integral

The flux vector  $\vec{F}$  is defined by the equation

$$\vec{F}(r, \theta', z) = \int_0^{\infty} \vec{F}_{\lambda}(r, \theta', z) d\lambda \quad (3)$$

where  $\lambda$  is the wavelength and  $r$  and  $\theta'$  are cylindrical coordinates. In turn,  $F_{\lambda}$  is given by

$$\vec{F}_{\lambda}(r, \theta', z) = \int_{\omega=4\pi} I_{\lambda}(r, \theta', z, \vec{\omega}) \vec{\omega} d\omega \quad (4)$$

where  $\vec{\omega}$  is a unit direction vector and  $I_{\lambda}(r, \theta', z, \vec{\omega})$  is the monochromatic intensity of radiation. In general the intensity  $I_{\lambda}$  depends on position coordinates  $r, \theta', z$  and the direction signified by the vector  $\vec{\omega}$ . To define  $I_{\lambda}$ , let  $\Delta A$  denote a small element of area;  $\vec{n}$  the outward drawn normal vector to  $\Delta A$ ;  $\vec{\omega}$  a vector enclosed by a solid angle  $\Delta\omega$  which makes an angle  $\gamma$  with  $\vec{n}$ ;  $\Delta\lambda$  the wavelength interval between  $\lambda$  and  $\lambda + \Delta\lambda$ ; and  $\Delta q_r$  the amount of radiant energy in the interval  $\Delta\lambda$  which is transferred across  $\Delta A$ , confined to the solid angle  $\Delta\omega$  during the time interval  $\Delta t$ . Then  $I_{\lambda}$  is given by the following limit:<sup>(1)</sup>

$$I_{\lambda}(r, \theta', z, \vec{\omega}) = \lim_{\Delta A, \Delta t, \Delta \omega, \Delta \lambda \rightarrow 0} \left| \frac{\Delta q_r}{(\cos \gamma) \Delta A \Delta \omega \Delta t \Delta \lambda} \right| \quad (5)$$

In Figure 1 is shown a point R in the arc with coordinates  $r, \theta'$ , 0. Through R is drawn a ray defined by the spherical coordinates  $\phi$  and  $\Theta$  which intersects the arc boundary at point Q. The integration of all radiation contributions from points on the ray from Q to R defines the intensity  $I_\lambda(r, \theta', 0, \vec{\omega})$  in the direction  $\vec{\omega}$  along the ray. Because of the definitions of  $\Theta$  and  $\phi$ , the vector  $\vec{\omega}$  is given by

$$\vec{\omega} = -\sin \theta \cos \phi \vec{i} - \sin \theta \sin \phi \vec{j} - \cos \theta \vec{k} \quad (6)$$

Expressing the Cartesian vectors  $\vec{i}$  and  $\vec{j}$  in terms of the cylindrical vectors  $\vec{r}$  and  $\vec{\theta}$

$$\vec{i} = \vec{r} \cos \theta' - \vec{\theta} \sin \theta' \quad (7)$$

and

$$\vec{j} = \vec{r} \sin \theta' + \vec{\theta} \cos \theta' \quad (8)$$

The vector  $\vec{\omega}$  in terms of  $\vec{r}$ ,  $\vec{\theta}$  and  $\vec{k}$  is given by

$$\vec{\omega} = f_1 \vec{r} + f_2 \vec{\theta} + f_3 \vec{k} \quad (9)$$

where

$$f_1 = -\sin \theta \cos \phi \cos \theta' - \sin \theta \sin \phi \sin \theta' \quad (10)$$

$$f_2 = \sin \theta \cos \phi \sin \theta' - \sin \theta \sin \phi \cos \theta' \quad (11)$$

$$f_3 = -\cos \theta \quad (12)$$

- 4 -

Using equation 9, equation 4 becomes

$$\vec{F}_\lambda(r, \theta', z) = \vec{r} \int_{\omega=4\pi}^{\infty} I_\lambda f_1 d\omega + \vec{\Theta} \int_{\omega=4\pi}^{\infty} I_\lambda f_2 d\omega + \vec{k} \int_{\omega=4\pi}^{\infty} I_\lambda f_3 d\omega \quad (13)$$

Assuming a symmetrical temperature distribution, the  $\vec{\Theta}$  and  $\vec{k}$  components of  $F_\lambda$  must vanish. Hence

$$\vec{F}_\lambda(r, \theta', z) = \vec{F}_\lambda(r) = \vec{r} \int_{\omega=4\pi}^{\infty} I_\lambda f_1 d\omega = \vec{r} F_\lambda(r) \quad (14)$$

Then

$$\vec{F} = \vec{r} F(r) \quad (15)$$

where

$$F(r) = \int_0^{\infty} \int_{\omega=4\pi}^{\infty} I_\lambda f_1 d\omega d\lambda \quad (16)$$

For convenience  $\theta'$  may be set equal to zero. Since  $d\omega = \sin\theta d\theta d\phi$ , and making use of symmetry, equation 16 becomes

$$F(r) = -4 \iiint_0^{\infty} I_\lambda \sin^2 \Theta \cos \phi d\theta d\phi d\lambda \quad (17)$$

An expression is now needed for  $I_\lambda(r, \theta, \phi)$ . In Figure 1, let  $s'$  represent a point along the ray from  $Q$  to  $R$ . The intensity satisfies the transfer equation

$$\frac{dI_\lambda}{ds'} = -K_\lambda(s') I_\lambda(s') + K_\lambda(s') B_\lambda(s') \quad (18)$$

where the Planck function  $B_\lambda$  is given by

$$B_\lambda(T) = \frac{2c^2 h}{\lambda^5 \left[ \exp\left(\frac{ch}{\lambda kT}\right) - 1 \right]} \quad (19)$$

where  $c$  is the velocity of light, and  $k$  and  $h$  are the Boltzmann and Planck constants respectively. Implicit in equation 18 is the assumption that the gas is non-scattering. An integrating factor of equation 18 is  $e^{-\int_s^{s'} K_\lambda ds'}$ .

Carrying out the integration yields

$$I_\lambda(s) = C_1 e^{-\int_0^s K_\lambda ds''} + \int_0^s K_\lambda(s') B_\lambda(s') e^{-\int_{s'}^s K_\lambda ds''} ds' \quad (20)$$

where  $C_1$  is a constant of integration which equals the intensity at  $s' = 0$ . Referring to Figure 1,  $s' = 0$  corresponds to point Q and  $s' = s$  corresponds to point R. The initial intensity of radiation entering the arc at point Q is assumed to be zero which makes  $C_1$  zero. In the numerical integration, it is more convenient to reverse the integration and to let  $s' = 0$  correspond to point R. Letting  $R_Q$  denote the length of the ray from R to Q, the intensity at R in the direction  $\vec{\omega}$  can be written as

$$I_\lambda(R, \vec{\omega}) = \int_0^{R_Q} K_\lambda(s') B_\lambda(s') e^{-\int_0^{s'} K_\lambda(s'') ds''} ds' \quad (21)$$

Using equation 21, equation 17 becomes

- 6 -

$$F(R) = -4 \int_0^\infty \int_0^\pi \int_0^{\pi/2} \int_0^{R_Q} X_\lambda(s') B_\lambda(s') e^{-\int_0^{s'} X_\lambda(s'') ds''} ds' \sin^2 \theta \cos \phi d\theta d\phi d\lambda \quad (22)$$

Equation 22 can be further simplified. Referring to Figure 1, consider point  $s'$  on the ray from  $Q$  to  $R$ , and its projection  $s$  on the ray from  $M$  to  $R$ . Point  $M$  is the projection of point  $Q$  onto the  $x$ - $y$  plane. Since  $ds' = ds/\sin \theta$ , then

$$\int_0^{s'} X_\lambda(s'') ds'' = \int_0^s \frac{X_\lambda(s'') ds''}{\sin \theta} \quad (23)$$

Furthermore, letting  $\beta_\lambda(s) = \int_0^s X_\lambda(s'') ds''$ , equation 22 can be written as

$$F(R) = -4 \int_0^\infty \int_0^\pi \int_0^{\pi/2} \int_0^{R_M(\phi)} X_\lambda(s) B_\lambda(s) e^{-\frac{\beta_\lambda(s)}{\sin \theta}} \sin \theta \cos \phi ds d\theta d\phi d\lambda \quad (24)$$

where  $R_M$  is the length of the ray from  $M$  to  $R$  and is a function of  $\phi$ . Defining the function  $G_n(x)$  by the equation

$$G_n(x) = \int_0^{\pi/2} e^{-\frac{x}{\sin \theta}} (\sin \theta)^n d\theta \quad (25)$$

and interchanging the orders of integration with respect to  $\theta$  and  $s$  in equation 24 yields

$$F(R) = -4 \int_0^\infty \int_0^\pi \int_0^{R_M(\phi)} X_\lambda(s) B_\lambda(s) G_1[\beta_\lambda(s)] \cos \phi ds d\theta d\lambda \quad (26)$$

Equation 26 is the desired integral expression for the flux as a function of radial position. In analyzing the radiation from an axisymmetric rocket engine plume, deSoto<sup>(2)</sup> evaluated an integral similar to the one in equation 22. For the arc, the cylindrical geometry permits equation 22 to be reduced to equation 26. To evaluate this integral, it is necessary to know how  $R_M$  varies with  $\phi$ , and for a given  $\phi$ , how temperature varies with  $s$  along the ray.

### Arc Geometry

The coordinate system in Figure 1 is redrawn in Figure 2 with  $\theta'$  set equal to zero. Let  $\vec{R}_{OM}$  and  $\vec{R}_{OR}$  denote vectors from the origin to points M and R respectively, and  $\vec{R}_{RM}$  the vector from R to M. Furthermore let  $R_A$  denote the radius of the arc, i.e.  $R_A = |\vec{R}_{OM}|$ . Then

$$\vec{R}_{OM} = R_A \cos \alpha \vec{r} + R_A \sin \alpha \vec{\theta} \quad (27)$$

and

$$\vec{R}_{OR} = R_0 \vec{r} \quad (28)$$

where  $R_0 = |\vec{R}_{OR}|$

Solving for  $\vec{R}_{RM}$  from the vector equation

$$\vec{R}_{OR} + \vec{R}_{RM} = \vec{R}_{OM} \quad (29)$$

gives

$$\vec{R}_{RM} = (R_A \cos \alpha - R_0) \vec{r} + R_A \sin \alpha \vec{\theta} \quad (30)$$

and

$$R_M = |\vec{R}_{RM}| = \left[ (R_A \cos \alpha - R_o)^2 + (R_A \sin \alpha)^2 \right]^{\frac{1}{2}} \quad (31)$$

To determine  $R_M$  as a function of  $\phi$  it is necessary to determine  $\alpha$  as a function of  $\phi$ . From Figure 2

$$\tan \phi = \frac{R_A \sin \alpha}{R_A \cos \alpha - R_o} \quad (32)$$

which yields the equation

$$\cos \alpha = \frac{\left(\frac{R_o}{R_A}\right) \tan^2 \phi \pm \sqrt{1 + (\tan^2 \phi)(1 - \left(\frac{R_o}{R_A}\right)^2)}}{1 + \tan^2 \phi} \quad (33)$$

Two values of  $\alpha$  are calculated from equation 33, the correct one being that value which also satisfies equation 32.

To evaluate the integrand  $\chi_\lambda(s) B_\lambda(s) G_1(\beta_\lambda(s))$  in equation 38, it is necessary to know the temperature distribution  $T(s)$  along the ray defined by  $\phi$ . A unit vector along the ray from  $R$  to  $M$  is given by  $\vec{R}_{RM}/R_M$ . Let  $\vec{R}_{OS}$  and  $\vec{R}_{RS}$  be vectors from the origin and point  $R$  to a point  $s$  on the vector  $\vec{R}_{RM}$ . Then

$$\vec{R}_{RS} = s \frac{\vec{R}_{RM}}{R_M} \quad (34)$$

where  $s$  denotes distance along the vector  $\vec{R}_{RM}$  and

$$\vec{R}_{os} = \vec{R}_{oR} + \vec{R}_{RS} \quad (35)$$

or

$$\vec{R}_{os} = R_o \vec{r} + \frac{s}{R_M} [(R_A \cos \theta - R_o) \vec{r} + R_A \sin \theta \vec{\theta}] \quad (36)$$

Solving for  $|\vec{R}_{os}|$ ,

$$|\vec{R}_{os}| = \left[ \left( R_o + \frac{s}{R_M} (R_A \cos \theta - R_o) \right)^2 + \left( \frac{s}{R_M} R_A \sin \theta \right)^2 \right]^{\frac{1}{2}} \quad (37)$$

Assuming that the radial temperature distribution  $T(r)$  is known for  $0 \leq r \leq R_A$ , the value of  $T(s)$  for a given value of  $s$  is defined by

$$T(s) = T[|\vec{R}_{os}|] \quad (38)$$

Knowing  $R_M(\phi)$  and  $T(s)$ , the integral in equation 26 can be evaluated.

As an aid in checking the computer program, it is convenient to consider the case of a grey isothermal arc. Let

$$\begin{aligned} K_s &= K = \text{constant} \\ T(r) &= T_0 = \text{constant} \end{aligned} \quad (39)$$

Then equation 26 reduces to

$$F(R) = \frac{4 \sigma' T_0^4}{\pi} \int_0^\pi G_2 [K R_M(\phi)] \cos \phi d\phi \quad (40)$$

Equation 40 was programmed and used to check the flux program for the evaluation of equation 26, under the conditions of equation 39.

### Flux Approximation

Before discussing flux computations for assumed temperature distributions, a word is in order on making approximate flux calculations. On a Burroughs B-5000 computer, it takes an average of 100 seconds to evaluate equation 26 for one value of  $r$ . Based on present computing rates, the corresponding cost is approximately \$10 per point. If the flux is evaluated at 10 points to compute a radial distribution, the cost of a flux distribution for an assumed temperature distribution is of the order of \$100. Since it is not known a priori how many iterations of equation 1 are needed to obtain a convergent solution, it is obvious that computing costs could become prohibitive. It is therefore necessary to consider the possibility of making approximate flux calculations.

For the case of a plane-parallel geometry, Sampson<sup>(3)</sup> used the general grey gas expression for the flux, but chose the mean absorption coefficient to be functions of the Planck and Rosseland mean absorption coefficients and the optical depth. By using Planck and Rosseland means, the integration with respect to wavelength is eliminated which significantly reduces machine time. Sampson's flux approximation is exact in the limits of very optically thin and very optically thick gases. For a non-grey gas of intermediate optical thickness, he found that exact and approximate flux calculations differed by no more than a factor of two. For a cylindrical geometry, the radiative intensity  $I_\lambda$  must be approximated instead of the flux, and the flux then obtained from the equation

$$F(r) = \int_0^\infty \int_{\omega=4\pi} I_\lambda \vec{\omega} d\omega d\lambda \quad (41)$$

Following Sampson, approximations<sup>(4)</sup> have been obtained for the radiative intensity and the flux. The quality of the approximation has not yet been checked, but if it is comparable to Sampson's, it will be useful in making temperature calculations with a significant reduction in cost.

Only the results of this approximation analysis are presented here. The approximate flux is given by the equation

$$\hat{F}(r) = -4 \int_0^{\pi} \int_0^{R_M(\phi)} K_a(s) B(s) G_1 \left[ \int_s^{R_M(\phi)} K_a(s) ds \right] \cos \phi ds d\phi \quad (42)$$

where  $B(s)$  is given by

$$B(s) = \int_0^{\infty} B_{\lambda} [T(s)] d\lambda = \frac{\sigma' T^4(s)}{\pi} \quad (43)$$

and the mean absorption coefficient  $K_a(s)$  is defined by the equation

$$K_a(s) = \left[ \frac{b}{b + \tilde{\tau}_p(s)} \right] \left[ \frac{b + \tilde{\tau}_R(s)}{b + \tilde{\tau}_p(s)} \right] K_p(s) + \left[ \frac{\tilde{\tau}_p(s)}{b + \tilde{\tau}_p(s)} \right] K_R(s) \quad (44)$$

The term  $b$  is a constant of the order of unity which can be varied to improve the approximation.

The terms  $\tilde{\tau}_R(s)$  and  $\tilde{\tau}_p(s)$  are the Rosseland and Planck optical lengths along the ray from point M to point R in Figure 2, and are given by

$$\tilde{\tau}_R(s) = \int_0^s K_R(s) ds \quad (45)$$

$$\tilde{\tau}_p(s) = \int_0^s K_p(s) ds \quad (46)$$

where the Planck and Rosseland absorption coefficients are given by

$$K_p(T) = \frac{\int_0^{\infty} K_{\lambda}(T) B_{\lambda}(T) d\lambda}{\frac{4 \sigma' T^4}{\pi}} \quad (47)$$

and

$$K_R(T)^{-1} = \frac{\int_0^{\infty} \frac{1}{\chi_{\lambda}(T)} \frac{dB_{\lambda}}{dT} d\lambda}{\frac{4 \sigma' T^3}{\pi}} \quad (48)$$

In equation 42, 45 and 46,  $s = 0$  corresponds to point M in Figure 1, and therefore the integration proceeds along a ray from the arc exterior to an internal point R. When  $s = R_M$ ,  $\tau_p$  and  $\tau_R$  represent optical thicknesses of the arc in the direction of the angle  $\phi$ . Depending on the temperature distribution, pressure and location of the point R, the arc could be optically thin when  $\phi = 0$  and optically thick when  $\phi = \pi$ . The dependence of the optical thickness on the angle  $\phi$  is a characteristic of the cylindrical geometry.

Under optically thin conditions, when  $\tau_p$  and  $\tau_R$  are much less than unity, the mean absorption coefficient  $K_a$  approaches the Planck absorption coefficient  $K_p$  and equation 42 is exact.

Under optically thick conditions when  $\tau_p$  and  $\tau_R$  are both much greater than unity,  $K_a$  approaches the Rosseland mean  $K_R$  and equation 42 is a good approximation. The quality of the approximation afforded by equation 42 when the rays are neither optically thin nor thick will be determined by comparison with exact flux calculations.

### Results

The purpose of this investigation is to determine radiant flux distributions throughout an arc corresponding to hypothetical temperature distributions. Calculations have been made for xenon at pressures of 15 and 50 atmospheres.

In Figures 3, 4, 5, and 6 the absorption coefficient of xenon is plotted versus wavelength for pressures of 15 and 50 atmospheres and for temperatures of 5,000°, 10,000°, 15,000° and 20,000°K respectively. These continuum absorptivities were calculated by Messrs. Church and Schlect<sup>(5)</sup> following the theory of Biberman and Norman<sup>(6,7)</sup> and Yankov<sup>(8)</sup>, using partition functions and particle densities derived from a modification of Dreilishaks<sup>(9,10,11)</sup> procedure. A separate computer program was written for the absorptivity calculations and the computed absorptivities stored on disc for the flux program.

The optical thickness  $\bar{\tau}_\lambda$  is defined by the equation

$$\bar{\tau}_\lambda = \int_0^{R_M(\phi)} K_\lambda(s) ds \approx \bar{K}_\lambda R_M(\phi) \quad (49)$$

From Figure 3, for a pressure of 50 atmospheres,  $\bar{K}_\lambda$  is of the order of  $1 \times 10^{-6} \text{ cm}^{-1}$ . If the arc radius is one centimeter, and  $R_M(\phi)$  is of the order of one centimeter,  $\bar{\tau}_\lambda \ll 1$  and a 5000°K arc is optically thin in all radial directions. From Figure 5, for a pressure of 50 atmospheres,  $\bar{K}_\lambda$  is of the order of 10 and  $\bar{\tau}_\lambda \gg 1$  so that a 15,000°K arc is optically thick in all radial directions. Between 10,000°K and 15,000°K the arc is neither optically thin nor thick. Furthermore between 5,000°K and 15,000°K, the absorptivity varies by eight orders of magnitude.

For the flux calculations, isothermal, linear and "parabolic" temperature distributions were assumed. Although the arc temperature is always conduction controlled near the flashtube wall, under certain conditions the arc may be fairly isothermal. In general, the arc temperature would be expected to be "parabolic", but a combination of isothermal and linear profiles might be used to bound the flux distribution.

In Figure 7 the flux distribution is shown for an isothermal arc of 20,000°K at a pressure of 50 atmospheres. From equation 26, when  $r = 0$ ,  $R_M(\phi)$  is equal to the arc radius for all values of  $\phi$  and the flux must

vanish. From Figure 6,  $\bar{\kappa}_\lambda$  is of the order of  $5 \text{ cm}^{-1}$ . Letting  $\bar{\kappa}_\lambda = \bar{\kappa}$ , then from equation 40, the shape of the flux curve is essentially determined by the integral  $\int_0^R G_2 [\bar{\kappa} R_m(\phi)] \cos \phi d\phi$

In Figure 8 are shown two temperature profiles  $T_1$  and  $T_2$  and the corresponding flux distributions  $F_1$  and  $F_2$ . Temperature  $T_1$  is constant at  $20,000^\circ\text{K}$  up to  $r = 0.9 \text{ cm}$  where it drops linearly to  $2000^\circ\text{K}$  at  $r = 1.0 \text{ cm}$ . This temperature profile to some extent simulates the effect of a thermal conduction layer near the arc boundary. The corresponding flux distribution  $F_1$  follows the flux distribution of Figure 7 until the "conduction layer" reduces its boundary value. Temperature  $T_2$  decreases linearly from  $20,000^\circ\text{K}$  at  $r = 0$  to  $2000^\circ\text{K}$  at  $r = 1.0 \text{ cm}$ . Both flux distributions  $F_1$  and  $F_2$  assume maximum values at interior points.

In Figure 9 the flux distribution is shown for an isothermal arc at  $15,000^\circ\text{K}$ . The fluxes in Figures 7 and 9 are almost in the ratio of  $(20,000/15,000)^4$  as would be expected from equation 40 since the "average" absorptivities are approximately equal, i.e., of the order of  $5$  to  $6 \text{ cm}^{-1}$ .

In Figure 10, the temperature varies linearly from  $15,000^\circ\text{K}$  at  $r = 0$  to  $12,000^\circ\text{K}$  at  $r = 1.0 \text{ cm}$ , and fluxes are shown for pressures of 15 and 50 atmospheres. An inspection of Figures 3 to 6 shows that the absorptivity for 15 atmospheres is always less than that for 50 atmospheres. From equation 26, the integrand  $\kappa_\lambda(s) B_\lambda(s) G_1[\beta_\lambda(s)]$  gives the amount of radiation leaving a point  $s$  which arrives at a fixed point  $R$ . The Planck function  $B_\lambda(s)$  is independent of pressure. Therefore, two arcs with the same temperature distribution, but at different pressures, will have different flux distributions because of differences in the product  $\kappa_\lambda G_1[\beta_\lambda(s)]$ . The term  $\kappa_\lambda(s) G_1[\beta_\lambda(s)]$  behaves like the function  $\kappa_\lambda e^{-\bar{\kappa}_\lambda s}$  which approaches zero for small and large values of  $\kappa_\lambda$  and which has a maximum for some value  $\kappa_\lambda^*$ . For a given  $s$ , if  $\kappa_\lambda < \kappa_\lambda^*$ , a reduction in  $\kappa_\lambda$  due to a reduction in pressure causes a reduction in the amount of radiation leaving  $s$  and arriving at point  $R$ . Therefore, the overall effect of a reduction in pressure is a reduction in flux distribution.

In Figure 11, the temperature varies linearly from 15,000°K to 2000°K. As in Figure 10, the flux at 15 atmospheres is less than the flux at 50 atmospheres for the reasons just given.

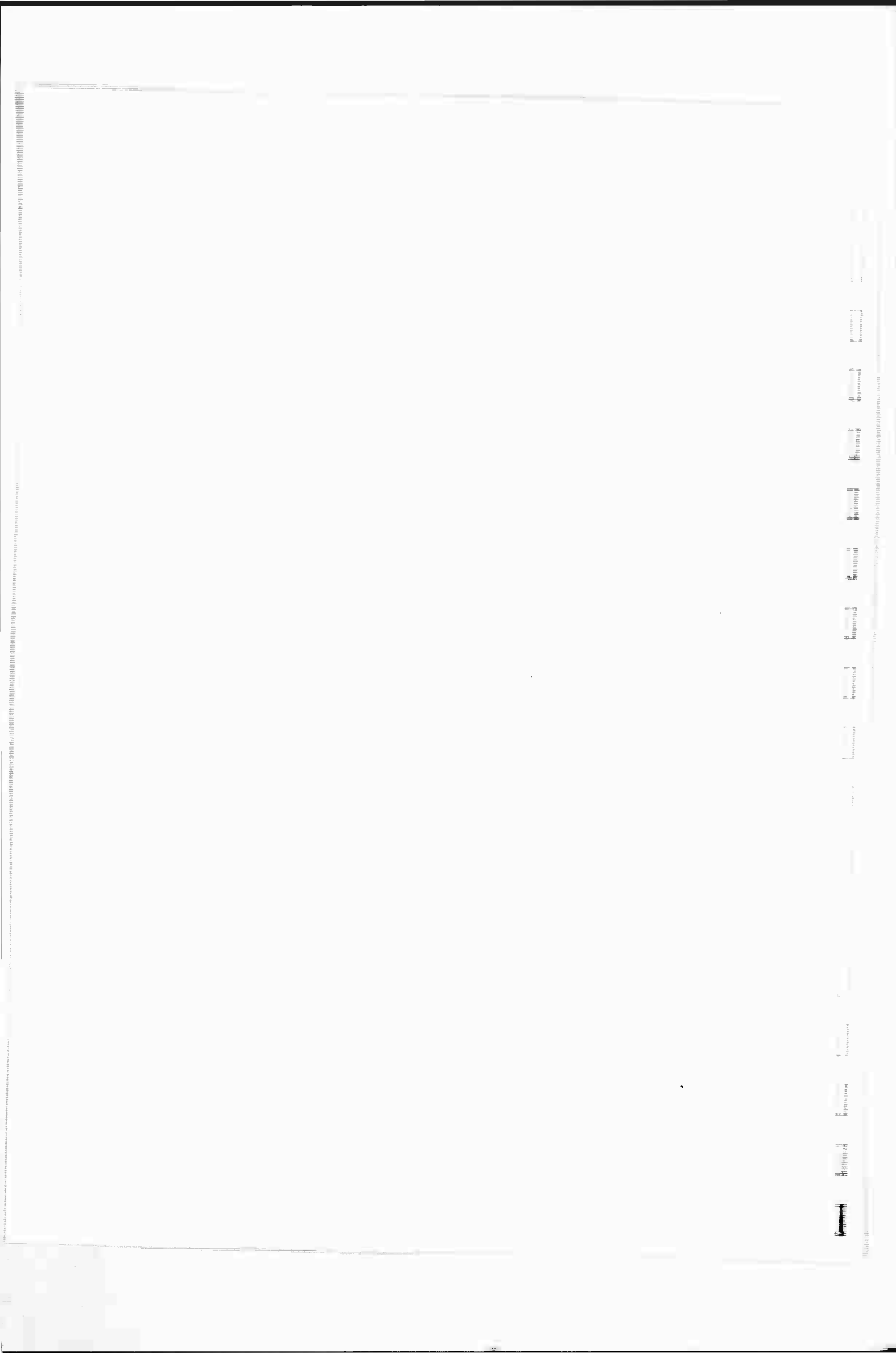
The last temperature distribution is shown in Figure 12. This "parabolic" temperature profile was observed in a nitrogen arc by Schmitz<sup>(12)</sup> and is most likely to occur in xenon. The flux distribution for 15 atmospheres is again less than that for 50 atmospheres and both flux profiles have maxima, which is characteristic of wall cooling effects.

These hypothetical temperature profiles have been used to illustrate radial flux computations for a one centimeter xenon arc. For operating conditions that could produce an isothermal arc with a thin conduction layer, or a "parabolic" arc, the value of the flux at  $r = 1.0$  cm gives the radiation of the arc to its surroundings.

For the arc temperature in Figure 8, the arc radiation is  $50 \times 10^4$  watts/cm<sup>2</sup> which is equivalent to  $1.59 \times 10^9$  Btu/hr ft<sup>2</sup>. Therefore, radiation from high pressure-high temperature self-absorbing arcs can be significant.

#### Acknowledgements

The author wishes to acknowledge the efficient computer programming by Mrs. E. Geil and Mr. B. Wang of the Computer Sciences Department, Westinghouse Research Laboratories.



## Appendix A

### Evaluation of $\vec{\nabla} \cdot \vec{F}$

From equation 14,

$$\vec{F}_\lambda = \int_{\omega=4\pi}^r \vec{r} I_\lambda f_1 d\omega \quad (A-1)$$

Taking the divergence of both sides of equation A-1

$$\vec{\nabla} \cdot \vec{F}_\lambda = \int_{\omega=4\pi}^r \vec{\nabla} \cdot (\vec{r} I_\lambda) f_1 d\omega \quad (A-2)$$

or

$$\vec{\nabla} \cdot \vec{F}_\lambda = \int_{\omega=4\pi}^{f_1 I_\lambda} \vec{\nabla} \cdot \vec{r} d\omega + \int_{\omega=4\pi}^{f_1 r} \vec{r} \cdot \vec{\nabla} I_\lambda d\omega \quad (A-3)$$

In cylindrical coordinates

$$\vec{\nabla} \cdot \vec{r} = \frac{1}{r} \quad (A-4)$$

Since the arc is symmetrical,

$$\vec{\nabla} I_\lambda = \vec{r} \frac{dI_\lambda}{dr} \quad (A-5)$$

and

A-2

$$\vec{r} \cdot \vec{\nabla} I_\lambda = \frac{dI_\lambda}{dr} \quad (A-6)$$

Now from equation 9,

$$\vec{\omega} = f_1 \vec{r} + f_2 \vec{\theta} + f_3 \vec{\tau} \quad (A-7)$$

and

$$\vec{\omega} \cdot \vec{\nabla} I_\lambda = \frac{dI_\lambda}{ds} = f_1 \frac{dI_\lambda}{dr} \quad (A-8)$$

Using equations A-4, A-6 and A-8, equation A-3 becomes

$$\vec{\nabla} \cdot \vec{F}_\lambda = \frac{1}{r} \int_{\omega=4\pi} f_1 I_\lambda d\omega + \int_{\omega=4\pi} \frac{dI_\lambda}{ds} d\omega \quad (A-9)$$

From equation 18,

$$\frac{dI_\lambda}{ds} = \kappa_\lambda B_\lambda - \kappa_\lambda I_\lambda \quad (A-10)$$

and from equation 14

$$F_\lambda(r) = \int_{\omega=4\pi} I_\lambda f_1 d\omega \quad (A-11)$$

Using equations A-10 and A-11, A-9 becomes

A-3

$$\vec{\nabla} \cdot \vec{F}_\lambda = 4\pi k_\lambda B_\lambda - k_\lambda \int_{\omega=4\pi}^{\infty} I_\lambda d\omega + \frac{F_\lambda}{r} \quad (A-12)$$

Since

$$F(r) = \int_0^\infty F_\lambda(r) dr \quad (A-13)$$

integrating equation A-12 with respect to  $\lambda$  from 0 to  $\infty$  yields

$$\vec{\nabla} \cdot \vec{F} = 4\pi \int_0^\infty k_\lambda B_\lambda d\lambda - \int_0^\infty k_\lambda \int_{\omega=4\pi}^{\infty} I_\lambda d\omega d\lambda + \frac{F(r)}{r} \quad (A-14)$$

also, since

$$\vec{\nabla} \cdot \vec{F} = \frac{dF}{dr} + \frac{F}{r} \quad (A-15)$$

it follows from equation A-14 that

$$\frac{dF}{dr} = 4\pi \int_0^\infty k_\lambda B_\lambda d\lambda - \int_0^\infty k_\lambda \int_{\omega=4\pi}^{\infty} I_\lambda d\omega d\lambda \quad (A-16)$$

### References

- 1) R. Viskanta, "Heat Transfer in Thermal Radiation Absorbing and Scattering Media," Dissertation, 1960, University Microfilms, Inc., Ann Arbor, Michigan.
- 2) S. deSoto, "The Radiation from an Axisymmetric, Real Gas System with a Non-Isothermal Temperature Distribution," A.I.Ch.E.-A.S.M.E. Heat Transfer Conference, August 1964.
- 3) D. H. Sampson, "Choice of an Appropriate Mean Absorption Coefficient for Use in the General Grey Gas Equations," General Electric Space Sciences Lab., Report R64SD77, November 1964.
- 4) B. W. Swanson, "Radiation Flux Approximation in a Non-Grey Cylindrical Arc," Westinghouse Research Report 65-8D8-GASDY-R1, 1965 (unpublished)
- 5) C. H. Church, R. G. Schlect, "Arc Discharge Radiation Sources for the Infrared - Some Simple Models," Westinghouse Scientific Paper 65-9C1-148-P3, 1965.
- 6) L. Biberman and G. Norman, "Plasma Radiation Due to Recombination and Bremsstrahlung Processes," J. Quant. Spect. Rad. Transfer 3, 221-245 (1963) General Atomics - San Diego Translation GA tr 4943.
- 7) L. M. Biberman, Yu. N. Toropkin, and K. N. Ulyanov, "The Theory of Multi-stage Ionization and Recombination," Sov. Phys. - Tech Phys. 7, 605-609 (1963).
- 8) V. V. Yankov, "On the Distribution of Energy in the Continuous Absorption Spectrum of Xenon," Optics and Spectroscopy 14, 14-17 (1963).
- 9) K. Drellishak, C. Knopp, and A. B. Cambel, "Partition Functions and Thermodynamic Properties of Argon Plasma," Phys. Fluids 6, 1280-1288 (1963).
- 10) K. S. Drellishak, C. F. Knopp, and A. B. Cambel, "Partition Functions and Thermodynamic Properties of Argon Plasma," AEDC-TDR-146, Northwestern University, Evanston, Illinois, August 1963.
- 11) C. H. Church and R. G. Schlect, "Arc Discharge Sources," Semi-Annual Technical Report in Contract N0NR 4647(00), Westinghouse Research Laboratories, Pittsburgh, Pennsylvania, May 15, 1965.
- 12) G. Schmitz, "The Profile of the Arc Column," Aeronautical Research Laboratories Report ARL 62-401, August 1962.

Curve 575238-A

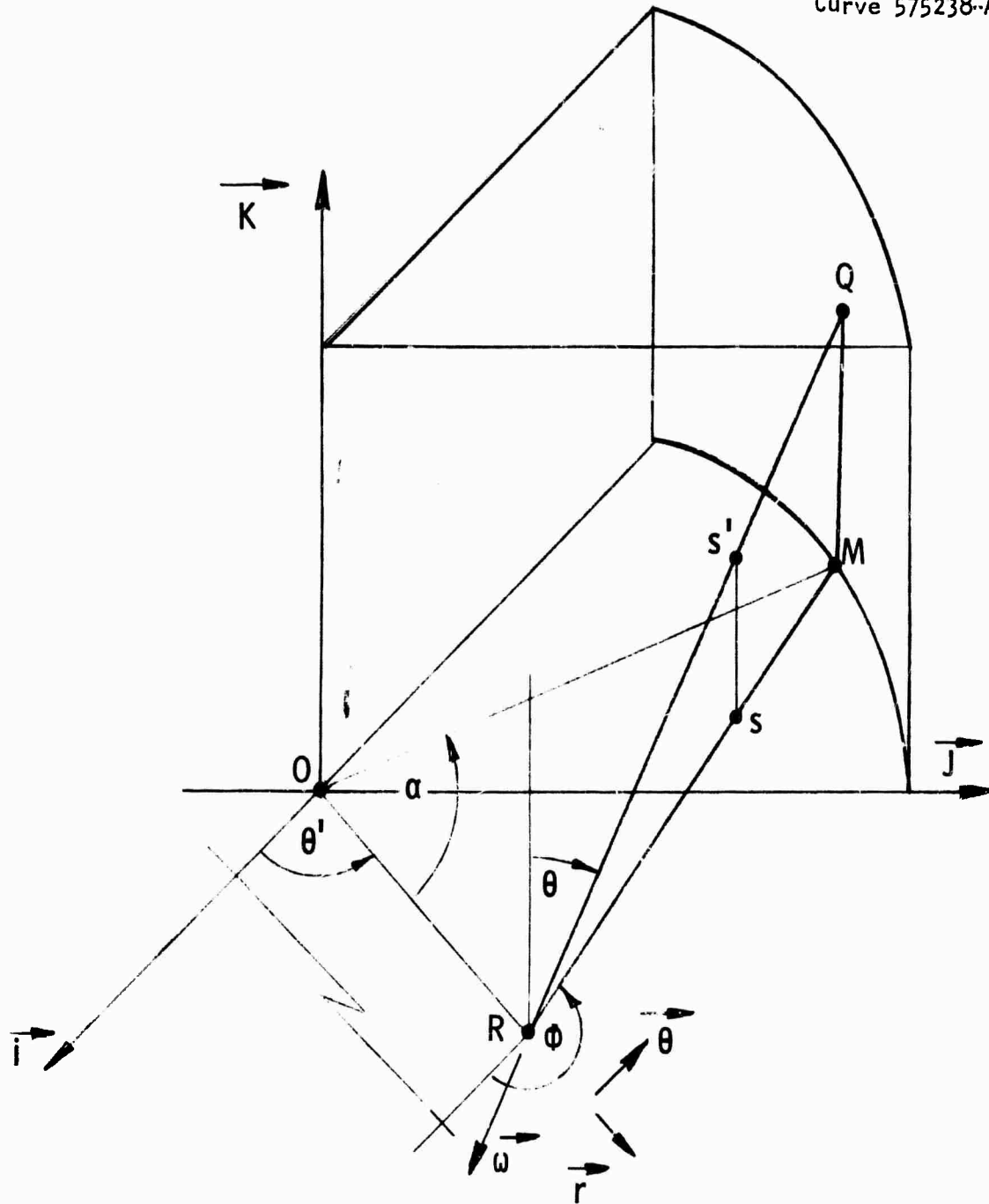


Fig. 1—Arc geometry

Curve 575240-A

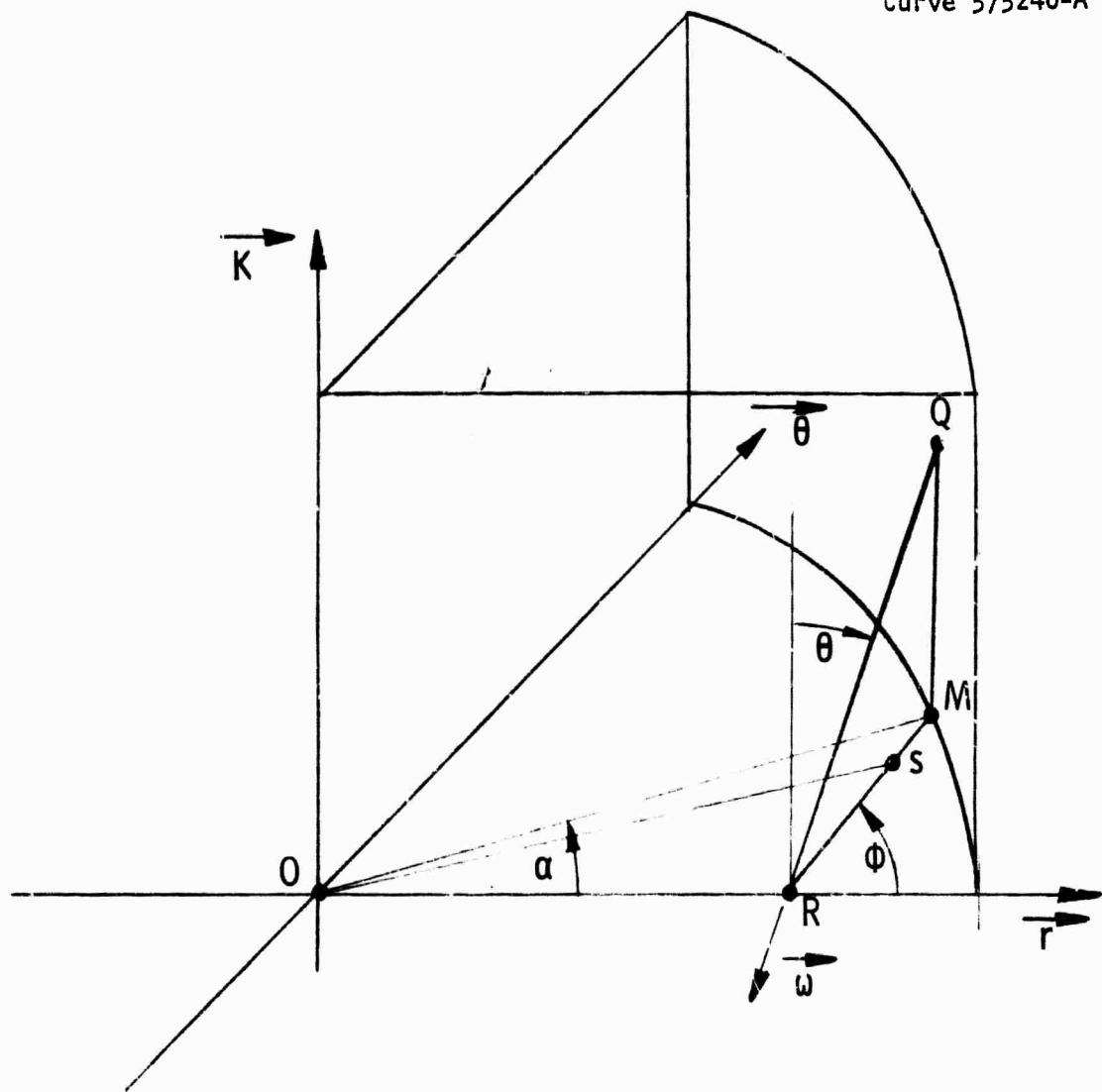


Fig. 2—Arc geometry with  $\theta' = 0$

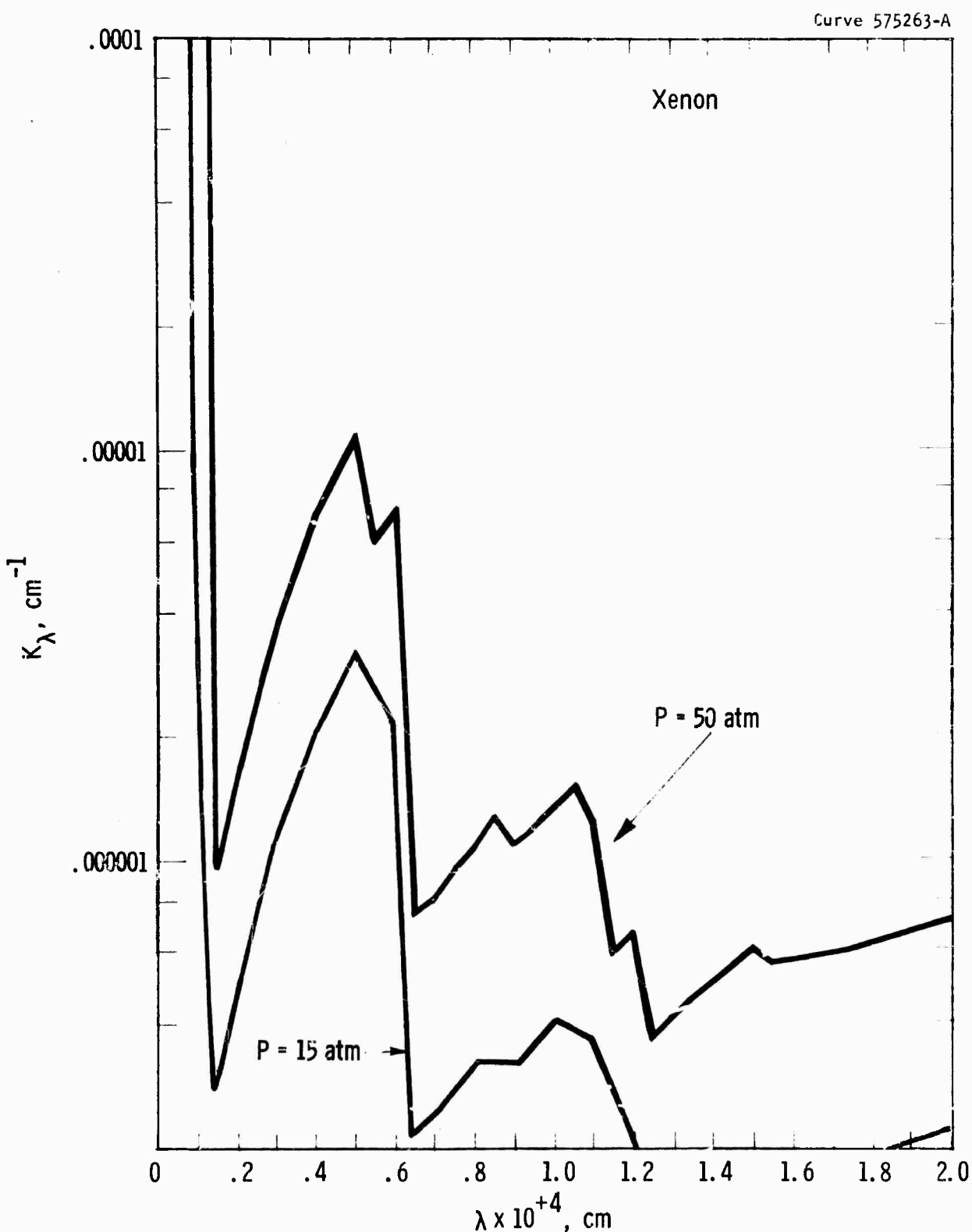


Fig. 3—Absorption coefficient vs wavelength:  $T = 5000^\circ\text{K}$

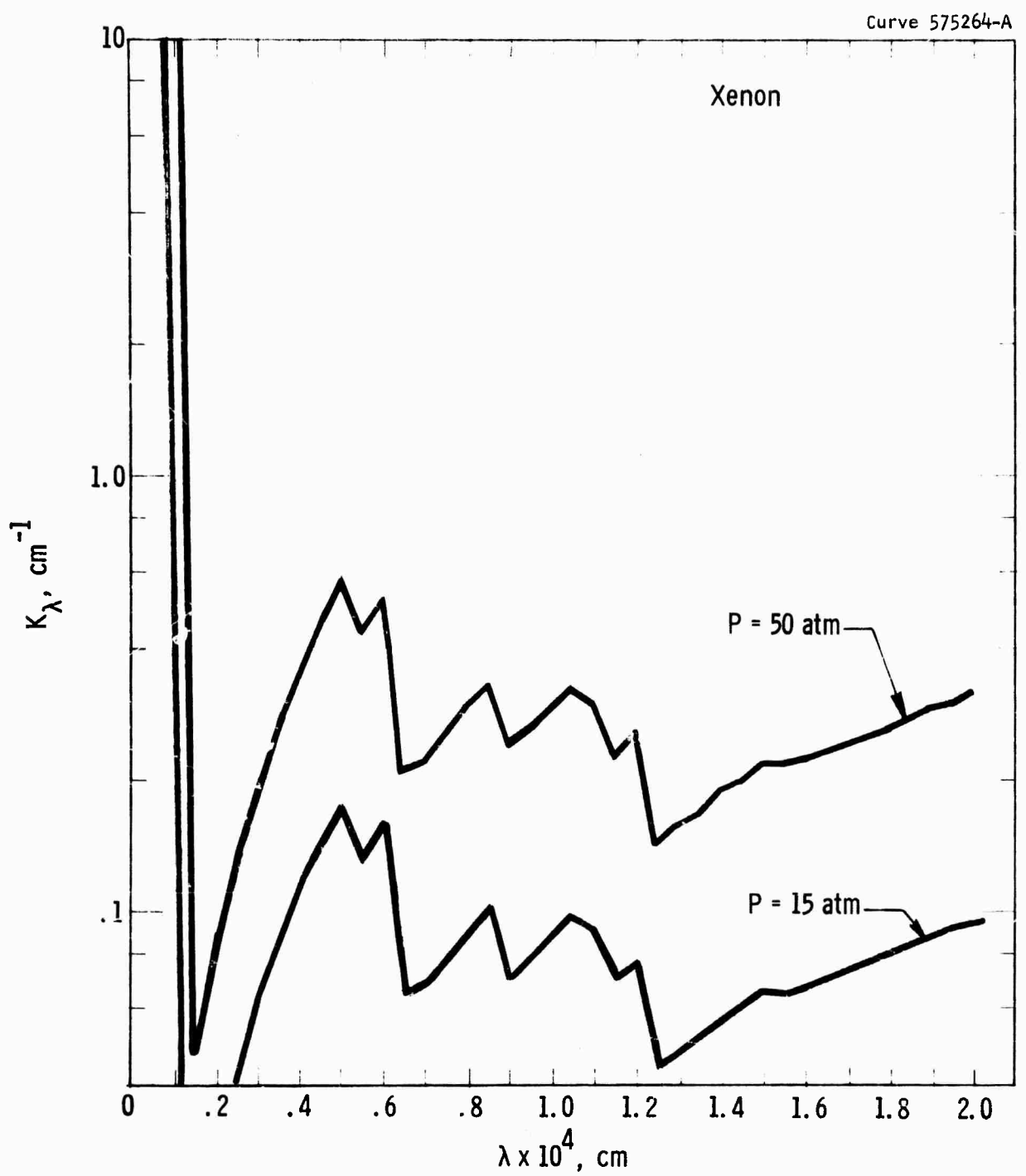


Fig. 4—Absorption coefficient vs wavelength:  $T = 10000^\circ\text{K}$

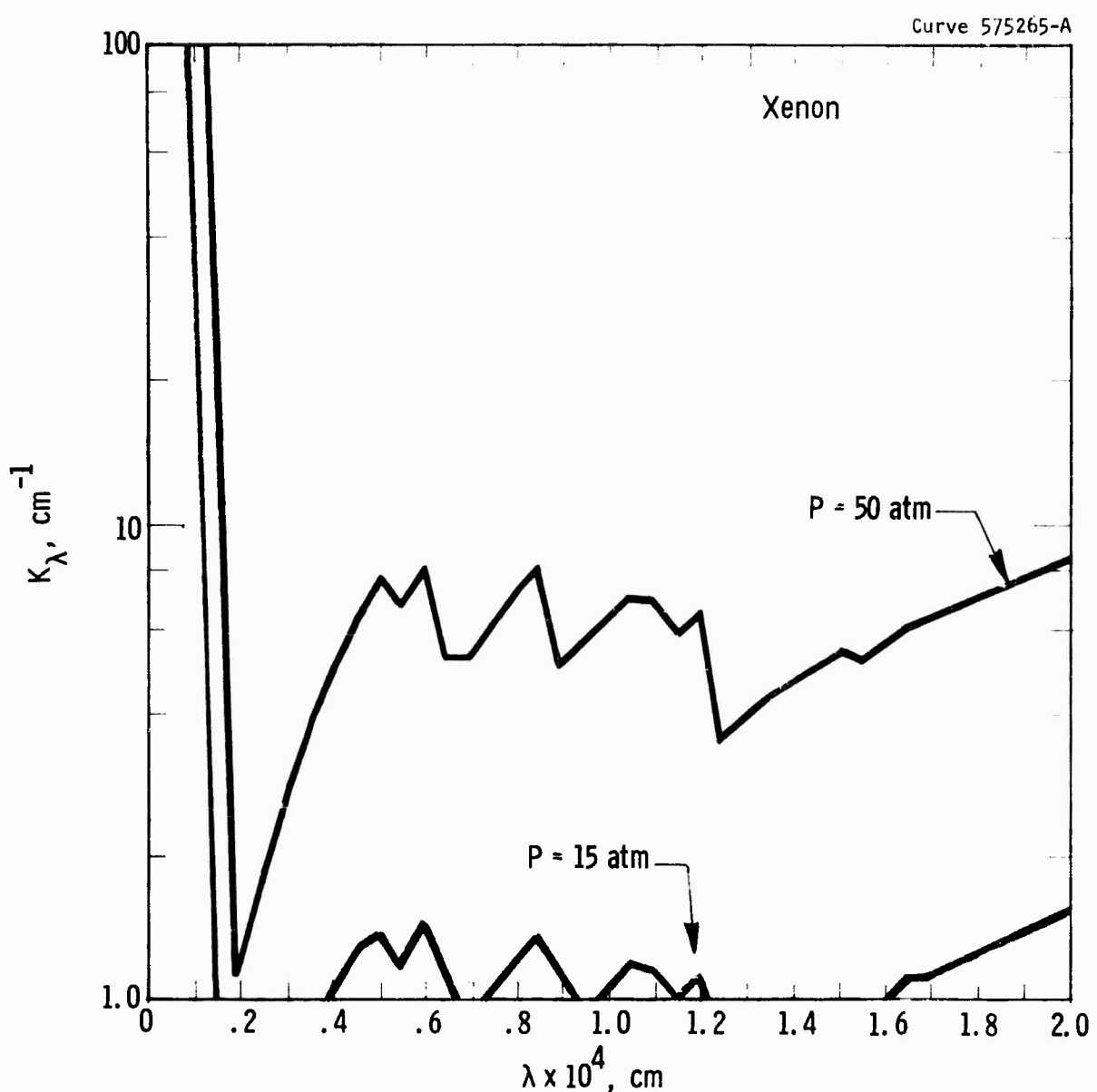


Fig. 5—Absorption coefficient vs wavelength:  $T = 15000^\circ\text{K}$

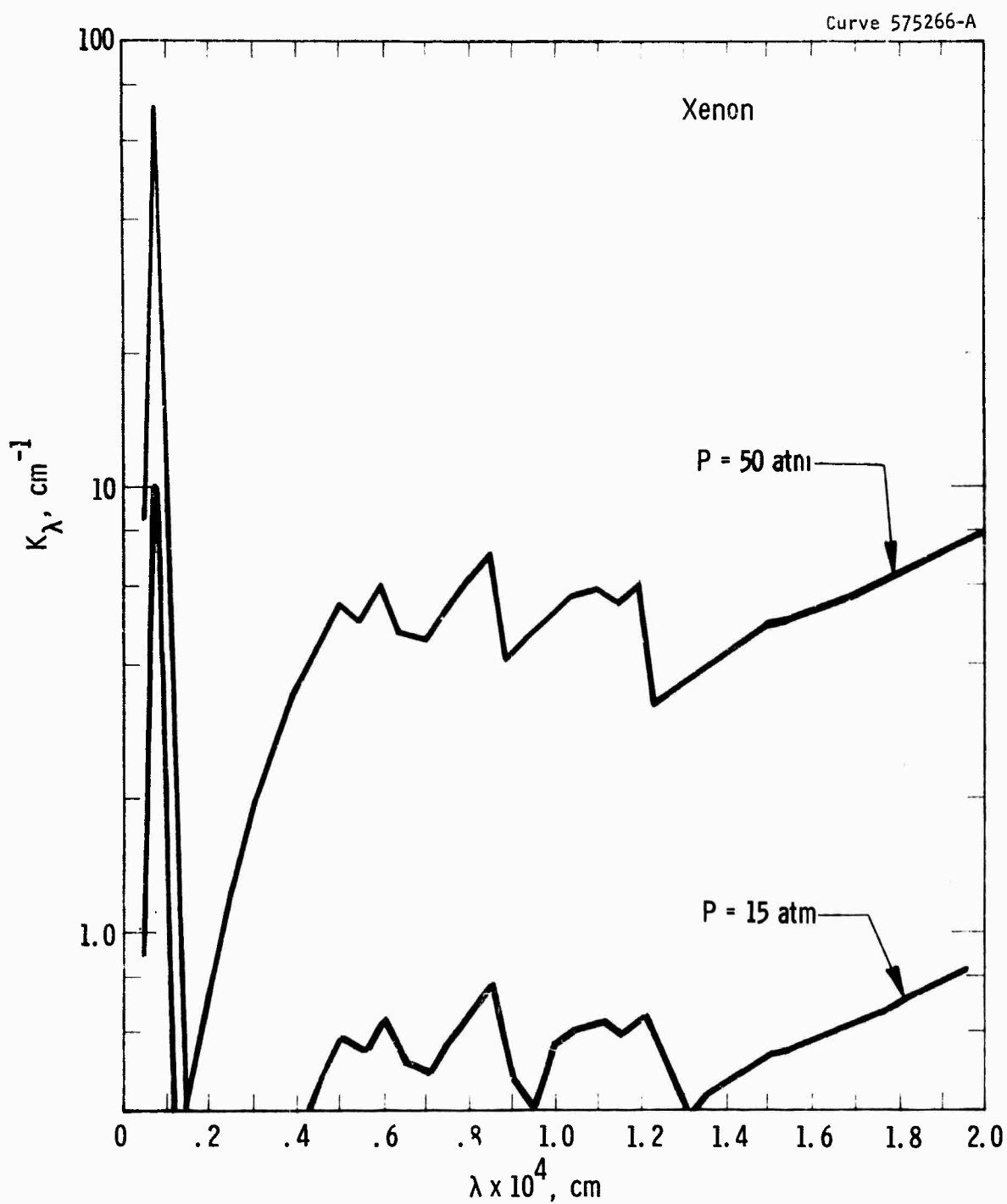


Fig. 6—Absorption coefficient vs wavelength:  $T = 20000^\circ\text{K}$

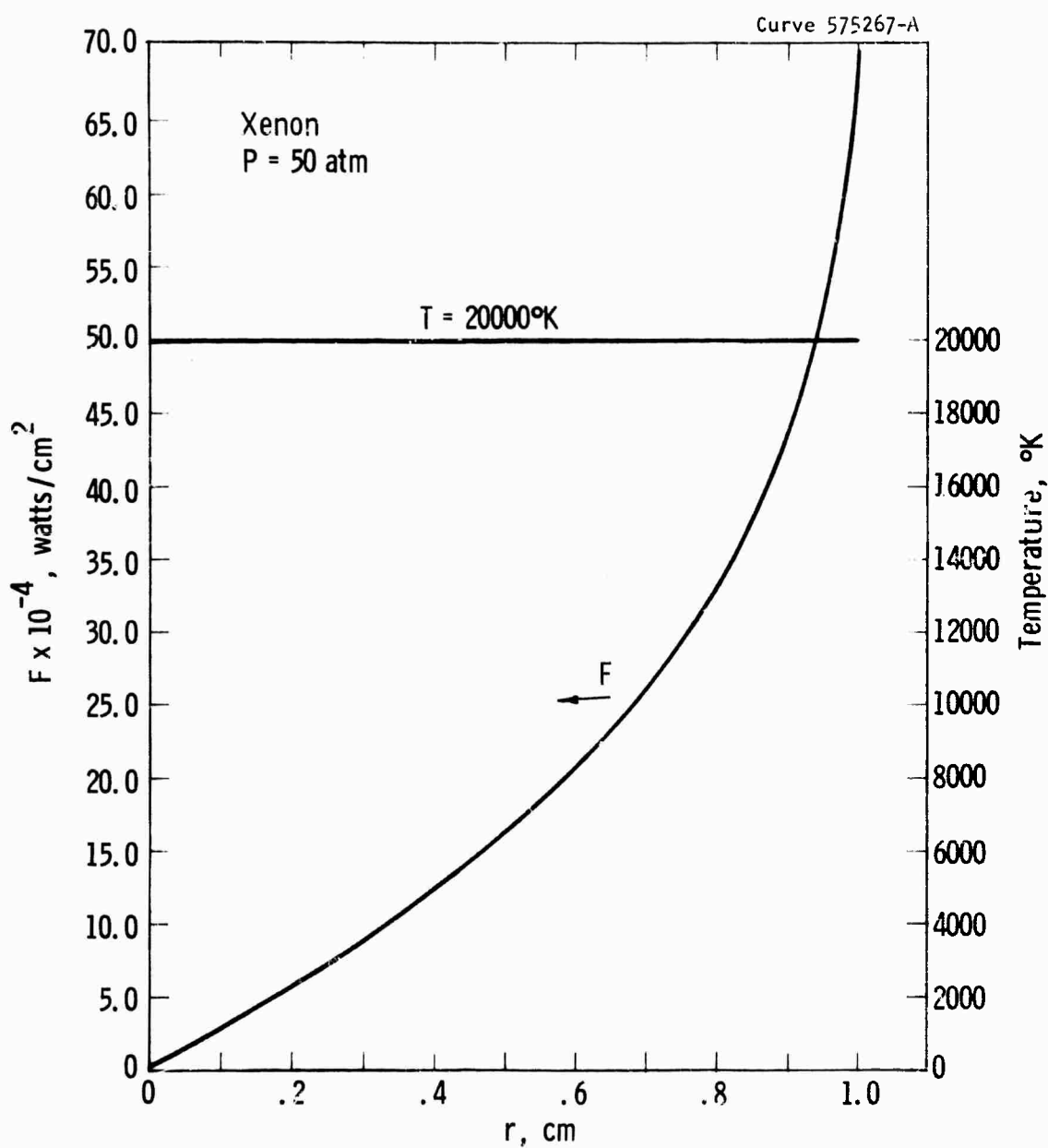


Fig. 7—Flux vs  $r$  for an isothermal arc

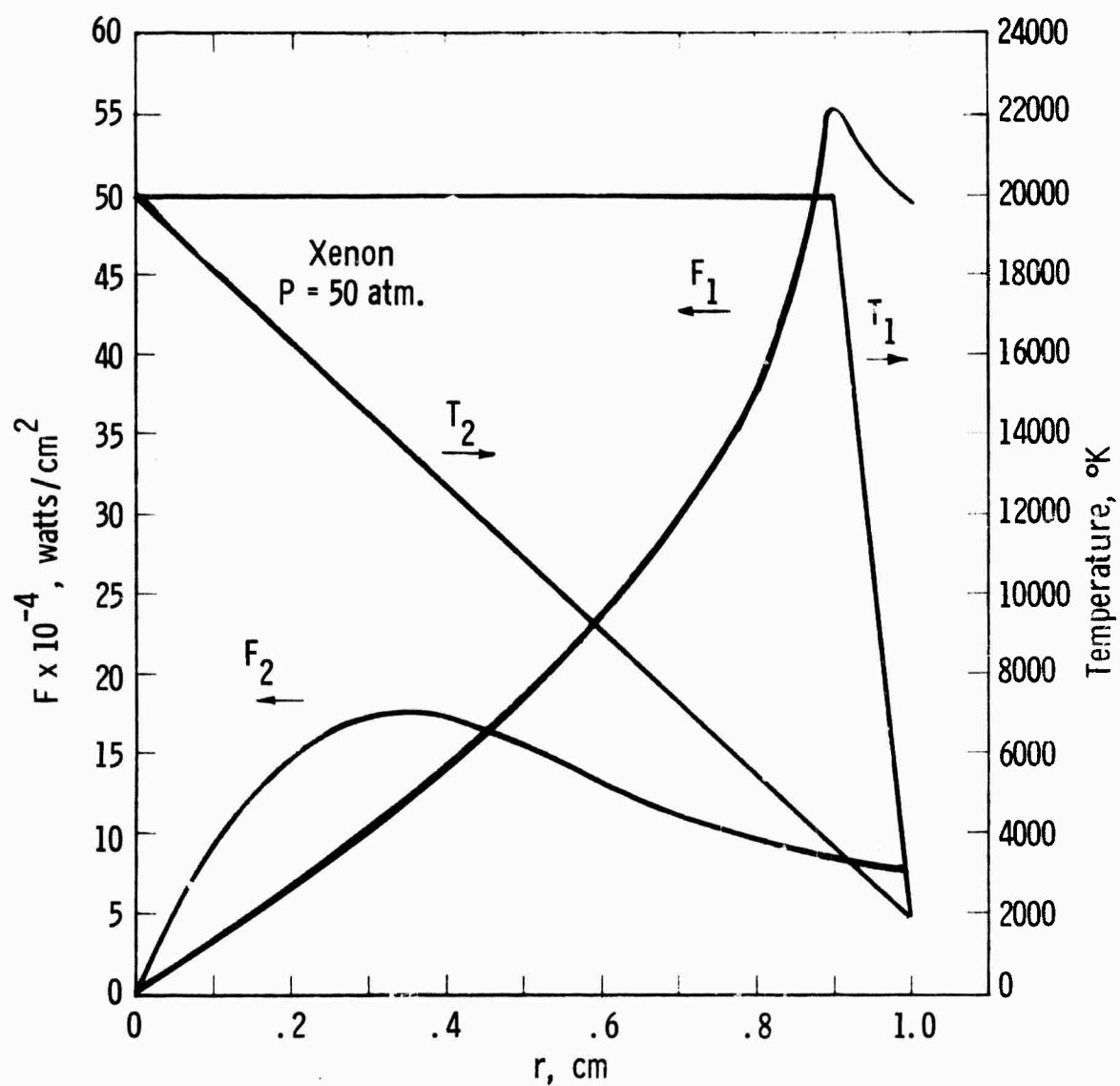


Fig. 8—Arc flux and temperature vs  $r$

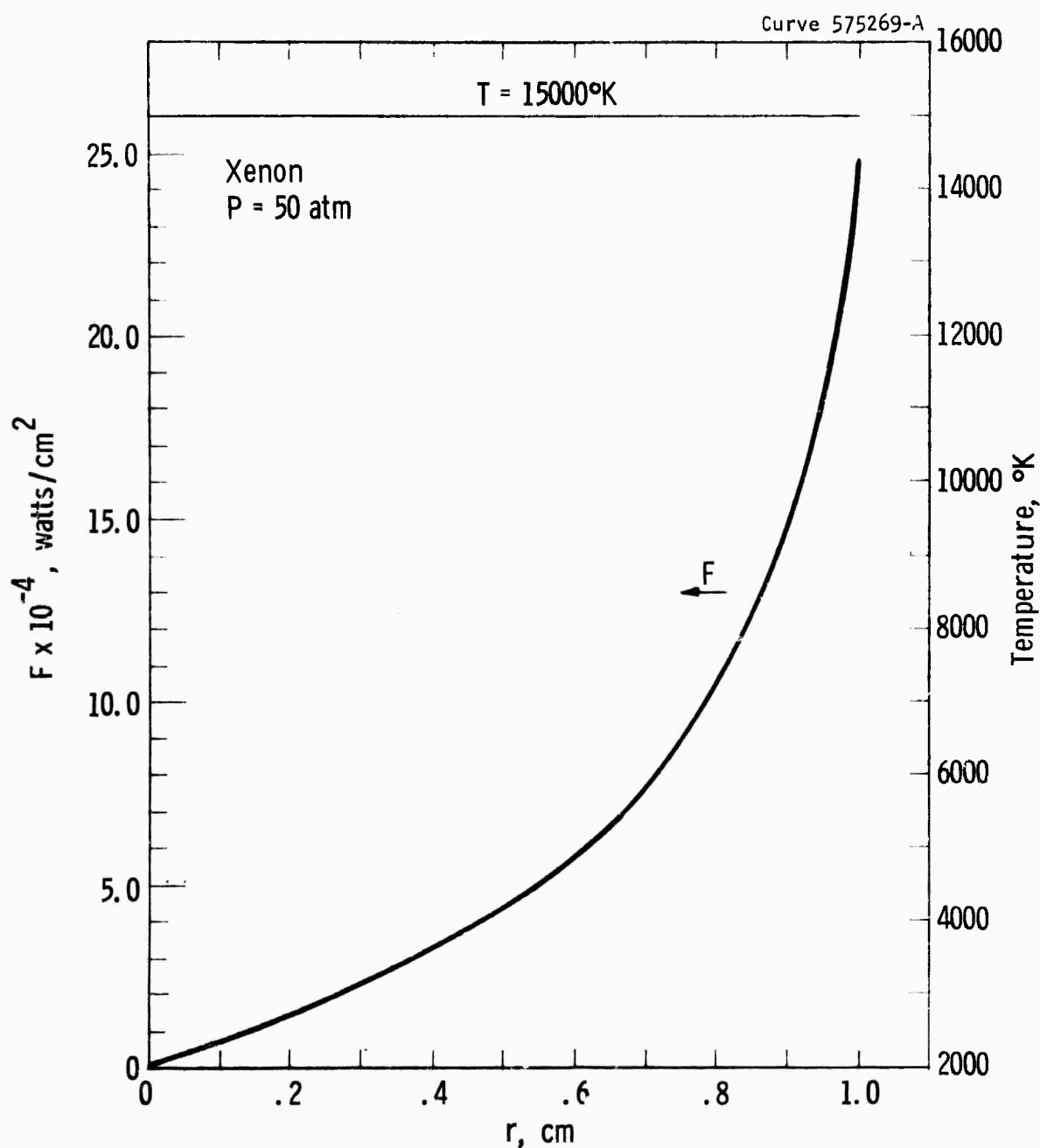


Fig. 9—Flux vs r for an isothermal arc

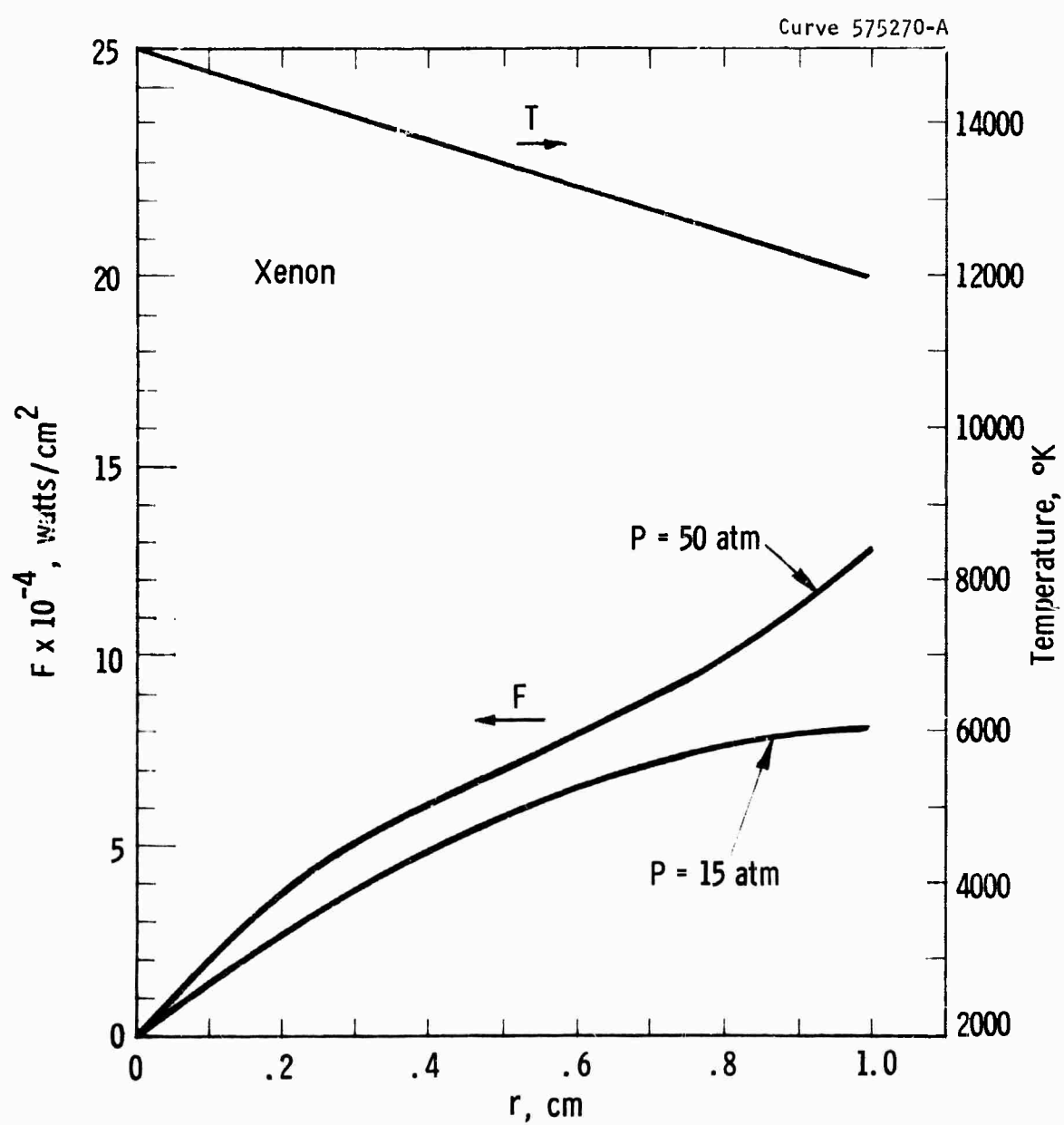


Fig. 10—Arc flux and temperature vs  $r$

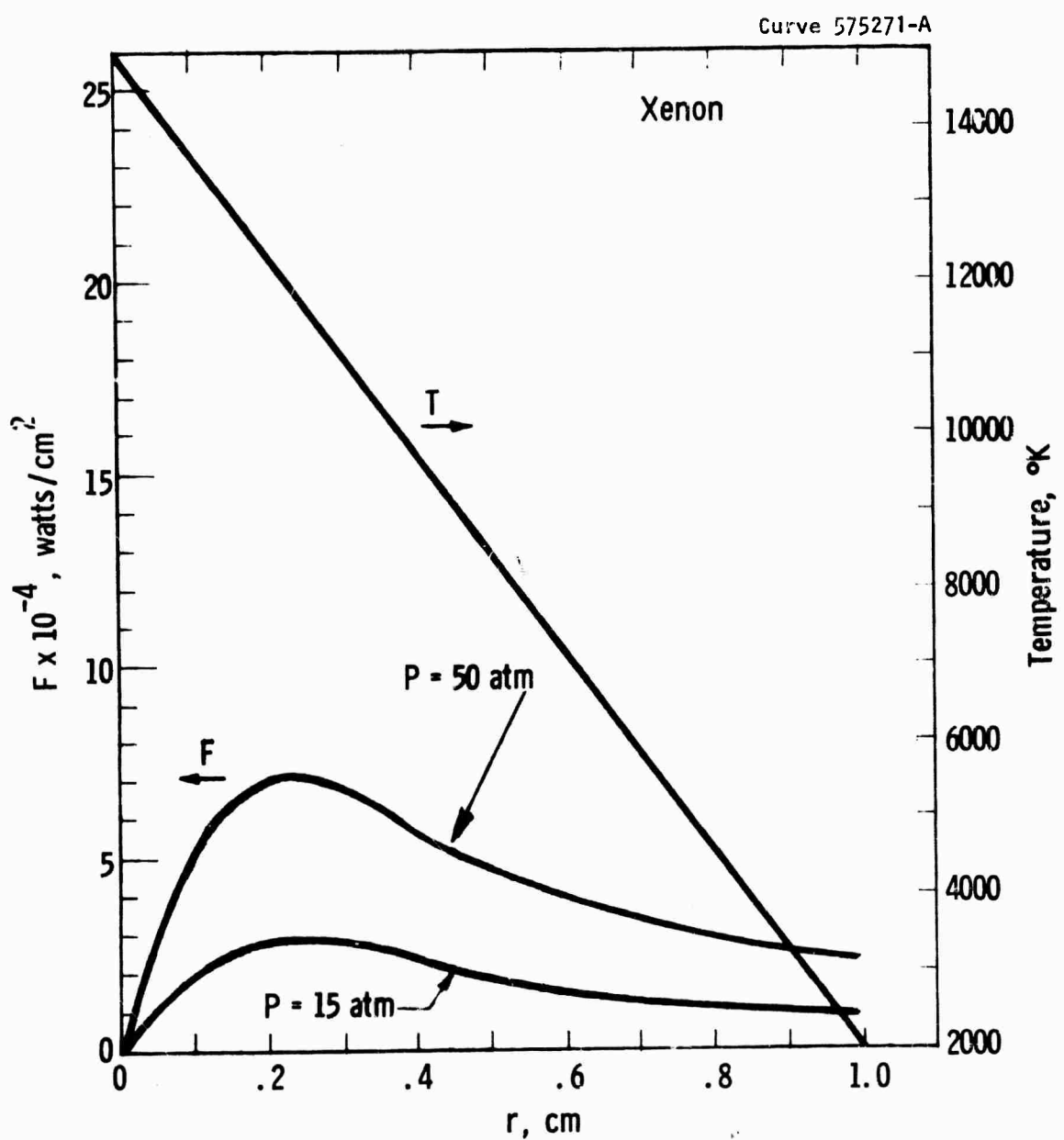


Fig. 11—Arc flux and temperature vs  $r$

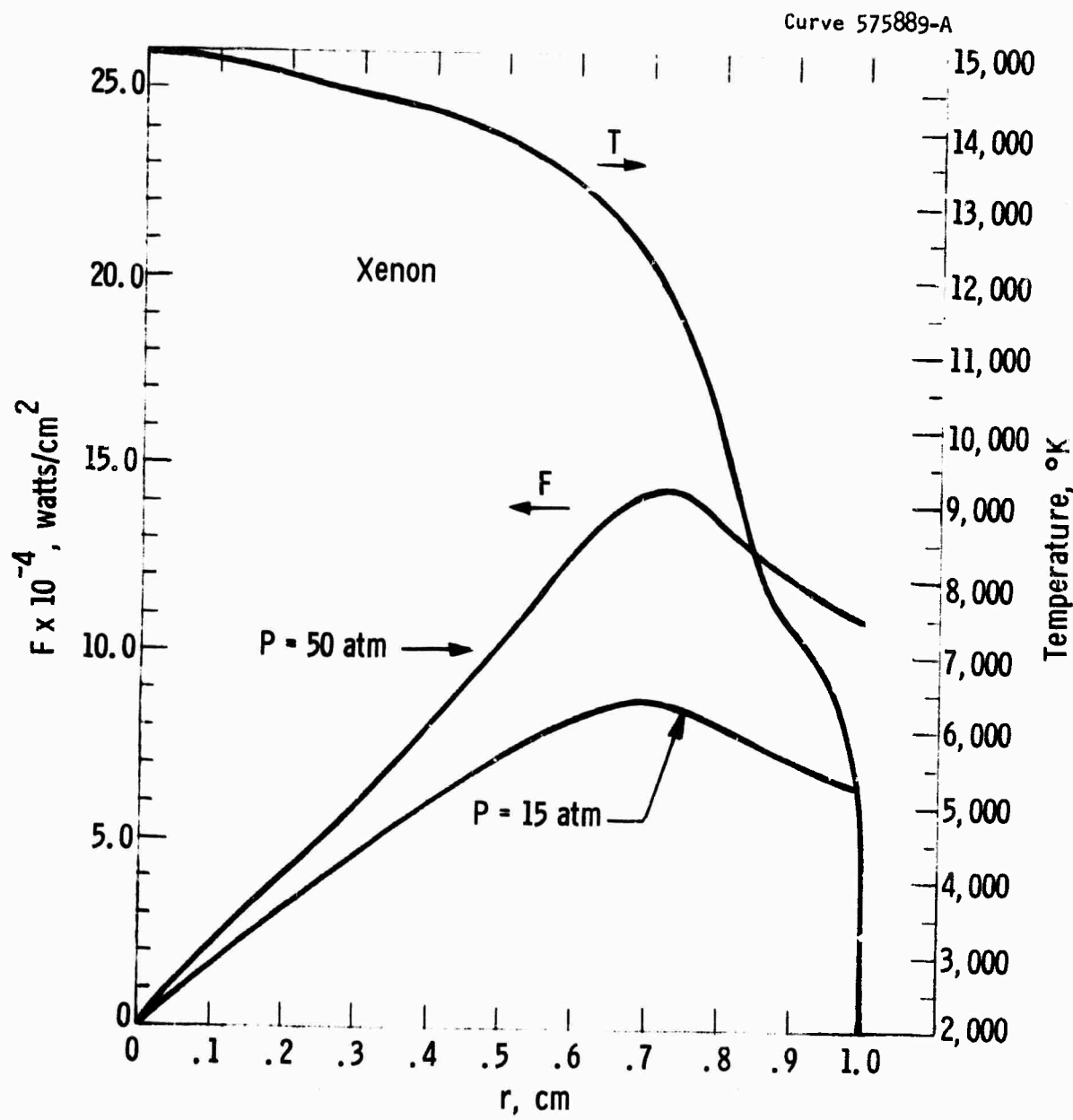


Fig. 12—Arc flux and temperature vs  $r$

**APPENDIX B**

**TRANSITION PROBABILITIES OF XENON I**

**by**

**E. G. F. Arnott**

## TRANSITION PROBABILITIES OF XENON I

by

E. G. F. Arnott

An investigation was made of the possibility of using the Bates-Damgaard<sup>(1)</sup> method for calculating transition probabilities and oscillator strengths for some of the spectral lines of the rare gases, particularly Xenon. The Bates-Damgaard approximation consists of assuming a Coulomb field for the atom and has given good agreement with experimental results for the simpler systems and for some more complicated systems.

The present work assumes that the approximation may be valid for the rare gases where it is thought that L-S coupling still occurs for some levels. The levels for which this might be expected are given in Moore's<sup>(2)</sup> tables where such designations are said to be significant for Ne, Ar and Kr but less so for Xe.

The oscillator strength is given by

$$f_{12} = \frac{304 S}{g_1 \lambda}$$

where  $g_1$  is the statistical weight of the lower level,  $\lambda$  is the wavelength in Angstrom units and the line strength

$$S = S(M) S(L) \sigma^2$$

where  $S(M)$  is a factor depending on the particular multiplet of the transition array,  $S(L)$  is a factor depending on the particular line. These values can be obtained from tables published by Goldberg<sup>(3)</sup> and White and Eliason<sup>(4)</sup> respectively.  $\sigma$  is the product of two quantities taken from Bates' and

Damgaard's (1) tables divided by C the excess charge in the nucleus when the active electron is removed. i.e., C=1 for a neutral atom.

$$\sigma = \frac{1}{C} F(n_{\ell}^*, \ell) I(n_{\ell-1}^*, n_{\ell}^*, \ell)$$

where  $n^* = C/E^{1/2}$ , where E is an energy parameter and  $\ell$  is the azimuthal quantum number. A sample calculation is given in the Appendix.

Calculations of  $f_{12}$  for the lines of A and Kr given by Moore as having LS coupling were made and the results are shown in Tables I and II compared with the experimental values of Pery-Thorne and Chamberlain<sup>(5)</sup> for the same spectral lines.

Table I

Absolute  $f_{12}$  Values for Argon

<u>Line (Å)</u>	<u>Transition (Paschen)</u>	<u><math>f(\text{exp})</math> P-T</u>	<u><math>f(\text{calc})</math> B-D</u>
6965	s <sub>5</sub> - p <sub>2</sub>	0.04	0.09
7384	s <sub>4</sub> - p <sub>3</sub>	0.12	0.14
7515	s <sub>4</sub> - p <sub>5</sub>	0.15	0.12
8015	s <sub>5</sub> - p <sub>8</sub>	0.09	0.08
8104	s <sub>4</sub> - p <sub>7</sub>	0.18	0.14
8115	s <sub>5</sub> - p <sub>9</sub>	0.27	0.45
8425	s <sub>5</sub> - p <sub>8</sub>	0.19	0.40

Table II

Absolute  $f_{12}$  Values for Krypton

<u>Line (Å)</u>	<u>Transition (Paschen)</u>	<u><math>f(\text{exp})</math> P-T</u>	<u><math>f(\text{calc})</math> B-D</u>
7601	$s_5 - p_6$	0.14	0.28
7695	$s_5 - p_7$	~0.03	0.006
8104	$s_5 - p_8$	0.07	0.085
8113	$s_5 - p_9$	0.23	0.48
8780	$s_4 - p_8$	0.44	0.42
8929	$s_5 - p_{10}$	0.20	0.104

The correspondence between calculated and observed values is remarkably good for argon and also for krypton except for the 7695A line. These results were sufficiently encouraging to suggest that similar calculations be made for Xe for the strong lines which might be expected to have L-S coupling. This was done for 15 of the strongest lines given in the table by Crosswhite and Dieke<sup>(6)</sup>.

As a check on the results three sets of three lines each were chosen:

$$\begin{array}{lll} 1s_4 - 2p_5 & 1s_5 - 2p_8 & 1s_4 - 2p_9 \\ 1s_4 - 3p_5 & 1s_5 - 3p_8 & 1s_4 - 3p_9 \\ 1s_4 - 4p_5 & 1s_5 - 4p_8 & 1s_4 - 4p_9 \end{array}$$

Following the method of Wilkerson<sup>(7)</sup> the quantity  $\log \frac{I \lambda^3}{g_1 f_{12}}$  where I is the intensity of the line was plotted against  $E_2$ , the energy of the upper level. A straight line should result whose slope will give the excitation temperature as given by

$$T^{\circ}\text{K} = 5041 \left( E_2^n - E_2^m \right) / \log_{10} \left( \frac{I \lambda^3}{g_1 f_{12}} \right)_m - \log_{10} \left( \frac{I \lambda^3}{g_1 f_{12}} \right)_n$$

The results are shown in the Fig. 1 for a 16 mm pressure microwave discharge. The  $1s_4 - np_9$  series does not seem to fall on the same line as the others and gives a slightly lower temperature. However, a temperature of  $2850^{\circ}\text{K}$  was chosen and the values of  $f_{12}$  were calculated from Wilkerson's expression

$$f_{12} = f_{12}^{\circ} \left( \frac{I \lambda^3}{g_1} \right) / \left( \frac{I \lambda^3}{g_1} \right) \leftrightarrow e^{-\frac{E_2^{\circ} - E_2}{kT}}$$

A value of 0.117 for  $f_{12}^{\circ}$  was chosen from the Bates-Damgaard calculations as a reasonable value for the strong line at 8280A.

Table III shows the values obtained in this way for 24 strong Xe lines and also gives the values calculated from the Bates-Damgaard approximation.

A more detailed study is necessary to determine the reliability of the values particularly where there are large differences between the two methods.

Curve 575808-A

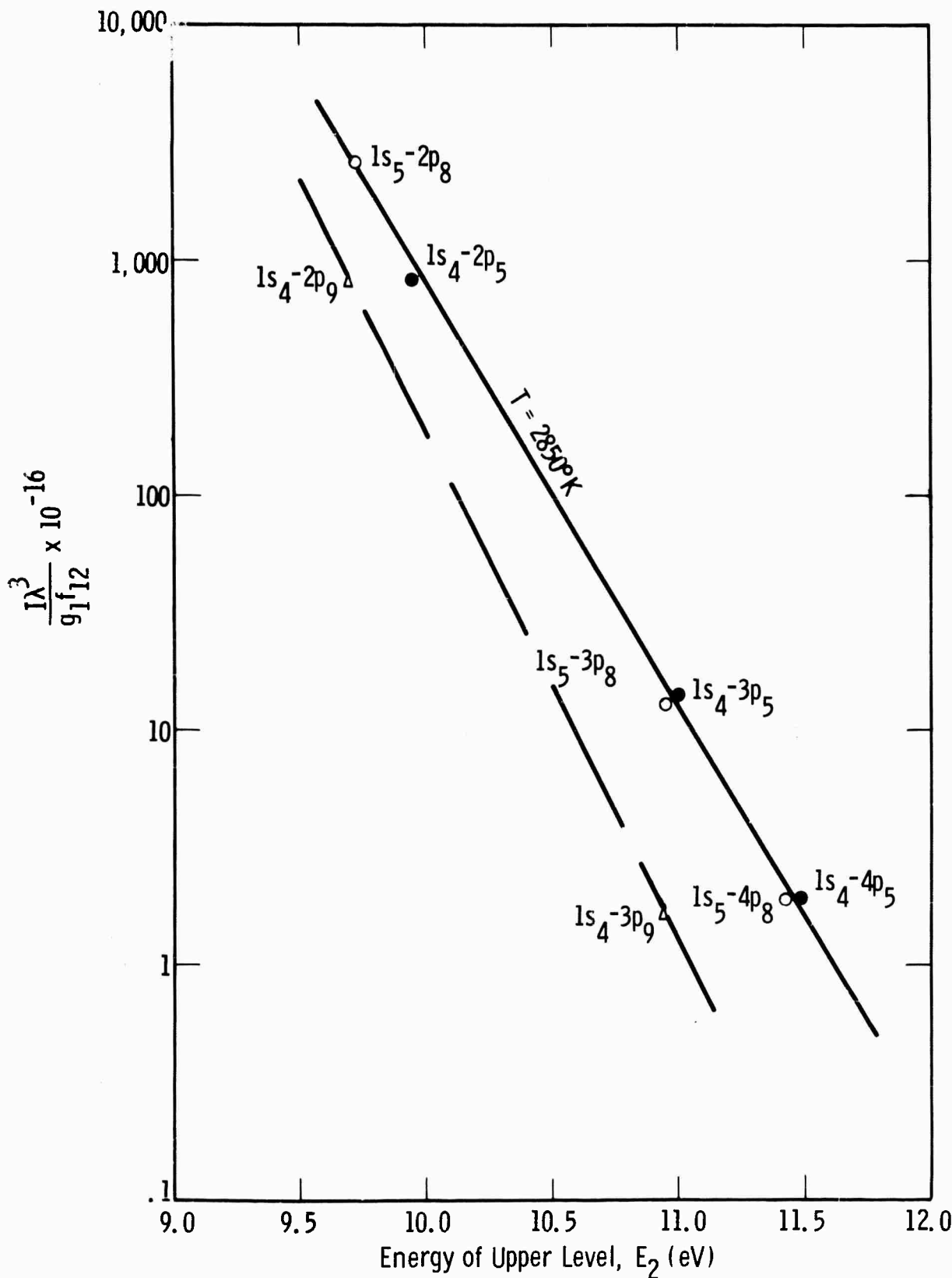


Fig. -1

Table III  
Absolute  $f_{12}$  Values for Xenon

<u>Line A</u>	<u>Transition</u>	<u><math>f_{12}(2850^{\circ}\text{K})</math></u>	<u><math>f(\text{calc})</math></u> <u>B-D</u>
10838	$1s_4 - 2p_{10}$		.106
9923	$1s_4 - 2p_9$	.152	.434
9800	$1s_5 - 2p_{10}$	.083	.110
9163	$1s_4 - 2p_7$	.145	.140
9045	$1s_5 - 2p_9$	.0034	.086
8952	$1s_4 - 2p_6$	.092	
8819	$1s_5 - 2p_8$	.074	.054
8409	$1s_5 - 2p_7$	.008	.006
8347	$1s_2 - 3p_3$	.151	
8280	$1s_4 - 2p_5$	.117	.117
8267	$1s_2 - 3p_2$	.222	
8232	$1s_5 - 2p_6$	.062	
7641	$1s_3 - 3p_2$	.380	
6318	$2p_8 - 6d_4^1$	.035	.140
4932	$1s_4 - 3p_9$	.005	.040
4917	$1s_4 - 3p_4$	.008	
4807	$1s_4 - 3p_5$	.0076	.006
4671	$1s_5 - 3p_8$	.016	.014
4624	$1s_5 - 3p_6$	.0125	
4525	$1s_5 - 3p_3$	.002	
4501	$1s_5 - 3p_2$	.006	
4079	$1s_4 - 4p_5$	.0034	.0032
3968	$1s_5 - 4p_8$	.0038	.0036
3693	$1s_5 - 5p_8$		.0002

Consider the transition  $1s_4 - 2p_5$  in Xe I. From Bacher and Goudsmit<sup>(8)</sup> the term values are  $1s_4$  29789.34

$$2p_5 \quad 17715.59$$

Dividing by 109,678 to express these in Rydbergs gives values of E of .2715 and .1615 respectively and therefore values of  $C_E^{1/2}$  or  $n^*$  for the two levels.

$$n_{\ell=1}^* = 1.92$$

$$n_{\ell}^* = 2.49$$

since C=1 for neutral Xenon. Therefore

$$n_{\ell=1}^* - n_{\ell}^* = -0.57$$

From the tables of Bates and Damgaard with  $\ell=1$

$$F(2.49, 1) = 4.9$$

$$I(-.57, 2.49, 1) = 0.65$$

From these values

$$\sigma^2 = (F I / C)^2 = 10.2$$

Goldberg's and White and Eliason's tables are reproduced in convenient form in Aller's book<sup>(9)</sup>.

From Aller's Table A-2 for a ps to pp transition

$$S(M) = 9$$

and from Table A-1 for a spin of 1

$$\log \frac{F}{S} = 9.95$$

$$S(L) = \frac{S}{\Sigma S} = 0.112$$

So that  $S = S(M)S(L) = 9 \times 0.112 \times 10.2 = 10.3$

The oscillator strength

$$f_{12} = \frac{304 s}{g_1 \lambda} = .117 \text{ for } \lambda = 8280\text{\AA} \text{ and } g_1 = 3.$$

REFERENCES

1. D. R. Bates and Agnete Damgaard, Philo. Trans. Roy. Soc. (London), Vol. 242A, 101 (1949).
2. C. E. Moore, "Atomic Energy Levels", Circular of the National Bureau of Standards 467, Vol. I, II and III (1949)(1952)(1958).
3. L. Goldberg, Astrophys. J. 82, 1 (1935).  
L. Goldberg, Astrophys. J. 84, 11 (1936).
4. H. E. White and A. Y. Eliason, Phys. Rev. 44, 753 (1933).
5. A. Fery-Thorne and J. E. Chamberlain, Proc. Phys. Soc. 82, 133 (1963).
6. American Institute of Physics Handbook, 2nd Edition, McGraw-Hill Book Co., New York (1963).
7. T. Wilkerson, Air Force Office of Scientific Research, Air Research and Development Command, Contract No. AF49(638)-439, Washington, D.C.
8. R. Bacher and S. Goudsmit, Atomic Energy States, McGraw-Hill Book Co., New York (1932).
9. L. H. Aller, The Atmospheres of the Sun and Stars, Ronald (1963).

**APPENDIX C**

**COMPUTER PROGRAMS USED IN THIS WORK**

**by**

**Esther Geil**

COMPUTER PROGRAMS USED IN THIS WORK

by

Esther Geil

The five computer programs written in ALGOL for the Burroughs B-5500 DISK computer used in this work are given in this appendix. The first four programs are preceded by a symbol table and followed by a sample calculation printout. The fifth program whose output is just the radiative flux does not have a sample calculation printout. The five programs are as follows: (The named references are at the end of this appendix)

- a) SIMPLIFIED - a calculation for the electron density and spectral absorptivity given the heavy particle density and temperature, based upon the Raizer-Penner model<sup>(1-4)</sup> for the plasma.
- b) DOUBLE - the calculation of the particle densities and then the spectral absorptivity and emissivity using methods similar to Drelliskak<sup>(5)</sup> et al. and Biberman and Norman<sup>(6)</sup>. The program is in two parts, particle density calculation, & spectral absorptivity calculation with separate symbol tables.
- c) DICSLAB - calculation of the spectral radiance, radiant emittance, and then the balancing current density using the particle densities and spectral absorptivities from DOUBLE and the electrical conductivity calculated according to Spitzer<sup>(7,8)</sup> et al. DICSLAB is the calculation for a plane parallel slab of homogeneous temperature and pressure.

- d) DICKCYL is a calculation of the same quantities in (c) for an infinite cylinder of homogeneous temperature and pressure.
- e) Radiative Flux throughout a non-isothermal non-grey cylindrical arc. This program is for the calculation of the radiative flux (radiant emittance) throughout a cylindrical arc of arbitrary spectral absorptivity and radial temperature distribution (the latter must be symmetrical about the center axis of the cylinder in this program). It uses the particle densities and spectral absorptivities calculated by program "DOUBLE".

Program a

Symbol Table for Raizer-Penner Model

Simplified Model for Electron Density and Spectral Absorptivity of Plasma

D = thickness of plasma

I[m] = ionization potential for mth degree of ionization from Penner's model

HNU(i) = hν = the energy corresponding to the ith frequency being used.

N = the heavy particle (atom and ion) density of the plasma

THETA = temperature in eV

M =  $\bar{m}$  = average number of electrons per atom

$$IM2 = I(\bar{m} - \frac{1}{2})$$

$$IM2P = I(\bar{m} + \frac{1}{2})$$

KAPPAPRIME =  $\kappa'$  = absorptivity including stimulated emission

Note: Total number of particles, temperature in degrees K, and pressure in atmospheres are calculated in the write statement following the computation of KAPPAPRIME.

Wavelength, tau = KAPPAPRIME x D,  $1 - e^{-\kappa' d}$ ,  $B_\nu$  and  $I_\nu$  for each frequency are calculated within the next write statement.

1712612A THURSDAY, OCTOBER 21, 1965

HRL ALGOL VERSION OF 9/1/65

BEGIN

SC 11 01C

START OF SEGMENT \*\*\*\*\* 0002

COMMENT GEIL, FOR CHURCH, 67A, FD0437, SIMPLIFIED PROBLEMS

SC 21 01C

FILE IN READER(2+10); FILE OUT GEIL 6(2+15);

SC 21 01C

COMMENT DAYTIME

/ SL 21 71C

TO OBTAIN LISTING MERGE IN BLANK CARD WITH SEQUENCE NUMBER 0000000301

S SL 21 71C

99999999 SC 21 71C

REAL A,K,N,THETA,COUNT,4,IM2,TEMP,E,MH,KE,TEMP1,J,EPSS

SC 21 71C

REAL OF

SC 21 71C

REAL IM2P,LITTLEA,AT3,X,HNU1,HNU3,HNUL,HNU,C1,C2,C2A,C2B,C3J

SC 21 71C

REAL L,M1,M2,F1+F2J

SC 21 71C

REAL EXPDN,RNU,FACCTS

SC 21 71C

ARRAY I[0:6],DI[0:6];

SC 21 71C

ARRAY KAPPAPRIME[ 0:1400],HNU[0:1400];

SC 21 1012

FORMAT TITLE("NAME OF THE GAS IS READ FROM TITLE CARD"),

SC 21 1410

START OF SEGMENT \*\*\*\*\* 0004

NTHETA("N=",R9,0,X5,"THETA=",R7,4),

SC 41 1410

IM("M=",X6,"I(M)/(I1,F10,3)),

SC 41 1410

IM5("I(M=1/2)=" ,F8,4,X5,"((M+1/2)%" ,F8,4),

SC 41 1410

NIS("NHH",E10,1),

SC 41 1410

TITLEPLOT(X10,"THETAN",F7,4," EVN",X7,"NTOTAL",E9,3,X7,"NDENSITY",E9,3,

SC 41 1410

" PARTICLES/CM3" //

SC 41 1410

X16,"T",F8,1," DEGREES K.",X7,"P",E9,3," ATN" // / / /

SC 41 1410

" HNU WAVELENGTH KAPPA=PRIME (-TAU) BNU",

SC 41 1410

X11,"INUM" /

SC 41 1410

" EV MICRONS 1/CM",X9,"1=E " ,X14,"WATTS/CW STER"/

SC 41 1410

),

SC 41 1410

LISPLOT(F5,1,E12,3,4E14,3),

SC 41 1410

MBAR("AFTER",15," ITERATIONS, MBAR=",F6,3," WHERE M=KEN",F8,4))

SC 41 1410

000A IS 0122 LONG, NEXT SEG 0002

DEFINE J00#FOR J+0 STEP 1 UNTIL 6 DO #;

SC 21 1410

J001#FOR J+1 STEP 1 UNTIL 6 DO #;

SC 21 1410

LABEL START,EXIT,PRINTITS

SC 21 1410

TIMEIT(GEIL');

SC 21 1410

FACT+1,1909#=12\*(11605/1.43A)\*3;

SC 21 1510

A+3#21J

SC 21 1713

EPS+.001;

SC 21 1812

START;

SC 21 1911

READ(READER,TITLE){EXIT}; WRITE(GEIL,PAGE)}; WRITE(GEIL,TITLE);

SC 21 2010

READ(READER,/,0);

SC 21 3011

READ(READER,/,J00 I(J));

SC 21 4213

WRITE(GEIL,IM,J00(J,I(J)));

SC 21 5413

READ(READER,/,FOR J+1 STEP 1 UNTIL 1000 DO HNU(.));

SC 21 6811

HNU+J=1;

SC 21 7913

CLOSE(READER,RELEASE);

SC 21 8110

```

FOR N=5#1A DO BEGIN
  WRITE(GEIL(PAGE))
  FOR THETA+1 DO BEGIN
    WRITE(GEIL,NTHETA,N,THETA)
    AT3=A#SQRT(THETA+3)
    K=AT3/N
    J001 DI[J]+I[J]=I[J-1]
    DI[0]+DI[1]
    M1+1/2
    M2+3/2
    F1=K#EXP(-I[D]/THETA)=M1
    F2=K#EXP(-I[1]/THETA)=M2
    FOR COUNT+1 STEP 1 UNTIL 1000 DO BEGIN
      M=(F2#M1-F1#M2)/(F2-F1)
      IM2+I[TEMP+ENTIER(TEMP1+M+1/2)]=(TEMP=TEMP1+1)#DI[TEMP]
      E=EXP(-IM2/THETA)
      KE+KE
      IF ABS(TEMP+KE-M) < EPS THEN GO PRINTIT
      F1=F2
      F2=TEMP
      M1=M2
      M2=M
    END OF COUNT LOOPJ
    SC 21 8212
    SC 21 8512
    SC 21 8811
    SC 21 9110
    SC 21 10111
    SC 21 10410
    SC 21 10511
    SC 21 11110
    SC 21 11212
    SC 21 11312
    SC 21 11510
    SC 21 11611
    SC 21 12112
    SC 21 12310
    SC 21 12611
    SC 21 13212
    SC 21 13412
    SC 21 13513
    SC 21 13811
    SC 21 13910
    SC 21 13913
    SC 21 14012
    SC 21 14111

PRINTIT:
  WRITE(GEIL,MBAR,COUNT,M,TEMP)
  LITTLEA+7.3#16
  IM2P+I[TEMP+ENTIER(TEMP1+M+3/2)]=(TEMP=TEMP1+1)#DI[TEMP1]
  WRITE(GEIL,IMS,IM2,IM2P)
  C1=LITTLEA/THETA+2*(N+2*M/AT3)*(M+2+,25)
  C2=LITTLEA/THETA+2*N#(M+,5)+2
  C2A+C2#N#M/(2#AT3)
  C2B=C2#IM2/THETA
  C3=LITTLEA/THETA+3*N#((M+,5)+2#IM2+(M+1,5)*2#IM2P)
  FOR J+1 STEP 1 UNTIL NHNU DO BEGIN
    X#HNUIJJ/THETA
    IF X#IM2 THEN KAPPAPRIMEC JJ=C1#EXP(X)/X+3 ELSE
      IF X#IM2P THEN KAPPAPRIMEC JJ=C3/X+3 ELSE
        KAPPAPRIMEC JJ=(C2A#EXP(X)+C2B)/X+3
  END OF J LOOPJ
  WRITE(GEIL(PAGE))
  WRITE(GEIL,TITLEPLOT,THETA,TEMP1+(1+M)*N,
    TEMP+11605#THETA,TEMP1#TEMP/(2.687#10#273)))
  WRITE(GEIL,LISTPLOT,FOR J+1 STEP 1 UNTIL NHNU DO (TEMP1+HNUIJ),
    1.2397/TEMP1, TEMP#KAPPAPRIMEC JJ,
    EXPON+1=EXP(-TEMP#D), BNU=FACT#TEMP1+3/(EXP(TEMP1/THETA
    )-1), EXPON X#BNU) ))
  SC 21 14312
  SC 21 14410
  SC 21 15511
  SC 21 15610
  SC 21 16211
  SC 21 16212
  SC 21 17411
  SC 21 17912
  SC 21 18311
  SC 21 18610
  SC 21 18713
  SC 21 19412
  SC 21 19910
  SC 21 20012
  SC 21 20512
  SC 21 21010
  SC 21 21413
  SC 21 21710
  SC 21 21913
  SC 21 22912
  SC 21 24211
  SC 21 25013
  SC 21 25713
  SC 21 26510

```

```

      WRITE(GE1L(PAGE)))
      SC 21 27511

      END OF THETA LOOP)
      SC 21 27810

      END OF N LOOP)
      SC 21 27812

      TIMEIT(GE1L))
      SC 21 27910

      EXIT! ENO.
      SC 21 28010

```

0002 IS 0203 LONG. NEXT SEG 0001

EXP	IS SEGMENT NUMBER 0005, PRT ADDRESS IS 0117
SORT	0003
OUTPUT(W)	0007
BLOCK CONTROL	0008
INPUT(W)	0009
GO TO SOLVER	0010
ALGOL WRITE	0011
ALGOL READ	0012
ALGOL SELECT	0013

NUMBER OF ERRORS DETECTED = 000 LAST CARD WITH ERROR HAS SEQ #  
PRT SIZE=00843 TOTAL SEGMENT SIZE=00593 WORDS3 DISK STORAGE REQ.=00693 WORDS3 NO. SEGS.=0014.  
ESTIMATED CORE STORAGE REQUIREMENT = 03522 WORDS.  
17126100 THURSDAY, OCTOBER 21, 1965 PROCESSOR TIME = 10.28 SECONDS I/O TIME = 17.20 SECONDS

LABEL 0000000000LINE 000453842 COMPILE 1050110 BY GEIL USING ALGOL

F0437EG

XENON

M	I(M)
0	12.127
1	21.200
2	32.100
3	46.000
4	57.000
5	62.000
6	100.000

N= 5.P+18 THETA= 1.0000  
AFTER 6 ITERATIONS, MBAR= 0.111 WHERE M=KE=0.0000  
 $I^{(M-1/2)} = 8.5965 \quad I^{(M+1/2)} = 17.6695$

THETA= 1.0000 EV      NTOTAL=5,5549+18      NDENSITY=5.000E+18 PARTICLES/CM<sup>3</sup>  
 T= 11605.0 DEGREES K.      P=8.787E+00 ATM

HNU EV	WAVELENGTH MICRONS	KAPPA=PRIME 1/CM	C-TAU 1=E	RNU WATTS/CM <sup>2</sup>	INU STER
0.0	1.240E+03	1.771E+08	1.000E+00	6.256E-07	6.256E-07
0.1	2.479E+01	1.488E+03	1.000E+00	1.524E-03	1.524E-03
0.2	1.240E+01	1.955E+02	1.000E+00	5.952E-03	5.952E-03
0.3	8.265E+00	6.090E+01	1.000E+00	1.305E-02	1.305E-02
0.4	6.199E+00	2.701E+01	1.000E+00	2.262E-02	2.262E-02
0.5	4.959E+00	1.454E+01	1.000E+00	3.443E-02	3.443E-02
0.6	4.132E+00	8.545E+00	9.995E-01	4.831E-02	4.830E-02
0.7	3.542E+00	5.855E+00	9.971E-01	6.404E-02	6.356E-02
0.8	3.099E+00	4.124E+00	9.939E-01	8.145E-02	8.013E-02
0.9	2.755E+00	3.045E+00	9.524E-01	1.004E-01	9.559E-02
1.0	2.479E+00	2.333E+00	9.030E-01	1.206E-01	1.089E-01
1.5	8.265E+01	2.349E+01	2.094E-01	6.068E-01	1.270E-01
2.0	4.132E+01	1.634E+01	1.508E-01	7.838E-01	1.182E-01
2.5	4.959E+01	1.379E+01	1.288E-01	8.746E-01	1.127E-01
3.0	4.132E+01	1.316E+01	1.233E-01	8.855E-01	1.092E-01
3.5	3.542E+01	1.366E+01	1.277E-01	8.356E-01	1.067E-01
4.0	3.099E+01	1.500E+01	1.401E-01	7.474E-01	1.047E-01
4.5	2.755E+01	1.748E+01	1.603E-01	6.408E-01	1.027E-01
5.0	2.479E+01	2.101E+01	1.895E-01	5.308E-01	1.006E-01
6.0	2.066E+01	3.304E+01	2.814E-01	3.360E-01	9.454E-02
7.0	1.771E+01	5.656E+01	4.320E-01	1.960E-01	8.465E-02
8.0	1.550E+01	1.030E+00	6.430E-01	1.075E-01	6.915E-02
9.0	1.377E+01	1.746E+01	1.000E+00	5.632E-02	5.632E-02
10.0	1.240E+01	1.448E+01	1.000E+00	2.842E-02	2.942E-02
12.0	1.033E+01	1.863E+01	1.000E+00	6.646E-03	6.646E-03
14.0	8.655E+02	5.942E+01	1.000E+00	1.428E-03	1.428E-03
16.0	7.748E+02	2.759E+02	1.000E+00	2.885E-04	2.885E-04
18.0	6.487E+02	3.070E+01	1.000E+00	5.560E-05	5.560E-05
20.0	6.199E+02	2.238E+01	1.000E+00	1.032E-05	1.032E-05
25.0	4.059E+02	1.146E+01	1.000E+00	1.358E-07	1.358E-07
30.0	4.132E+02	6.632E+00	9.987E-01	1.581E-09	1.579E-09
35.0	3.542E+02	4.176E+00	9.846E-01	1.692E-11	1.666E-11
40.0	3.099E+02	2.798E+00	9.391E-01	1.702E-13	1.598E-13
45.0	2.755E+02	1.965E+00	8.594E-01	1.633E-15	1.604E-15
50.0	2.479E+02	1.433E+00	7.613E-01	1.509E-17	1.149E-17
55.0	2.254E+02	1.076E+00	6.591E-01	1.353E-19	8.921E-20
60.0	2.066E+02	8.290E-01	5.635E-01	1.184E-21	6.672E-22
65.0	1.907E+02	6.520E-01	4.790E-01	1.014E-23	4.655E-24
70.0	1.771E+02	5.221E-01	4.067E-01	8.535E-26	3.471E-26
75.0	1.653E+02	4.244E-01	3.459E-01	7.073E-28	2.646E-28
80.0	1.550E+02	3.497E-01	2.951E-01	5.784E-30	1.707E-30
85.0	1.458E+02	2.916E-01	2.529E-01	4.675E-32	1.182E-32
90.0	1.377E+02	2.456E-01	2.175E-01	3.739E-34	8.143E-35
95.0	1.305E+02	2.089E-01	1.885E-01	2.963E-36	5.585E-37
100.0	1.240E+02	1.791E-01	1.639E-01	2.329E-38	3.818E-39

Program b<sub>1</sub>  
Symbol Table for DOUBLE  
Program to Calculate Spectral Absorptivities and  
Emissivities Given Temperature and Pressure

JT1 = initial temperature desired

JTINC = temperature step size desired

JTMAX = maximum temperature desired

JBOLTZ = Boltzmann's constant

NW = input as upper limit, becomes actual value, of number of energy states input  
for the atom

NW1 = input as upper limit, becomes actual value, of number of energy states input  
for the first ion

NW2 = input as upper limit, becomes actual value, of number of energy states input  
for the second ion

NW3 = input as upper limit, becomes actual value, of number of energy states input  
for the third ion

NW4 = input as upper limit, becomes actual value, of number of energy states input  
for the fourth ion

JC = a constant used in calculating electron density

IP[i] = ionization potential of the ith species

NP = number of pressures desired

P[i] = the ith pressure, input in atmospheres but converted internally to mm  
mercury

SVENGA[i] = ith energy level of the atom

SVENG1[i] = ith energy level of the first ion

SVENG2[i] = ith energy level of the second ion

SVENG3[i] = ith energy level of the third ion

SVENG4[i] = ith energy level of the fourth ion

**SV<sub>AMEGA</sub>[i]** = total angular momenta for the ith energy level of the atom  
**SV<sub>AMEG1</sub>[i]** = total angular momenta for the ith energy level of the first ion  
**SV<sub>AMEG2</sub>[i]** = total angular momenta for the ith energy level of the second ion  
**SV<sub>AMEG3</sub>**[i] = total angular momenta for the ith energy level of the third ion  
**SV<sub>AMEG4</sub>[i]** = total angular momenta for the ith energy level of the fourth ion  
**NLAMBDA** = number of wavelengths desired  
**ALAMBDA[i]** = ith wavelength  
**JELEC** = electron density (called NELEC on output sheet)  
**JT** = current value of temperature  
**JP** = current value of pressure  
**JT<sub>PTL</sub>** = total particle density (called NT<sub>PTL</sub> on output sheet)  
**JNQ** = cutoff energy for the atom  
**JN1** = cutoff energy for the first ion  
**JN2** = cutoff energy for the second ion  
**JN3** = cutoff energy for the third ion  
**JN4** = cutoff energy for the fourth ion  
**JAT<sub>PM</sub>** = atomic particle density (called NO on output sheet)  
**JCHR1** = particle density for the first ion (called N1 on output sheet)  
**JCHR2** = particle density for the second ion (called N2 on output sheet)  
**JCHR3** = particle density for the third ion (called N3 on output sheet)  
**JCHR4** = particle density for the fourth ion (called N4 on output sheet)  
**JSUMA** = internal partition function for the atom (called Q0 on output sheet)  
**JSUM1** = internal partition function for the first ion (called Q1 on output sheet)  
**JSUM2** = internal partition function for the second ion (called Q2 on output sheet)  
**JSUM3** = internal partition function for the third ion (called Q3 on output sheet)  
**JSUM4** = internal partition function for the fourth ion (called Q4 on output sheet)  
**JV1** = ionization potential lowering for the atom

Program b<sub>2</sub>  
Symbol Table for the Spectral Absorptivity Part of DOUBLE

T = temperature

NO = atomic density

Q0 = internal partition function for the atom

Q1 = internal partition function for the first ion

NU =  $\nu$  = frequency

K0 = total spectral absorptivity for the atom

KOPRIME = effective spectral absorptivity for the atom, including stimulated  
emission

XI[INU] = the Biberman-Norman factor for the frequency INU  $\times 10^{-14}$  cycles/sec

H = Planck's constant

K = Boltzmann's constant

V6P =  $\nu_{6p}$  = ionization frequency from the 6P state

V7P =  $\nu_{7p}$  = ionization frequency from the 7P state

V5D =  $\nu_{5d}$  = ionization frequency from the 5D state

V6D =  $\nu_{6d}$  = ionization frequency from the 6D state

VLMVG =  $\nu_1 - \nu_g$  where  $\nu_1$  = ionization frequency of lowest level not considered  
individually, and

$\nu_g$  = ionization frequency of the ground state where  $h\nu_g$  = ionization  
potential

GP = degeneracy of each of the p levels

GD = degeneracy of each of the d levels

A6P = cross section of the 6P state

A6D = cross section of the 6D state

A7P = cross section of the 7P state

A7D = cross section of the 7D state

Note: The emission coefficient,  $\epsilon$ , is calculated within the final write statement.

**JV2 = ionization potential lowering for the first ion**

**JV3 = ionization potential lowering for the second ion**

**JV4 = ionization potential lowering for the third ion**

14159849 MONDAY, OCTOBER 25, 1965

WRL ALGOL VERSION OF 9/1/65

```

BEGIN                                     SC  11  010
                                         START OF SEGMENT ***** 0002

SAVE FILE PASSK&PPA DISK SERIAL [20/1200](2,60,1200,SAVE 100)          SC  21  010
FILE IN READER (2,10))                      SC  21  312
FILE OUT PRINT #> CHURCH(2,15))           SC  21  710
REAL RISL,RISU,NB$TEPS,R1SLNTH$          SC  21  1012
COMMENT      DABTINE                   /  SL  21  1012
      TO OBTAIN LISTING MERGE IN BLANK CARO WITH SEQUENCE NUMBER 000000308   S  SL  21  1012
                                         09999999 SC  21  1210

REAL NLAMR04,ILANR04)                      SC  21  1210
ARRAY X10:20))                            SC  21  1210
ARRAY KARRAY[I:90])                        SC  21  1313
ARRAY ALAMBOA[0:90])                       SC  21  1512
REAL JT,JATON,JSUNA,JSUM))                SC  21  1711
DEFINE GEIL#PRINT$)
BEGIN
  DEFINE STILH+I STEP 1 UNTIL #)
                                         SC  21  1711
                                         START OF SEGMENT ***** 0004

REAL TEMP,TENPI,TEMP2)
INTEGER INOEIJ)
INTEGER NN,NW1,NW2,NW3,NW4)
INTEGER OX1)
                                         SC  41  010
                                         SC  41  010
                                         SC  41  010
                                         SC  41  010

REAL X0,Y0,XM,YM)                         SC  41  010
REAL KTS
  INTEGER JKX,JK1,JK2,JK3,JKC,JK,        JN, JJ
  REAL       JT1, JZEFF,           JTINC, JFXX, JEX1, JEXB, JEXC)
  INTEGER JN0, JN1, JN2, JN3, JN4, JL, JI, JN5, JNTCHK, JLLL)
  REAL JTMAX, JRDLTZ, JC, JATHY, JCULE,    JELEG, JP,   JT01L,
JON, JON1, JON2, JON3, JONA, JOEL1, JOEL2, JOEL3, JDELA,
JSUM2, JSUM3, JSUNA, JP0W1, JP0W2, JP0W3, JP0W4, JC1, JC2, JC3, JC4,
JR, JRR, JA1, JA2, JA3, JA4, JA5, JA6,   JOPOLA, JAAA, JBBB,
JCHR1, JCHR2, JCHR3, .CHR4, JSNCH, JV, JV1, JV2, JV3, JV4,
JP)
  ARRAY IP[0:8],      PW[0:8])
  ARRAY OEI[0:8])
PROCEDURE BISECT(X, A, B, N, Y)  REAL X, A, B, N, Y)
  BISECT1 SC  41  511
  BISECT & < X < B TO ERROR IN X S 2**N X (B-A) FOR Y = 0.
  BISECT2 SC  41  511
  BEGIN REAL O,I,S; X + B; S + Y; X + A; S + SIGN(Y-S)) O + (B-A)/2)
  BISECT3 SC  41  511
                                         START OF SEGMENT ***** 0005

  FOR I + 0 STEP 1 UNTIL N DO
    BEGIN X + X + O ; O + SIGN(Y * S) * ABS(O)/2 )
    END ;
  END BISECT )
                                         RISECT4 SC  51  712
                                         RISECT5 SC  51  910
                                         RISECTA SC  51  1413
                                         RISECTB SC  51  1710
                                         0005 IS 0020 LONG, NEXT SFG 0004

DEFINE

```

```

JPOLA=JELEC*(JA1*(JELEC*JELEC))+JELEC*(JA2*JELEC)+JA3*JELEC+JA4+((
SC 41 511
JA5/JELEC)/JRR)+(1/JELEC)*((JA6/JELEC)/JRR)#
SC 41 511
PROCEDURE OORDER2(ENG,OMEG,NH)
SC 41 511
VALUE NH
SC 41 511
INTEGER NH
SC 41 511
ARRAY ENG,OMEG(0:)
SC 41 511
BEGIN
SC 41 511
INTEGER I,J
SC 41 511
SC 42 511
START OF SEGMENT *****
0006
FOR I=1 STEP 1 UNTIL NH DO BEGIN
SC 61 010
TENP+ENG(I)
SC 61 110
TENP1+I
SC 61 210
FOR J=I+1 STEP 1 UNTIL NH DO
SC 61 213
IF TEMP2+ENG(J) < TEMP THEN BEGIN TENP+TENP2) TENP1+J ENDS
SC 61 911
DOUBLE(ENG(TENP1),ENG(1),+,ENG(1),ENG(TENP1))
SC 61 1311
DOUBLE(OMEG(TENP1),OMEG(1),+,ONEG(1),ONEG(TENP1))
SC 61 1610
END OF I LOOPS
SC 61 1813
END OF PROCEDURE OORDER2
SC 61 2110
0006 IS 0024 LONG, NEXT SEG 0004

PROCEDURE FINO(SVENG,ENER,NW,NQ)
SC 41 511
VALUE ENER
SC 41 511
ARRAY SVENG(0:)
SC 41 511
INTEGER NW,NQ
SC 41 511

REAL ENER
SC 41 511
BEGIN
SC 41 511
LABEL RETURN
SC 41 511
SC 42 511
START OF SEGMENT *****
0007
FOR NQ=NW STEP -1 UNTIL 1 DO
SC 71 010
IF ENER > SVENG(NQ) THEN GO TO RETURN
SC 71 110
RETURN ENDS
SC 71 511
0007 IS 0007 LONG, NEXT SEG 0004

REAL Q,X9R3
SC 41 511
INTEGER COUNT,COUNTT,NP,TI
SC 41 511
INTEGER KJ
SC 41 511
LABEL EXIT
SC 41 511
FORMAT FLF(5E20.12)
SC 41 511
SC 42 511
START OF SEGMENT *****
0008
0008 IS 0004 LONG, NEXT SEG 0004

FORMAT
SC 41 511
TITLE1("OUTPUT OF PROGRAM 1"),
SC 41 511
FL216(6E16.8)
SC 41 511
SC 42 511
START OF SEGMENT *****
0009
0009 IS 0011 LONG, NEXT SEG 0004
SC 41 511
BEGIN
SC 41 511
ARRAY P,NELLC(0:120)
SC 41 511

```

```

LIST LIST0(JT1>JTINC,JTMAX,          JRDLTZ,NW,NW1,NW2,NW3,NW4,          SC 101 281
      JC,IP[1],IP[2],IP[3],IP[4],NP,
      FOR INDEX1+1 STEP 1 UNTIL NP DO P[INDEX1]))          SC 101 1483
FORMAT CONSTANTS("JT1>JTINC,JTMAX,"      "JRDLTZ,NW,NW1,NW2,NW3,NW4,"          SC 101 2311
                  START OF SEGMENT ***** 0011
      "JC,IP[1],IP[2],IP[3],IP[4],"          "NP,FDR...,P[NP]"          SC 111 3012
      /(5R20.5))          SC 111 3012
                  0011 15 0024 LENGTH NEXT SEG 0010
COMMENT VERIFY INPUT TO PARTITION SERIES PROGRAM I          SC 101 3012
FORMAT OUT  EFORM(7E15.7),  IFORM(10I4) I          SC 101 3012
                  START OF SEGMENT ***** 0012
                  0012 IS 0008 LONG, NEXT SEG 0010
TIMEIT(PRIN1))
READ(READER, />,LIST0 )[EXIT])
WRITE(GE1L,CONSTANTS,LIST0)
WRITE(PRINT(OBL))
FOR DX1 + 1 STEP 1 UNTIL
      NP DO P1DX1+P1DX1*x760)
BEGIN
LABEL      L508,L516,L517,L608,L615,L708,L715,L808,L815,L908,L915)
                  START OF SEGMENT ***** 0013
REAL ARRAY  SVENGA{0:NW},  SVENG1{0:NW1},  SVENG2{0:NW2},
      SVENG3{0:NW3},  SVENG4{0:NW4},  SVOMEGA1{0:NW},  SVOMEG1{0:NW1},
      SVOMEG2{0:NW2},  SVOMEG3{0:NW3},  SVOMEG4{0:NW4},  SVSUMA{0:NW},
      SVS1{0:NW1},  SVS2{0:NW2},  SVS3{0:NW3},  SVS4{0:NW4},
      SVS10{NW})
LIST LIST1(FOR DX1+1 STEP 1 UNTIL NW  DO SVENGA {DX1}))
LIST LIST2(FOR DX1+1 STEP 1 UNTIL NW  DO SVOMEGA{DX1}))
LIST LIST3(FOR DX1+1 STEP 1 UNTIL N+1 DO SVENG1 {DX1}))
LIST LIST4(FOR DX1+1 STEP 1 UNTIL NW1 DO SVOMEG1{DX1}))
LIST LIST5(FOR X1+1 STEP 1 UNTIL NW2 DO SVENG2 {DX1}))
LIST LIST6(FOR DX1+1 STEP 1 UNTIL NW2 DO SVOMEG2{DX1}))
LIST LIST7(FOR DX1+1 STEP 1 UNTIL NW3 DO SVENG3 {DX1}))
LIST LIST8(FOR DX1+1 STEP 1 UNTIL NW3 DO SVOMEG3{DX1}))
LIST LIST9(FOR DX1+1 STEP 1 UNTIL NW4 DO SVENG4 {DX1}))
LIST LIST10(FOR DX1+1 STEP 1 UNTIL NW4 DO SVOMEG4{DX1}))
LIST LIST11(FOR INDEX1+1 STEP 1 UNTIL NW  DO SVS{INDEX1},FOR INDEX1+1
STEP 1 UNTIL NW1 DO SVS1{INDEX1}, FOR INDEX1+1 STEP 1 UNTIL NW2 DO SVS2{
INDEX1},FOR INDEX1+1 STEP 1 UNTIL NW3 DO SVS3{INDEX1},FOR INDEX1+1
STEP 1 UNTIL NW4 DO SVS4{INDEX1},JT))
READ(READER, / >,LIST1)
NW +DX1+1
READ(READER, / >,LIST2)
READ(READER, / >,LIST3)
NW1+DX1+1
READ(READER, / >,LIST4)

```

```

READ(READER, / >LIST5)
NW2+DX1=13
READ(READER, / >LIST6 )
READ(READER, / >LIST7)
NW3+DX1=13
READ(READER, / >LIST8 )
READ(READER, / >LIST9)
NW4+DX1=13
READ(READER, / >LIST10)
READ(READER, / >NLAMBOA, FOR DX1+1 STEP 1 UNTIL NLAMBOA DO ALAMBOA[DX1])
READ(READER, / >NSTEP5)
CLOSE(READER,RELEASE)
WRITE(PASSKAPPAs, JT1, / *TNC, JTMAX)
WRITE(PASSKAPPAs, NLAMBOA)
WRITE(PASSKAPPAs, NLAMBOA+1, ALAMBOA[*])
ORDER2(SVENGA, SVOMEGA, NW)
ORDER2(SVENG1, SVOMEG1, NW1)
ORDER2(SVENG2, SVOMEG2, NW2)
ORDER2(SVENG3, SVOMEG3, NW3)
ORDER2(SVENG4, SVOMEG4, NW4)
FOR DX1 + 1 STEP 1 UNTIL
    NW DO SVOMEGA[DX1]+2*SVOMEGA[DX1]+1
FOR DX1 + 1 STEP 1 UNTIL
    NW1 DO SVOMEG1[DX1]+2*SVOMEG1[DX1]+1
FOR DX1 + 1 STEP 1 UNTIL
    NW2 DO SVOMEG2[DX1]+2*SVOMEG2[DX1]+1
FOR DX1 + 1 STEP 1 UNTIL
    NW3 DO SVOMEG3[DX1]+2*SVOMEG3[DX1]+1
FOR DX1 + 1 STEP 1 UNTIL
    NW4 DO SVOMEG4[DX1]+2*SVOMEG4[DX1]+1
FINOC(SVENGA, IP[1], NW, NW)
IF FALSE THEN BEGIN
    WRITE(PRINT, EFORM, LIST1)
    WRITE(PRINT[DBL])
    WRITE(PRINT, EFORM, LIST2)
    WRITE(PRINT[DBL])
    WRITE(PRINT, EFORM, LIST3)
    WRITE(PRINT[DBL])
    WRITE(PRINT, EFORM, LIST4)
    WRITE(PRINT[DBL])
    WRITE(PRINT, EFORM, LIST5)
    WRITE(PRINT[DBL])
    WRITE(PRINT, EFORM, LIST6)
    WRITE(PRINT[DBL])
    WRITE(PRINT, EFORM, LIST7)
    WRITE(PRINT[DBL])

```

```

        WRITE(PRINT,EOFHM,LIST8 )          SC  131 33613
        WRITE(PRINT,DAL))                SC  131 34010
        WRITE(PRINT,EFORM, LEST9 )       SC  131 34213
        WRITE(PRINT,DAL))                SC  131 34610
        WRITE(PRINT,EFORM,L1SY10)        SC  131 34813
        WRITE(PRINT,DBL))                SC  131 35210
END OF IF FALSE)
KT+JBOLTZ*JT1)
TEMP =   JCXSQRT(JT1)*3*SVOMEGA[1]/
           [SVOMEGA[1]]*EXP[-P[1]/KT])          SC  131 35413
FOR DX1 = 1 STEP 1 UNTIL
    NP DO                                SC  131 36211
BEGEN
NELEC[DX1]=SQR(TEMP*(TEMP+P[DX1]*6.712818/KT))-TEMP
NELEC[DX1]=NELEC[DX1]*.1            SC  131 36310
ENOF
TIMEIT(PRINT)
FOR JT=JTI STEP JTINC UNTIL JTMAX DO BEGEN
KT+JBOLTZ*JT)
SVS[1]*SVOMEGA[1]*EXP=SVENG[1]/KT)
JJ+2)
DO BEGEN
L5161*SVS[JJ]*SVS[JJ=1]*SVOMEGA[JJ]*EXP=SVENG[JJ]/KT)
SC  131 36912
SC  131 37113
SC  131 37213
SC  131 37410
SC  131 37610
SC  131 37711
SC  131 38013
SC  131 38112
SC  131 38112

L5171 END UNTIL JJ+JJ+1 > NW1
SVS1[1]*SVOMEGA[1]*EXP=SVENG1[1]/KT)
JJ+2)
DO BEGEN
SVS1[JJ]*SVS1[JJ=1]*SVOMEGA1[JJ]*EXP=SVENG1[JJ]/KT)
L6151 END UNTIL JJ+JJ+1 > NW1
SVS2[1]*SVOMEGA2[1]*EXP=SVENG2[1]/KT)
JJ+2)
DO BEGEN
SVS2[JJ]*SVS2[JJ=1]*SVOMEGA2[JJ]*EXP=SVENG2[JJ]/KT)
L7151 END UNTIL JJ+JJ+1 > NW2
SVS3[1]*SVOMEGA3[1]*EXP=SVENG3[1]/KT)
JJ+2)
DO BEGEN
SVS3[JJ]*SVS3[JJ=1]*SVOMEGA3[JJ]*EXP=SVENG3[JJ]/KT)
L8151 END UNTIL JJ+JJ+1 > NW3
SVS4[1]*SVOMEGA4[1]*EXP=SVENG4[1]/KT)
JJ+2)
DO BEGEN
SVS4[JJ]*SVS4[JJ=1]*SVOMEGA4[JJ]*EXP=SVENG4[JJ]/KT)
L9151 END UNTIL JJ+JJ+1 > NW4
BEGEN

```

COMMENT SECOND MAJOR PORTION OF PROGRAM  
 FORMAT F3("PARTITION FUNCTIONS")  
 SC 131 43711  
 SC 131 43711

	START OF SEGMENT *****	0014
	START OF SEGMENT *****	0015
"Q0=">E16.8,X5,"Q1=">E16.8,X5,"Q2=">F16.8,X5/	SC 151 010	
"Q3=">E16.8,X5,"Q4=">E16.8/),	SC 151 010	
FORB1SECT("NUMBER OF BISECTING STEPS TAKEN=",16),	SC 151 010	
F4("DENSITIES IN INVERSE CM3")	SC 151 010	
"N0=">E16.8,X5,"N1=">E16.8,X5,"N2=">E16.8,X5/	SC 151 010	
"N3=">E16.8,X5,"N4=">E16.8,X5/	SC 151 010	
"NELEC=">E16.8,X5,"NTUTL=">E16.8/),	SC 151 010	
F6("IONIZATION POTENTIAL LOWERINGS IN INVERSE CM FOR"),	SC 151 010	
"ATUM=">E16.8,X3,"ION1=">E16.8,X3,"ION2=">E16.8,X3,	SC 151 010	
"ION3=">E16.8/),	SC 151 010	
FTP("TEMP=",16," DEGREES K.,"X5,"PRESSURE=",E16.8," ATMOSPHERES"))	SC 151 010	
L1ST LIST3(JSUMA,JSUM1,JSUM2,JSUM3,JSUM4 )	SC 151 010	
0015 IS 0102 LONG, NEXT SEG 0014		
LIST LIST4(JATOM,JCHR1,JCHR2,JCHR3,JCHR4,JELEC,JTOTL )	SC 141 1012	
L1ST LIST6( JV1,JV2,JV3,JV4 )	SC 141 2312	
BEGIN	SC 141 3212	
LABEL L10, L51,L52,L55,L56,L59,L60,L66,L71,L72,L74,L81,L84,	SC 141 3212	
L87,L90,L101,L118)	SC 161 080	
START OF SEGMENT *****	0016	
TIMEIT(GEIL)) .	SC 161 080	
WRITE(GEIL))	SC 161 180	
FOR TI+1 STEP 1 UNTIL NP 00 BEGIN	SC 161 313	
WRITE(GEIL[PAGE]))	SC 161 510	
JP+P[II])	SC 161 713	
JELEC+NELEC[II])	SC 161 813	
WRITE(GEIL,FORB1SECT,NBSTEP))	SC 161 913	
JTOTL+JP*6.712015/(JBOLTZ*JT))	SC 161 1711	
JP*W1+SVENG1[NW1]/KT)	SC 161 1912	
JP*W2+SVENG1[NW1]/KT+JP*W1)	SC 161 2110	
JP*W3+SVENG2[NW2]/KT+JP*W2)	SC 161 2310	
JP*W4+SVENG3[NW3]/KT+JP*W3)	SC 161 2510	
JN0+NW3	SC 161 2710	
JN1+NW1)	SC 161 2713	
JN2+NW2)	SC 161 2812	
JN3+NW3)	SC 161 2911	
JN4+NW4)	SC 161 3010	
L101	SC 161 3013	
JSUMA+SVS [JN0])	SC 161 3110	
JSUM1+SVS1[JN1])	SC 161 3210	
JSUM2+SVS2[JN2])	SC 161 3310	
JSUM3+SVS3[JN3])	SC 161 3410	
JSUM4+SVS4[JN4])	SC 161 3510	

6-6

```

JC1+JCX*(JT*1.5)*EXP(-JPOW1)*(JSUM1/JSUMA))
SC 161 3610

JC2+JCX*(JT*1.5)*EXP(-JPOW2+JPOW1)*(JSUM2/JSUM1))
SC 161 4112

COMMENT

IF (5995>JT) THEN GO TO L51)
SC 161 4712

JC3+JCX*(JT*1.5)*EXP(-JPOW3+JPOW2)*(JSUM3/JSUM2))
SC 161 4712

GO TO L52)

L51) JC3=0)

L52)

COMMENT

IF (8995>JT) THEN GO TO L55)
SC 161 5710

JC4+JCX*(JT*1.5)*EXP(-JPOW4+JPOW3)*(JSUM4/JSUM3))
SC 161 5710

GO TO L56)

L55) JC4=0)

L56) IF (12995<JT) THEN GO TO L59)
SC 161 6510

JR+1#-15)
SC 161 6513

JRR+1)

GO TO L60)

L59) JR+1#=35)
SC 161 6813

JRR+1#=20)

L60) JA1+JR)

JA2+2*JC1*JR)
SC 161 7312

JA3+3*(JC2*(JC1*JR))=JC1*(JTDTL*JR))
SC 161 7413

JA4+4*(JC3*(JC2*(JC1*JR)))-2*(JTDTL*(JC2*(JC1*JR)))))
SC 161 7612

SC 161 8011

```

```

JAT5=5*(JC1*JR1)*(JC3*(JC2*(JC1*JR)))-3*(JT0TL*JR1)*(JC3*(JC2*(JC1*JR)))
JA6=-AX*(JT0TL*JR1)*(JC4*(JC3*(JC2*(JC1*JR)))) SC 161 8512
L661 SC 161 9113
BSECT(JELEC,100,5#20,NBSTEPSPJPOLA)
JAAA+JC1+(2*JC1*(JC2/JELEC))+3*JC1*JC2*(JC3/(JELEC*2)))
JRRR+AX*(JC1/JELEC)*(JC2/JELEC)*(JC3/JELEC)*JC4) SC 161 9810
JATOM+(JELEC*2)/(JAAA+JBBB) SC 161 11410
JCHR1+JC1*XATOM/JELEC) SC 161 11913
IF (JCHR1>1) THEN GO TO L81) SC 161 12410
JCHR1=0) SC 161 12611
L811 JCHR2+JC2*XCHR1/JELEC) SC 161 12810
IF (JCHR2>1) THEN GO TO L84) SC 161 12911
JCHR2=0) SC 161 13113
L841 JCHR3+JC3*XCHR2/JELEC) SC 161 13310
IF (JCHR3>1) THEN GO TO L87) SC 161 13313
JCHR3=0) SC 161 13513
L871 JCHR4+JC4*XCHR3/JELEC) SC 161 13710
IF (JCHR4>1) THEN GO TO L90) SC 161 13713
JCHR4=0) SC 161 13913
L901 SC 161 14110
JV1=7#3.95792359#-5#SQRT((3.1415926536/KT)*(JELEC+JCHR1+4*XJCHR2+
9*XJCHR3+16*XJCHR4))) SC 161 14210
IV2=2*XJV1) SC 161 14413

```

```

JV3=3*XJV1;
JV4=4*XJV1;

IF IP[1]=JPOW1*KT< JV1 THEN
  BEGIN
    TEMP+IP[1]=JV1;
    FIND(SVENG1,TEMP      ,NW1,JNQ);
    JPOW1=SVENG1[JNQ]/KT;
    TEMP+IP[2]=JV2;
    FIND(SVENG1,TEMP      ,NW1,JN1);
    JPOW2=SVENG1[JN1]/KT+JPOW1;
    TEMP+IP[3]=JV3;
    JPOW3=SVENG2[JN2]/KT+JPOW2;
    TEMP+IP[4]=JV4;
    FIND(SVENG2,TEMP      ,NW2,JN2);
    FIND(SVENG3,TEMP      ,NW3,JN3);
    JPOW4=SVENG3[JN3]/KT+JPOW3;
    GO TO L10;
  END;
  WRITE(GEIL[0BL],FTP,JP/760);
  WRITE(GEIL,F3,LIST3);
  WRITE(GEIL,F4,LIST4);
  WRITE(GEIL,F6,LIST6);
  NELEC[II]=JELECS;

```

BEGIN  
COMMENT GEIL, ABSORPTION COEFFICIENT FOR THE XENON ATOM, SCHLECHT, 576;  
REAL LITTLECOEF,BIGCOEF;

```

REAL V6P,V7P,V5D,V6D,
      TEMP,
      GP,GO,VIHVG,I,
      COEF,C1,      H,K,
      DNU2,
EV1MVG,EV6P,EV6D,EV7P,EV5D,
HOK,C12,
E6P,E6D,E7P,E5D,
      NU      PINUS,
      KO,KOPRIME,
      AGS1,AGS2,A6P,A6D,A7P,A5D,ACOEF;
DEFINE T=JTE,NO=JATOM#,Q0=JSUMA#,Q1=JSUM1#;
FORMAT INPUT("T=",16," DEGREES K",X6,"NO=",E10.3,X6,
            "Q0=",E10.3,X6,"Q1=",E10.3),
        OUTPUT(4E15.3),
        TITLEOUT(/,
        NU      LAMBDA "
        KAPPAPRIME   EMISSION COEF"

```

```

/
SC 181 010
" CYCLES/SEC      MICRONS "
SC 181 010
" INVERSE CM      WATTS/CM3 STER SEC-1"
SC 181 010
/
SC 181 010
;;
SC 181 010

0018 IS 0049 LONG, NEXT SEG 0017

REAL PROCEDURE LAG ( X , X0 , DX , Y , N ) ;
COMMENT ORDER 3 LAGRANGE INTERPOLATION. EQUAL INDEPENDENT STEP.
SINGLE DEPENDENT,INDEPENDENT VARIABLE,EXTRAPOLATE IF NOT X0SXDX=N*DX.
X = DESIRED INDEPENDENT VALUE
X0 = FIRST INDEPENDENT VALUE OF Y TABLE (FOR Y(0))
DX = TABLE STEP FOR INDEPENDENT
Y = NAME,DEPENDENT VARIABLE VALUE TABLE (MUST BE SINGLE SUBSCRIPT)
N = MAX INDEX OF Y TABLE ( ≥ 4 )
VALUE X , X0 , DX , N ;
REAL X , X0 , DX ; INTEGER N ; ARRAY Y(D) ;
BEGIN
INTEGER I ; REAL S ;
START OF SEGMENT ***** 0019
IF (I = ENTIER((X - X0)/DX + 1)) < 0 THEN I = 0 ELSE
  IF I + 3 > N THEN I + N = 3 ;
  S = (X - X0)/DX + 1 ;
  LAG = ((Y[I + 3] * S - Y[I] * (S - 3)) * ((S - 3) * S + 2))/3
  LAG + (Y[I + 1] * (S - 2) - Y[I + 2] * (S - 1)) * (S - 3) * S)/2
END LAG ;
LAG 1 SC 171 010
LAG 2 SC 171 010
LAG 3 SC 171 010
LAG 4 SC 171 010
LAG 5 SC 171 010
LAG 6 SC 171 010
LAG 7 SC 171 010
LAG 8 SC 171 010
LAG 9 SC 171 010
LAG 10 SC 171 010
LAG 11 SC 171 010
LAG 12 SC 171 010
LAG 13 SC 191 010
LAG 14 SC 191 510
LAG 15 SC 191 1010
LAG 16 SC 191 1211
LAG 17 SC 191 1712
LAG 18 SC 191 2410
0019 IS 0028 LONG, NEXT SEG 0017
SC 171 010
LABEL START=EXIT;
FILL X(I*) WITH 1.,6.,5,I,2.25,2.8,3,3.1, 3,
SC 171 010
START OF SEGMENT ***** 0020
2.9,2.8,2.6,2.4,2.1,I,8,1.6,1.4,I,25,
I,2,I,1,I
SC 171 113
SC 171 113
0020 IS 0021 LONG, NEXT SEG 0017
H=6.623178=27;
SC 171 113
K=I,380448=16;
SC 171 212
HDK=H/K;
SC 171 311
V6P=2.35536@15;
SC 171 412
V7P=2.65419@15;
SC 171 511
V5D=2.43618@15;
SC 171 610
V6O=2.67309@15;
SC 171 613
VIMVG=2.7252@15;
SC 171 712
EVIMVG=HDKxV1MVG;
SC 171 811
EV6P=HDKxV6P;
SC 171 912
EV6D=HDKxV6D;
SC 171 1013
EV7P=HDKxV7P;
SC 171 1210
EV5D=HDKxV5D;
SC 171 1311
GP=24;
SC 171 1412

```

```

GD+40J
ACDEF +1.20423x9013J
AGS2+2.598=32J
AGS1+98=17+AGS2x2.93#15J
A6P+ACDEFx.072xG0J
A6D+ACDEFx.025xG0J
A7P+ACDEFx.021xG0J
A50+ACDEFx.076xG0J
C1+89#24J
C12+C1x2J
START:
WRITE(GEIL{08L })
WRITE(GEIL{DRL},INPUT,T,N0,Q0,Q1)
WRITE(GEIL      -TITLEOUT)
LITTLECOEF+C12x01xT
BIGCOEF=LITTLECOEFxEXP(-EV1(HVG/T))
ESP+A6PxEXP(-EV6P/T)
E6D+A60xEXP(-EV60/T)
E7P+A7PxEXP(-EV7P/T)
E50+A50xEXP(-EV50/T)
FOR 1LAMROA#1 STEP 1 UNTIL NLAMBOA 00 BEGIN
NU+3#14/ALAMBOA{ILAMBOA})
INU+NUxP=14J
SC 171 1511
SC 171 1610
SC 171 1711
SC 171 1810
SC 171 1913
SC 171 2112
SC 171 2311
SC 171 2510
SC 171 2613
SC 171 2712
SC 171 2813
SC 171 2910
SC 171 3113
SC 171 6011
SC 171 6311
SC 171 6510
SC 171 6712
SC 171 7010
SC 171 7212
SC 171 7510
SC 171 7712
SC 171 7910
SC 171 8012

IF NU<2#14 THEN COEF+LITTLECOEFxEXP(HOKx(NU-2.935#15)/T) ELSE
COEF+BIGCOEFJ
ONU2+1.0/NU  *2J
KO +NU/Q0 x (COEF/NU  *3 x
(IF INU#20 THEN 1 ELSE IF INU#2 THEN X{INU} ELSE LAG(INU,0,1,X1,40))+
(IF NU  22.93#15 THEN AGS1=AGS2xNU  ELSE 0)+
(IF NU  25.7966#14 THEN E6PxONU2 ELSE 0)+
(IF NU  22.6193#14 THEN E6DxONU2 ELSE 0)+
(IF NU  22.8083#14 THEN EPPxONU2 ELSE 0)+
(IF NU  24.9884#14 THEN E50xONU2 ELSE 0)))+
KOPRIME+KOx{1-EXP(-HxNU/(KxT)))}
KARRAY{ILAMBOA}+KOPRIME)
WRITE(GEIL,OUTPUT,NU,3#14/NU,KOPRIME,IF TEMP+HOKxNU/T>15 THEN
EXP(LN (KOPRIMEx2xHxNU#3)-64.36715-TEMP) ELSE
KOPRIMEx2xHxNU#3/(9#27x
(EXP(HOKxNU/T)=1)))}
ENO OF INU)
WRITE(PASSKAPPAs,JP))
END OF JP LOOP
ENO ENOJ
SC 171 8113
SC 171 8611
SC 171 9113
SC 171 9312
SC 171 9610
SC 171 10212
SC 171 10611
SC 171 10911
SC 171 11211
SC 171 11511
SC 171 11910
SC 171 12310
SC 171 12413
SC 171 14411
SC 171 15010
SC 171 15310
SC 171 16211
SC 171 16412
SC 171 16712
DD017 IS 0169 LONG, NEXT SEG 0016
SC 161 20110
SC 161 20811
SC 161 21012

```

EXP	IS SEGMENT NUMBER	PRT ADDRESS IS
LN	0022	0307
SORT	0023	0276
OUTPUT(W)	0024	0041
BLOCK CONTROL	0025	0005
INPUT(W)	0026	0235
X TO THE I	0027	0310

G0 TO SOLVER	0028	0234
ALGOL WRITE	0029	0014
ALGOL READ	0030	0015
ALGOL SELECT	0031	0016

NUMBER OF ERRORS DETECTED = 000 LAST CARD WITH ERROR HAS SEG #  
PRT SIZE=02543 TOTAL SEGMENT SIZE=01431 WORDS) DISK STORAGE REQ.=01733 WORDS) NO. SEGS.=0032.  
ESTIMATED CORE STORAGE REQUIREMENT = 06689 WORDS.  
15:00:29 MONDAY, OCTOBER 25, 1965 PROCESSOR TIME = 22.75 SECONDS I/O TIME = 52.48 SECONDS

15100133 MONDAY, OCTOBER 25, 1965

JT1=JTINC, JTMAX, JBLTZ=NW,NH1,NH2,NH3,NH4,JC,IP[1],IP[2],IP[3],IP[4],NP,FOR,,,P[NP]

9000.00000	1000.00000	10000.00000	0.69502	400.00000
200.00000	150.00000	100.00000	2.00000	4.83000E+15
97834.40000	171068.40000	259089.00000	371037.00000	1.00000
1.00000				

15101104 MONDAY, OCTOBER 25, 1965 PROCESSOR TIME = 18.80 SECONDS I/O TIME = 28.47 SECONDS

15101105 MONDAY, OCTOBER 25, 1965 PROCESSOR TIME = 19.47 SECONDS I/O TIME = 28.58 SECONDS

NUMBER OF BISECTING STEPS TAKEN= 75  
TEMP= 9000 DEGREES K. PRESSURE= 1.00000000E+00 ATMOSPHERES

PARTITION FUNCTIONS

Q0= 1.00082966E+00	Q1= 4.37106237E+00	Q2= 6.22667678E+00
Q3= 4.67216147E+00	Q4= 1.00000000E+00	

DENSITIES IN INVERSE CM<sup>-3</sup>

N0= 7.19930480E+17	N1= 4.77863084E+16	N2= 7.13042656E+10
N3= 6.21119317E+01	N4= 0.00000000E+00	
NELEC= 4.77864511E+16	NTOTL= 8.15503311E+17	

IONIZATION POTENTIAL LOWERINGS IN INVERSE CM FOR

ATOM= 5.48428661E+02	ION1= 1.09685732E+03	ION2= 1.64528598E+03	ION3= 2.19371464E+03
----------------------	----------------------	----------------------	----------------------

T= 9000 DEGREES K N0= 7.199E+17 Q0= 1.001E+00 Q1= 4.371E+00

NU CYCLES/SEC	LAMBDA MICRONS	KAPPAPRIME INVERSE CM	EMISSION COEF WATTS/CM <sup>3</sup> SEC <sup>-1</sup>
6.000E+15	5.000E-02	7.544E+00	3.052E+20
5.455E+15	5.500E-02	1.771E+01	9.865E+19
5.000E+15	6.000E-02	2.617E+01	1.268E+17
4.615E+15	6.500E-02	3.334E+01	9.879E+17
4.286E+15	7.000E-02	3.948E+01	5.433E+16
4.000E+15	7.500E-02	4.481E+01	2.300E+15
3.750E+15	8.000E-02	6.946E+01	7.937E+15
3.333E+15	9.000E-02	5.723E+01	5.949E+14
3.000E+15	1.000E+01	6.344E+01	2.844E+13
2.857E+15	1.050E+01	1.348E+04	1.118E+10
2.000E+15	1.300E+01	2.759E+04	7.587E+17
1.500E+15	2.000E+01	4.966E+04	8.290E+16
1.200E+15	2.500E+01	7.908E+04	3.352E+15
1.000E+15	3.000E+01	1.155E+03	8.254E+15
8.571E+14	3.500E+01	1.582E+03	1.534E+14
7.500E+14	4.000E+01	2.082E+03	2.414E+14
6.667E+14	4.500E+01	2.636E+03	3.383E+14
6.000E+14	5.000E+01	3.236E+03	4.375E+14
5.455E+14	5.500E+01	2.368E+03	3.264E+14
5.000E+14	6.000E+01	2.816E+03	3.071E+14
4.615E+14	6.500E+01	9.768E+04	1.319E+14
4.286E+14	7.000E+01	1.014E+03	1.331E+14

4.000E+14	7.500E-01	1.194E-03	1.512E-14
3.750E+14	6.000E-01	1.389E-03	1.688E-14
3.529E+14	6.500E-01	1.600E-03	1.860E-14
3.333E+14	9.000E-01	1.137E-03	1.262E-14
3.158E+14	9.500E-01	1.275E-03	1.308E-14
3.000E+14	1.000E+00	1.421E-03	1.430E-14
2.857E+14	1.050E+00	1.575E-03	1.507E-14
2.727E+14	1.100E+00	1.447E-03	1.317E-14
2.609E+14	1.150E+00	1.041E-03	9.010E-15
2.500E+14	1.200E+00	1.150E-03	9.547E-15
2.400E+14	1.250E+00	6.422E-04	5.035E-15
2.308E+14	1.300E+00	7.084E-04	5.299E-15
2.222E+14	1.350E+00	7.780E-04	5.536E-15
2.143E+14	1.400E+00	8.512E-04	5.775E-15
2.069E+14	1.450E+00	9.279E-04	6.007E-15
2.000E+14	1.500E+00	1.008E-03	6.232E-15
1.935E+14	1.550E+00	9.844E-04	5.815E-15
1.875E+14	1.600E+00	1.017E-03	5.747E-15
1.818E+14	1.650E+00	1.055E-03	5.706E-15
1.765E+14	1.700E+00	1.098E-03	5.686E-15
1.714E+14	1.750E+00	1.145E-03	5.680E-15
1.667E+14	1.800E+00	1.197E-03	5.696E-15
1.622E+14	1.850E+00	1.252E-03	5.720E-15
1.579E+14	1.900E+00	1.311E-03	5.753E-15
1.538E+14	1.950E+00	1.374E-03	5.794E-15
1.500E+14	2.000E+00	1.440E-03	5.841E-15
6.000E+13	5.000E+00	1.030E-02	8.763E-15
3.000E+13	1.000E+01	4.473E-02	1.025E-14
1.500E+13	2.000E+01	1.849E-01	1.103E-14
6.000E+12	5.000E+01	1.177E+00	1.151E-14
3.000E+12	1.000E+02	4.734E+00	1.167E-14

15:01:08 MONDAY, OCTOBER 25, 1965      PROCESSOR TIME = 21.55 SECONOS      I/O TIME = 29.52 SECONOS

NUMBER OF BISECTING STEPS TAKEN= 75  
 TEMP= 10000 DEGREES K.      PRESSURE= 1.000000000+00 ATMOSPHERES

PARTITION FUNCTIONS

Q0= 1.00287680E+00	Q1= 4.43919789E+00	Q2= 6.47496687E+00
Q3= 5.12092000E+00	Q4= 1.00000000E+00	

DENSITIES IN INVERSE CM<sup>3</sup>

N0= 5.35669130E+17	N1= 9.91403413E+16	N2= 1.05582966E+12
N3= 1.28505295E+02	N4= 0.00000000E+00	
NELEC= 9.91424529E+16	NTOTL= 7.33952980E+17	

IONIZATION POTENTIAL LOWERINGS IN INVERSE CM FOR

ATOM= 7.49412317E+02    ION1= 1.49882463E+03    ION2= 2.24823695E+03    ION3= 2.99764927E+03

T= 10000 DEGREES K      N0= 5.357E+17      Q0= 1.003E+00      Q1= 4.439E+00

NU CYCLES/SEC	LAMBDA MICRONS	KAPPAPRIME INVERSE CM	EMISSION COEF WATTS/CM <sup>3</sup> SEC <sup>-1</sup>
6.000E+15	5.000E-02	5.601E+00	5.556E-10
5.455E+15	5.500E-02	1.315E+01	1.343E-17
5.000E+15	6.000E-02	1.944E+01	1.355E-16
4.615E+15	6.500E-02	2.476E+01	8.596E-16
4.286E+15	7.000E-02	2.932E+01	3.966E-15
4.000E+15	7.500E-02	3.327E+01	1.442E-14
3.750E+15	8.000E-02	3.673E+01	4.353E-14
3.333E+15	9.000E-02	4.249E+01	2.613E-13
3.000E+15	1.000E+01	4.710E+01	1.046E-12
2.857E+15	1.050E+01	3.645E+04	1.388E-17
2.000E+15	1.500E+01	7.472E+04	5.969E-16
1.500E+15	2.000E+01	1.350E+03	5.015E-15
1.200E+15	2.500E+01	2.161E+03	1.739E-14
1.000E+15	3.000E+01	3.165E+03	3.870E-14
8.571E+14	3.500E+01	4.342E+03	6.690E-14
7.500E+14	4.000E+01	5.722E+03	9.999E-14
6.667E+14	4.500E+01	7.240E+03	1.313E-13
6.000E+14	5.000E+01	8.876E+03	1.679E-13
5.455E+14	5.500E+01	6.745E+03	1.268E-13
5.000E+14	6.000E+01	8.022E+03	1.474E-13
4.615E+14	6.500E+01	3.244E+03	5.753E-14
4.286E+14	7.000E+01	3.341E+03	5.677E-14

4.000E+14	7.500E+01	3.929E-03	6.362E-14
3.750E+14	8.000E+01	4.569E-03	7.027E-14
3.529E+14	5.500E+01	5.260E-03	7.668E-14
3.333E+14	9.000E+01	3.630E-03	5.000E-14
3.158E+14	9.500E+01	4.069E-03	5.311E-14
3.000E+14	1.000E+00	4.533E-03	5.597E-14
2.857E+14	1.050E+00	5.022E-03	5.865E-14
2.727E+14	1.100E+00	4.695E-03	5.189E-14
2.609E+14	1.150E+00	3.545E-03	3.711E-14
2.500E+14	1.200E+00	3.942E-03	3.909E-14
2.400E+14	1.250E+00	2.180E-03	2.051E-14
2.308E+14	1.300E+00	2.401E-03	2.144E-14
2.222E+14	1.350E+00	2.634E-03	2.233E-14
2.143E+14	1.400E+00	2.577E-03	2.320E-14
2.069E+14	1.450E+00	3.133E-03	2.404E-14
2.000E+14	1.500E+00	3.399E-03	2.485E-14
1.935E+14	1.550E+00	3.344E-03	2.331E-14
1.875E+14	1.600E+00	3.664E-03	2.303E-14
1.818E+14	1.650E+00	3.600E-03	2.287E-14
1.765E+14	1.700E+00	3.753E-03	2.279E-14
1.714E+14	1.750E+00	3.921E-03	2.278E-14
1.667E+14	1.800E+00	4.104E-03	2.263E-14
1.622E+14	1.850E+00	4.300E-03	2.292E-14
1.579E+14	1.900E+00	4.510E-03	2.306E-14
1.538E+14	1.950E+00	4.732E-03	2.322E-14
1.500E+14	2.000E+00	4.967E-03	2.341E-14
6.000E+13	5.000E+00	3.686E-02	3.512E-14
3.000E+13	1.000E+01	1.600E-01	4.107E-14
1.500E+13	2.000E+01	6.643E-01	4.422E-14
6.000E+12	5.000E+01	4.238E+00	4.613E-14
3.000E+12	1.000E+02	1.706E+01	4.677E-14

15101110 MONDAY, OCTOBER 25, 1965      PROCESSOR TIME = 22.93 SECONOS      I/O TIME = 30.27 SECONOS

LABEL 0 GEIL 0 CHURCH000652987 EXECUTE DOUBLE/GEIL

R0636EG

Symbol Table for DICSLAB (c) and DICKCYL (d)

ZBAR =  $\bar{Z}$  = mean ionic charge

DELTE[i] =  $\delta_{T_\epsilon}$  for the ith given value of  $\bar{Z}$ . A correction factor to the electrical conductivity  $\sigma$ .

DELTk[i] =  $\delta_{T_k}$  for the ith given value of  $\bar{Z}$ . A correction factor to the thermal conductivity.

Z[i] = the ith integral value of  $\bar{Z}$ , at which  $\delta_{T_\epsilon}$  and  $\delta_{T_k}$  are tabulated

KAPPA[t,λ] =  $\kappa$ , for temperature t and wavelength λ

D = thickness of plasma

NT = number of temperatures to be solved for (they must be in equal increments)

NLAMBDA = number of wavelengths to be solved for

P = pressure

FNU[j] = input as jth wavelength, changed within program to jth energy  $h\nu$

BT = lowest temperature desired

DT = temperature step size

ET = maximum temperature desired

T = current temperature

THETA = temperature in eV

KAPPAPRIME[j] =  $\kappa'$  at jth frequency and current temperature

NE = electron density

NTOTAL = total particle density

N = heavy particle density

M = average number of electrons per heavy particle

SIGMA = electrical conductivity

KK = thermal conductivity

TAU =  $\kappa'D$

EI = approximation to exponential integral  $\int_1^\infty \frac{e^{-\tau u}}{u} du$

FNU[j] =  $F_\nu(j)$  = spectral radiant emittance corresponding to jth given energy  
 $h\nu(j)$

BNU[j] = the Planck function for the jth given energy

FNUDNU = radiant emittance between energies bounding optically thick or thin regions ( $\tau > 3$  or  $\tau < 3$  respectively)

SUM = total radiant emittance =  $\int_0^{\infty} F_{\nu} d\nu$

EXPO =  $1 - e^{-K'D}$

Note: The electric field, E, and current density, J, are calculated within the write statement following the printout of SUM. The quantities  $h\nu$ ,  $\lambda$ ,  $K'$ ,  $\tau$ ,  $1 - e^{-\tau}$ ,  $B_{\nu}$ , the spectral radiance  $I_{\nu}$ , and  $F_{\nu}$  are printed out in the final write statement, and  $\lambda$ ,  $\tau$ , and  $I_{\nu}$  are calculated there.

Procedure CHOP prints out  $\int_{\lambda_1}^{\lambda_2} F_{\nu} d\nu$  where  $\lambda_1$  and  $\lambda_2$  are the bounds on optically thick or thin region

Procedure INTERP does a linear interpolation to find the value of  $\delta_{T_e}$  or  $\delta_{T_k}$  corresponding to a given value of  $Z$ .

Procedure SIMPSON performs a numerical integration (used in DICKCYL only)

LPHI = minimum  $\phi$  value at which integral will be calculated during integration.

MPHI = maximum  $\phi$  value at which integral will be calculated during integration.

LENGTH = length of ray from point  $R_i$  to cylinder wall in PHI direction

N = maximum number of intervals into which ray may be divided (input).

NDS = actual number of intervals into which a particular ray is divided.

DS = step size along a particular ray.

APPR $\phi$ XDS = approximate step size (input)

DS =  $\frac{\text{LENGTH}}{\min(\text{NDS}, \text{N})}$  where NDS is an integer such that  $\text{NDS} \geq \frac{\text{LENGTH}}{\text{APPR}\phi\text{XDS}} > \text{NDS}-1$ .

S = point along ray at which integrand is numerically evaluated.

LS = minimum value of S along a particular ray.

MS = maximum value of S along a particular ray.

RSMXY = radial distance from axis of cylinder to point S.

TM = temperature at the radial distance RSMXY.

KIM = interpolated value of KAPPA at ILAMBDA<sub>A</sub> wavelength and temperature TM.

IBB = Planck function = amount of radiation emitted by a black body as a function of frequency and temperature.

YMT = value of the integrand (without multiplier DLAMBDA [ILAMBDA] x DS x COS( $\phi$ ) x DPHI x (-4)).

SUMF = total flux at point  $R_i$  (output).



```

SUM=SUM+NUDUS
PNUONU=0$                                SC 21 4813
LDW+JS                                SC 21 4410
END OF PROCEDURE CHOP$                   SC 21 4413
PROCEDURE INTERP(DT$,DELT$) REAL DT$, ARRAY DELT()
BEGIN                                     SC 21 4512
LABEL JUMPS                               SC 21 4710
                                         SC 21 4710
                                         SC 21 4710
J001                                     START OF SEGMENT ***** 0007
IF ZBAR47CHP6Z$J THEN BEGIN           SC 71 010
    DT$=DELT(J)=DELT(J)+DELT(J-1)*TEMP=ZBAR$/
    (TEMP=Z(J-1)) ; GO JUMP EN0$          SC 71 110
JUMPS                                     SC 71 110
                                         SC 71 612
                                         SC 71 1113
                                         SC 71 1210
END OF PROCEDURE INTERP$                 0007 IS 0013 LONG, NEXT SEG 0002

LABEL START,EXITS
TIMEIT(DELT())
FILL DELT(+) WITH 0.,5816.,6833.,7849.,9225.,13
                                         SC 21 4710
                                         SC 21 4710
                                         SC 21 4810
START OF SEGMENT ***** 0008
FILL DELT(+) WITH 0.,225.,356.,513.,791.,13
                                         SC 21 4913

```

```

FILL Z (*) WITH 0,1,2,4,16,100} SC 21 5112
READ(PASSKAPPA,*,&BT,&DT,&ET)} START OF SEGMENT **** 0010
WRITE(GEIL,DEBUG,&BT,&DT,&ET)} 0010 IS 0006 LONG, NEXT SEG 0002
NT=(ET-BT)/DT} SC 21 5311
READ(PASSKAPPA,*,&NLAMBDA)} SC 21 5610
WRITE(GEIL,DEBUG,&NLAMBDA)} SC 21 6913
READ(PASSKAPPA,&NLAMBDA+1,&HNUC*)} SC 21 8011
WRITE(GEIL,DEBUG,FOR IT=0 STEP 1 UNTIL NLAMBDA DO HNUC(IT)} SC 21 8210
READ(READER,TITLE)EXIT} WRITE(GEIL,PAGE)} WRITE(GEIL,TITLE)} SC 21 8913
WRITE(GEIL,DESCRIPTION)} SC 21 9711
READ(READER,/*D*/} SC 21 10111
READ(READER,TITLE)EXIT} WRITE(GEIL,PAGE)} WRITE(GEIL,TITLE)} SC 21 11311
WRITE(GEIL,DESCRIPTION)} SC 21 12312
READ(READER,/*D*/} SC 21 12612
READ(READER,/*D*/} SC 21 13413
NNUO=NLAMBDA} SC 21 13612
FOR J=1 STEP 1 UNTIL NLAMBDA DO HNUC(J)=1.2397/HNUC(J)} SC 21 13713
NNUCLAMBDA=0.12397 SC 21 14211
BEGIN SC 21 14410
ARRAY BNK,KAPPAPRIME,NNUO>NNNUJ} SC 21 14610
START OF SEGMENT ***** 0021
IT=1} SC 111 311
FOR I=1 STEP 1 UNTIL ET-1 DO BEGIN SC 111 461

```

\*\*\*\*\*

```

WRITE(GEIL,WRITE377)} SC 111 510
IT=IT+1} SC 111 1271
YTHETA=IT/11605} SC 111 1312
READ(PASSKAPPA,NLAMBDA,KAPPAT,I,*)} SC 111 1473
WRITE(GEIL,DEBUG,FOR J=1 STEP 1 UNTIL NLAMBDA DO KAPPAC(IT,J)} SC 111 1610
READ(PASSKAPPA,NLAMBDA,KAPPAT,I,*)} SC 111 1613
WRITE(GEIL,DEBUG,P7)} SC 111 3011
WRITE(GEIL,DEBUG,P7)} SC 111 4113
PnP/7601} SC 111 4611
WRITE(GEIL,PP28,P7)} SC 111 5012
WRITE(GEIL,PP28,P7)} SC 111 6011
FOR J=1 STEP 1 UNTIL NLAMBDA DO KAPPAPRIME(I,J)=KAPPAC(IT,J)} SC 111 6310
READ(PASSKAPPA,NLAMBDA,KAPPA,I,*)} SC 111 6610
WRITE(GEIL,DEBUG,NE,NTOTE)} SC 111 7813
NTOTE=NE} SC 111 8811
NODENS} SC 111 8912
IF NE>3 THEN ZBAR=1 ELSE SC 111 9013
ZBAR=M**.25/V1} SC 111 9213
INTERP(DTE,DELTE)} SC 111 9413
INTERP(DTK,DELTk)} SC 111 9511
DENOM=ZBARM*.434294481903X { PRINT+ LNC(2.401*20*XTHETA+3/
(ZBAR*2*XNN*(1+ZBAR*XNN)))} SC 111 9913
SIGMA=286*X0THETA+3*XOTE/DENOM} SC 111 10212

```

```

KK=.2465XSQTHETA+5XDTK/OCENOMS
WRITE(GEIL    )3
WRITE(GEIL,SIGMAK,PRINT,SIGMA,KK)
FOR J=1 STEP 1 UNTIL NHNU DO BEGIN
TAU*KAPPAPRIME(J)KD1
IF TAU>1 THEN
E1=-.57721566+TAUXC,.99999193+TAUC(-.24991055+TAUXC,.05519968+TAUX
(-.00976004+TAUXC,.00107857)) ELSE
E1+EXP(-TAU/TAU+0.330657*TAU+.250621)/
(TAU=2+3.330657*TAU+1.681534))
BNUE(J)=FACT(TEMP1+HNUE(J)+3/(EXP(TEMP1/THETA)-1))
FHNU(J)=3.330657*HNUE(J)      RECALL(TAU=1)HEXP(-TAU)+TAU+BNE1)
END OF J LOOPS
WRITE(GEIL,CDALJ)
OB48/32
SUM=0;
L0H=18
TEMP0=KAPPAPRIME(J)+BNE1)
FNUONU=FNU(1)*(HNUE(1)-HNUE(2))
IF FNUONU>0 THEN T0H=18 ELSE
T0H=178
DO100: THEN CH0PS
FOR J=2 STEP 1 UNTIL NHNU DO BEGIN
IF TEMP0>TEMP1(KAPPAPRIME(J)=0) THEN CH0PS

```

SC 111 11011  
SC 111 11480  
SC 111 11613  
SC 111 12111  
SC 111 13210  
SC 111 13312  
SC 111 13481  
SC 111 13711  
SC 111 14111  
SC 111 15210  
SC 111 15510  
SC 111 16012  
SC 111 16912  
SC 111 17211  
SC 111 17312  
SC 111 17411  
SC 111 17510  
SC 111 17811  
SC 111 18043  
SC 111 18213  
SC 111 19113  
SC 111 19410

```

DNUE(HNUE(J)+BNE1)
FNUONU=FNUONU*TEMP0*BNUE(J)*HNUE(J)
END OF J LOOPS
CM00P
WRITE(GEIL,FINAL,0UM)
WRITE(GEIL,EJ,TEMP+3GRY(2*SUM/(SIGNA0)),SIGNA0TEMP)
WRITE(GEIL,00000000)
WRITE(GEIL,TITLE,PCOT3THETA,TEMP1+(1+HNUE,N,
TEMP+11605*THETA,TEMP1*TEMP/(2.687019*273)))
WRITE(GEIL,L0H,PRINT,PNR,J=1 STEP 1 UNTIL NHNU DO (TEMP1+HNUE(J),
1.23977*TEMP1, TEMP0KAPPAPRIME(J), TEMP0,
EXPN+1=EXP(-TEMP0),BNUE(J),EXPON*BNUE(J),FNU(J)))
WRITE(GEIL,00000000)
END OF THETA LOOPS
TIMEIT(GEIL)
END DYNAMIC(NNU).

```

SC 111 19813  
SC 111 20110  
SC 111 20312  
SC 111 20513  
SC 111 20811  
SC 111 21411  
SC 111 22811  
SC 111 23110  
SC 111 24012  
SC 111 25311  
SC 111 26113  
SC 111 27111  
SC 111 28611  
SC 111 29410

```

EXIT1 ENO.
0011 IS 0299 LONG, NEXT SEG 0002
SC 21 14610
0002 IS 0150 LONG, NEXT SEG 0001

```

EXP	IS SEGMENT NUMBER 0012, PRT ADDRESS IS 0207	
LN	0013	0205
SORT	0014	0176
OUTPUT(W)	0015	0035

BLOCK CONTROL	0016	0005
INPUT(8)	0017	0161
GO TO SOLVER	0018	0167
ALGOL WRITE	0019	0014
ALGOL READ	0020	0015
ALGOL SELECT	0021	0016

NUMBER OF ERRORS DETECTED = 000

LAST CARD WITH ERROR WAS SEQ #

PNT SIZE=0141) TOTAL SEGMENT SIZE=00296 WORDS) DISK STORAGE REQ.=01075 WORDS) NO. SEGS.=0022.

ESTIMATED CORE STORAGE REQUIREMENT = 06298 WORDS.

17:11:49 MONDAY, OCTOBER 25, 1965 PROCESSOR TIME = 13.00 SECONDS I/O TIME = 33.73 SECONDS

LABEL 00000000LINE 000652989 COMPILE DICSLAB BY GEIL IN ALGOL TO LIBRARY

R0630EG

LABEL 000000000GEIL 00065299? EXECUTE D16SLAB BY GEIL

R0636EG

1711154 MONDAY, OCTOBER 29, 1968

9.00000000E+03	1.00000000E+03	1.00000000E+04		
5.30000000E+01				
0.00000000E+00	5.00000000E-02	5.50000000E-02	6.00000000E-02	6.50000000E-02
7.00000000E-02	7.50000000E-02	8.00000000E-02	9.00000000E-02	1.00000000E-01
1.05000000E-01	1.30000000E-01	2.00000000E-01	2.50000000E-01	3.00000000E-01
3.50000000E-01	4.00000000E-01	4.50000000E-01	5.00000000E-01	5.50000000E-01
6.00000000E-01	6.50000000E-01	7.00000000E-01	7.50000000E-01	8.00000000E-01
8.50000000E-01	9.00000000E-01	9.50000000E-01	1.00000000E+00	1.05000000E+00
1.10000000E+00	1.15000000E+00	1.20000000E+00	1.25000000E+00	1.30000000E+00
1.35000000E+00	1.40000000E+00	1.45000000E+00	1.50000000E+00	1.55000000E+00
1.60000000E+00	1.65000000E+00	1.70000000E+00	1.75000000E+00	1.80000000E+00
1.85000000E+00	1.90000000E+00	1.95000000E+00	2.00000000E+00	2.05000000E+00
1.00000000E+01	2.00000000E+01	5.00000000E+01	1.00000000E+02	5.00000000E+02

XENON  
PLANE PARALLEL SLAB FOR HOMOGENEOUS TEMPERATURE, NEGLECTING THERMAL CONDUCTIVITY  
T= 9000 DEGREES

	1.770591229E+01	2.617463859E+01	3.334011639E+01	3.948212759E+01
4.480520559E+01	4.946290059E+01	5.722572979E+01	6.343599439E+01	1.347456539E+01
2.759479249E+01	4.986132949E+01	7.900433507E+01	1.154762139E+01	1.582397899E+01
2.082341739E+01	2.635711399E+01	3.236033409E+01	2.367541339E+01	2.815702719E+01
9.768478829E+01	1.014361968E+01	1.193556699E+01	1.388486539E+01	1.599427239E+01
1.137262099E+01	1.073328779E+01	1.421160459E+01	1.574719399E+01	1.447250919E+01
1.040785769E+01	1.159133719E+01	6.422264209E+01	7.083765279E+01	7.780304319E+01
8.911999139E+01	9.278934769E+01	1.008126519E+01	9.843529319E+01	1.017363409E+01
1.055421359E+01	1.098187629E+01	1.149376709E+01	1.196746739E+01	1.252091639E+01
1.311234439E+01	1.374224289E+01	1.440328429E+01	1.039091189E+01	1.472800919E+01
1.849085759E+01	1.176815749E+01	4.734358019E+00		
7.600000009E+02				
0.00 1.00	FM 1.00 ATM			

4.778045110E+00 6.193033819E+01

LN CANADA = 7.0860E+00  
ELECTRICAL CONDUCTIVITY SIGMA = 3.7029E+01 INVERSE OHMS INVERSE CM  
THERMAL CONDUCTIVITY K = 9.5729E-03 WATTS/CM DEGREES

FROM NUM=0.00 TO NUM=0.025 THE VALUE OF THE INTEGRAL OF FNU IS 3.6129E+00 WATTS/CM<sup>2</sup>  
FROM NUM=11.807 TO NUM= 0.012 THE VALUE OF THE INTEGRAL OF FNU IS 1.1379E+02 WATTS/CM<sup>2</sup>  
FROM NUM= 0.012 TO NUM= 0.012 THE VALUE OF THE INTEGRAL OF FNU IS 2.3199E-02 WATTS/CM<sup>2</sup>

THICK  
THIN  
THICK

REFRACTIVE INDEX = 1.1272E+00  
REFRACTIVE INDEX = 2.9160E+00 VOLTS/CM  
CURRENT DENSITY J<sub>W</sub> = 0.2800481 AMP/CM<sup>2</sup>

THETA=0.78 EV NTOTAL=8.1559E+17 NOENSITY=7.6779E+17 PARTICLES/CM<sup>3</sup>  
T= 9000.0 DEGREES K<sub>0</sub> P=1.0010E+00 ATM

NU	WAVELENGTH EV	KAPPA-PRIME MICRONS	TAU 1/CM	(-TAU) 1-E	BNU	INU WATTS/CM STER	FNU WATTS/CM
2.00794	5.0000E-02	7.5448E+00	7.5448E+00	9.9959E-01	1.2449E-10	1.2449E-10	3.1539E-06
2.00560	5.0000E-02	1.07719E+01	1.07719E+01	1.0000E+00	1.7109E-09	1.7109E-09	4.3339E-05
2.00562	6.0000E-02	8.66178E+01	2.6179E+01	1.0000E+00	1.4849E-08	1.4849E-08	3.7619E-04
17.072	8.5000E-02	3.9330E+01	3.9330E+01	1.0000E+00	9.0039E-08	9.0039E-08	2.2979E-03
17.710	7.0000E-02	3.9489E+01	3.9489E+01	1.0000E+00	4.2049E-07	4.2049E-07	1.0659E-02
16.529	7.5000E-02	4.4819E+01	4.4819E+01	1.0000E+00	1.5669E-06	1.5669E-06	3.9699E-02
18.494	8.0000E-02	4.9466E+01	4.9466E+01	1.0000E+00	4.8909E-06	4.8909E-06	1.2399E-01
22.774	9.0000E-02	9.7237E+01	5.7230E+01	1.0000E+00	3.1639E-05	3.1639E-05	8.0159E-01
12.397	1.0000E-01	6.3848E+01	6.3848E+01	1.0000E+00	1.3629E-04	1.3629E-04	3.4519E+00
11.807	1.0500E-01	1.3489E+01	1.3489E+01	1.0000E+00	2.5199E-04	3.3949E-05	1.7209E-03
8.265	1.5000E-01	2.7599E+01	2.7599E+01	2.7599E+01	5.3189E-03	2.2058E-06	1.1639E-01
6.199	2.0000E-01	4.9669E+01	4.9669E+01	4.9669E+01	5.0409E-03	2.5029E-05	1.2688E+00
8.939	2.3000E-01	7.9388E+01	7.9068E+01	7.9059E+01	1.2789E-01	1.0109E-04	5.1209E+00
4.932	3.0000E-01	1.1559E+01	1.1559E+01	1.1549E+01	2.1939E-01	2.4459E-04	1.2609E+01
3.932	3.9000E-01	1.9382E+01	1.9382E+01	1.9381E+01	2.9199E-01	4.6169E-04	2.3409E+01
3.079	4.0000E-01	2.0829E+01	2.0829E+01	2.0828E+01	3.4909E-01	7.2559E-04	3.6709E+01
2.753	4.5000E-01	2.6369E+01	2.6369E+01	2.6329E+01	3.8519E-01	1.0169E-03	5.1529E+01
2.479	5.0000E-01	3.2369E+01	3.2369E+01	3.2319E+01	4.0679E-01	1.3149E-03	6.6609E+01
2.254	5.5000E-01	2.3689E+01	2.3689E+01	2.3659E+01	4.1459E-01	9.8039E-04	4.9699E+01
2.066	6.0000E-01	2.8169E+01	2.8169E+01	2.8129E+01	4.1349E-01	1.1629E-03	5.8919E+01
1.907	6.5000E-01	9.7689E+00	9.7689E+00	9.7649E+00	4.0609E-01	3.9649E-04	2.0099E+01
1.771	7.0000E-01	1.0149E+01	1.0149E+01	1.0149E+01	3.9469E-01	4.0009E-04	2.0279E+01

1.653	7.500E-01	1.194E-03	1.194E-03	1.193E-03	3.806E-01	4.541E-04	2.301E+01
1.650	9.000E-01	1.309E-03	1.309E-03	1.309E-03	3.653E-01	5.070E-04	2.570E+01
1.648	8.500E-01	1.600E-03	1.600E-03	1.599E-03	3.494E-01	5.586E-04	2.831E+01
1.637	9.000E-01	1.137E-03	1.137E-03	1.137E-03	3.334E-01	3.789E-04	1.920E+01
1.635	9.500E-01	1.275E-03	1.275E-03	1.275E-03	3.176E-01	4.949E-04	2.051E+01
1.623	1.000E+00	1.421E-03	1.421E-03	1.420E-03	3.022E-01	4.292E-04	2.175E+01
1.611	1.050E+00	1.575E-03	1.575E-03	1.573E-03	2.875E-01	4.524E-04	2.293E+01
1.600	1.100E+00	1.647E-03	1.647E-03	1.646E-03	2.733E-01	3.954E-04	2.004E+01
1.588	1.150E+00	1.041E-03	1.041E-03	1.040E-03	2.601E-01	2.705E-04	1.371E+01
1.573	1.200E+00	1.159E-03	1.159E-03	1.158E-03	2.475E-01	2.867E-04	1.453E+01
1.562	1.250E+00	6.422E-04	6.422E-04	6.420E-04	2.355E-01	1.512E-04	7.664E+00
1.554	1.300E+00	7.084E-04	7.084E-04	7.084E-04	2.243E-01	1.580E-04	9.050E+00
1.549	1.350E+00	7.780E-04	7.780E-04	7.777E-04	2.137E-01	1.662E-04	8.425E+00
1.546	1.400E+00	8.512E-04	8.512E-04	8.508E-04	2.036E-01	1.734E-04	6.789E+00
1.535	1.450E+00	9.270E-04	9.279E-04	9.275E-04	1.945E-01	1.804E-04	9.141E+00
1.526	1.500E+00	1.008E-03	1.008E-03	1.008E-03	1.857E-01	1.871E-04	9.463E+00
1.519	1.550E+00	9.844E-04	9.844E-04	9.844E-04	1.775E-01	1.748E-04	5.848E+00
1.511	1.600E+00	1.017E-03	1.017E-03	1.017E-03	1.697E-01	1.726E-04	8.745E+00
1.504	1.650E+00	1.055E-03	1.055E-03	1.055E-03	1.624E-01	1.713E-04	5.682E+00
1.497	1.700E+00	1.098E-03	1.098E-03	1.098E-03	1.555E-01	1.707E-04	8.632E+00
1.490	1.750E+00	1.145E-03	1.145E-03	1.145E-03	1.491E-01	1.706E-04	8.648E+00
1.489	1.800E+00	1.197E-03	1.197E-03	1.197E-03	1.430E-01	1.710E-04	6.666E+00
1.470	1.850E+00	1.232E-03	1.232E-03	1.231E-03	1.372E-01	1.717E-04	8.701E+00
1.462	1.900E+00	1.311E-03	1.311E-03	1.310E-03	1.318E-01	1.727E-04	8.752E+00
1.456	1.950E+00	1.374E-03	1.374E-03	1.373E-03	1.266E-01	1.739E-04	6.814E+00
1.442	2.000E+00	1.440E-03	1.440E-03	1.439E-03	1.218E-01	1.753E-04	8.685E+00
1.438	5.000E+00	1.039E-02	1.039E-02	1.038E-02	2.533E-02	2.618E-04	1.327E+01
1.424	1.000E+01	4.673E-02	4.673E-02	4.674E-02	6.680E-03	3.009E-04	1.327E+01
1.412	2.000E+01	1.849E-01	1.849E-01	1.848E-01	1.792E-03	3.095E-04	1.526E+01
1.402	5.000E+01	1.177E+00	1.177E+00	1.176E+00	2.937E-04	2.031E-04	6.154E+00
1.392	1.000E+02	4.734E+00	4.734E+00	4.912E-01	7.401E-05	7.336E-05	1.871E+00

T= 10000 DEGREES

5.601618418E+00	1.631671912E+01	1.943582115E+01	2.475590789E+01	2.931630938E+01
3.326903919E+01	3.072769938E+01	4.249161699E+01	4.710291078E+01	3.045152338E+01
7.47164119E+04	1.34957127E+03	2.160576079E+03	3.16530231E+03	4.341928889E+03
5.72203667E+03	7.24014722E+03	8.87604714E+03	6.74481466E+03	9.02248167E+03
3.24382229E+03	3.24123442E+03	3.92927136E+03	4.56868346E+03	5.26031188E+03
3.62967234E+03	4.669223912E+03	4.33345379E+03	3.02223651E+03	4.6948336E+03
3.56529328E+03	3.947748568E+03	2.160422588E+03	2.401336739E+03	2.63383431E+03
3.87739966E+03	3.12801649E+03	3.399284677E+03	3.34410800E+03	3.46357410E+03
3.60024052E+03	3.75304458E+03	3.921087499E+03	4.10360444E+03	4.29994097E+03
4.50953410E+03	4.73189711E+03	4.966607309E+03	3.68553866E+02	1.60016295E+01
6.64264922E+01	4.287957988E+00	1.70631389E+01		
7.60000000E+00				

DE 1.00 PR 1.00 ATM

9.914245298+14 7.339429800+17

LN LAMBDA = 6.6538+00  
ELECTRICAL CONDUCTIVITY SIGMAS = 4.6050+01 INVERSE CMWS INVERSE CM  
THERMAL CONDUCTIVITY K = 1.3230+02 WATTS/CM DEGREES

FROM NU=94.794 TO NU= 12.397 THE VALUE OF THE INTEGRAL OF FNU IS 1.5608401 WATTS/CM<sup>2</sup>  
FROM NU=11.807 TO NU= 9.612 THE VALUE OF THE INTEGRAL OF FNU IS 4.5958+02 WATTS/CM<sup>2</sup>  
FROM NU= 9.025 TO NU= 9.012 THE VALUE OF THE INTEGRAL OF FNU IS 1.2818+01 WATTS/CM<sup>2</sup>

THICK  
THIN  
THICK

RADIANT EMITTANCE FR = 8.8038+02 WATTS/CM<sup>2</sup>  
ELECTRIC FIELD E = 4.6053+00 VOLTS/CM  
CURRENT DENSITY J = 2.1210+02 AMP/CM<sup>2</sup>

THETABG=0.86 EV NTOTAL=7.3408+17 NDENSITY=6.3400+17 PARTICLES/CM<sup>3</sup>  
TAU = 10000.0 DEGREES C. P=1.0010+00 ATM

NU EV	WAVELENGTH MICRONS	KAPPA-PRIME 1/CM	TAU	(=TAU)	FNU WATTS/CM <sup>2</sup> STER	INU WATTS/CM <sup>2</sup>
24.794	5.0000+02	5.6010+00	5.6010+00	9.9630+01	3.0440+00	3.0330+00
22.547	5.5000+02	1.3150+01	1.3150+01	1.0000+00	3.1240+00	3.1240+00
20.662	6.0000+02	1.9440+01	1.9440+01	1.0000+00	2.1310+07	2.1310+07
19.072	6.5000+02	2.4760+01	2.4760+01	1.0000+00	1.0600+06	1.0600+06
17.710	7.0000+02	2.9320+01	2.9320+01	1.0000+00	4.1250+06	4.1250+06
16.529	7.5000+02	3.3270+01	3.3270+01	1.0000+00	1.3200+05	1.3200+05
15.495	8.0000+02	3.6730+01	3.6730+01	1.0000+00	3.6070+05	3.6070+05
13.774	9.0000+02	4.2400+01	4.2400+01	1.0000+00	9.1400+01	9.1400+01
12.397	1.0000+01	4.7100+01	4.7100+01	1.0000+00	1.5680+04	1.5680+04
11.807	1.0500+01	3.6450+04	3.6450+04	1.0000+00	5.7500+04	5.7500+04
0.265	1.5000+01	7.8720+04	7.8720+04	1.0000+00	4.2070+07	4.2070+07
0.197	2.0000+01	1.3500+03	1.3500+03	1.0000+00	1.8030+05	1.8030+05
0.140	2.5000+01	2.1610+03	2.1610+03	1.0000+00	1.3120+04	1.3120+04
0.132	3.0000+01	3.1650+03	3.1650+03	1.0000+00	2.4200+01	2.4200+01
0.982	3.5000+01	4.3420+03	4.3420+03	1.0000+00	3.6820+01	3.6820+01
3.098	4.0000+01	5.7220+03	5.7220+03	1.0000+00	4.0380+01	4.0380+01
2.795	4.5000+01	7.2400+03	7.2400+03	1.0000+00	5.2520+01	5.2520+01
2.479	5.0000+01	8.8740+03	8.8740+03	1.0000+00	6.0370+01	6.0370+01
2.294	5.5000+01	6.7850+03	6.7850+03	1.0000+00	5.0280+01	5.0280+01
2.034	6.0000+01	8.0220+03	8.0220+03	1.0000+00	3.8110+01	3.8110+01
1.907	6.5000+01	3.2840+03	3.2840+03	1.0000+00	4.4120+01	4.4120+01
1.771	7.0000+01	3.3410+03	3.3410+03	1.0000+00	1.7260+01	1.7260+01
					1.7030+01	1.7030+01
					8.6340+01	8.6340+01

1.083	7.5000+01	3.7290+03	3.9200+03	3.9220+03	4.8050+01	1.9080+03	9.6730+01
1.550	8.0000+01	4.5690+03	4.5690+03	4.5580+03	4.6220+01	2.1070+03	1.0680+02
1.455	8.5000+01	5.2100+03	5.2800+03	5.2470+03	4.3500+01	2.2990+03	1.1650+02
1.377	9.0000+01	3.6300+03	3.6300+03	3.6230+03	4.1460+01	1.5020+03	7.6140+01
1.375	9.5000+01	4.0600+03	4.0600+03	4.0610+03	3.9220+01	1.5930+03	8.0730+01
1.280	1.0000+00	4.5330+03	4.5330+03	4.5230+03	3.7090+01	1.6780+03	8.5040+01
1.181	1.0300+00	3.0220+03	5.0220+03	5.0220+03	9.0100+03	3.5090+01	8.0100+01
1.127	1.1000+00	4.6950+03	4.6950+03	4.6840+03	3.3210+01	1.7380+03	8.8840+01
1.075	1.1500+00	3.5450+03	3.5450+03	3.5390+03	3.1480+01	1.5510+03	7.8840+01
1.033	1.2000+00	3.0420+03	3.0420+03	3.0420+03	3.1480+01	1.1130+03	5.6400+01
0.992	1.2500+00	2.1800+03	2.1800+03	2.1780+03	2.9790+01	1.1720+03	5.0410+01
0.954	1.3000+00	2.4010+03	2.4010+03	2.3980+03	2.8250+01	6.1540+04	3.1190+01
0.918	1.3500+00	2.6300+03	2.6300+03	2.6340+03	2.6620+01	6.4320+04	3.2600+01
0.886	1.4000+00	2.8770+03	2.8770+03	2.8730+03	2.5470+01	8.7000+04	3.3960+01
0.855	1.4500+00	3.1330+03	3.1330+03	3.1280+03	2.4420+01	6.9590+04	3.5270+01
0.824	1.5000+00	3.3990+03	3.3990+03	3.3940+03	2.3050+01	7.2090+04	3.6540+01
0.800	1.5500+00	3.3440+03	3.3440+03	3.3440+03	2.1960+01	7.4510+04	3.7770+01
0.775	1.6000+00	3.4640+03	3.4640+03	3.4680+03	2.0930+01	6.9480+04	3.5420+01
0.751	1.6500+00	3.6000+03	3.6000+03	3.5940+03	1.9980+01	6.9070+04	3.5010+01
0.729	1.7000+00	3.7530+03	3.7530+03	3.7460+03	1.9050+01	6.8760+04	3.4750+01
0.708	1.7500+00	3.9210+03	3.9210+03	3.9130+03	1.8240+01	6.8390+04	3.4630+01
0.689	1.8000+00	4.1040+03	4.1040+03	4.0950+03	1.7350+01	6.8290+04	3.4610+01
0.670	1.8500+00	4.3000+03	4.3000+03	4.2910+03	1.6510+01	6.8420+04	3.4680+01
0.652	1.9000+00	4.5100+03	4.5100+03	4.4900+03	1.6010+01	6.8700+04	3.4820+01
0.635	1.9500+00	4.7320+03	4.7320+03	4.7210+03	1.5360+01	6.9090+04	3.5020+01
0.620	2.0000+00	4.9670+03	4.9670+03	4.9540+03	1.4740+01	6.9370+04	3.5270+01
0.606	2.0500+00	3.6540+02	3.6540+02	3.6180+02	1.4160+01	7.0130+04	3.5530+01
0.592	1.0000+01	1.5700+01	1.5700+01	1.4700+01	1.3620+02	1.0350+03	5.2530+01
0.582	2.0000+01	5.6430+01	5.6430+01	4.8540+01	7.7070+03	1.1400+03	5.7630+01
0.573	5.0000+01	4.2380+00	4.2380+00	3.8560+01	3.2680+04	9.7100+04	4.2090+01
0.562	1.0000+02	1.7060+01	1.7060+01	1.0000+00	8.2300+05	9.2300+05	2.0850+00



FORMAT FORGOT("SIMPSON REQUIRED EVEN NUMBER OF POINTS")

SC 21 2381

START OF SEGMENT \*\*\*\*\* 0009

0009 IS 0010 LONG, NEXT SEG 0002

FORMAT TITLE("NAME OF THE GAS IS READ FROM TITLE CARD"),

SC 21 2381

START OF SEGMENT \*\*\*\*\* 0010

DPC("D=",F5.2,X5,"P=", F7.2," ATM"),

SC 101 2811

WR1ET("T=",I6," DEGREES"),

SC 101 2811

DESCRIPTION("CYLINDER FOR HOMOGENEOUS TEMPERATURE")

SC 101 2811

"> NEGLECTING THERMAL CONDUCTIVITY"),

SC 101 2811

DOUT("D=",R9.4),

SC 101 2811

NTHETA("N=",R9.0,X5,"THETA=",R5.2," EV"),

SC 101 2811

IM("N",X6,I[M]/[1,F10.3]),

SC 101 2811

IMS("I[M+1/2]"= ,F8.4,X5,"I[M+1/2]"= ,F8.4),

SC 101 2811

NIS("N",E10.1),

SC 101 2811

TITLEPLOT(X10,"THETA=",F4.2," EV",X7,"NTOTAL=",E0.3,X7,"DENSITY=",E0.3,

SC 101 2811

" PARTICLES/CM3" /

SC 101 2811

X16,"T=",F8.1," DEGREES K," X7,"P=",E9.3," ATM" //

SC 101 2811

" HNU WAVELENGTH KAPPA=PRIME"

SC 101 2811

" TAU (=-TAU) BNU,"

SC 101 2811

X11,"INUM" ,X11,"FNU" /

SC 101 2811

" EV MICRONS 1/CM" ,X23,"1-E" ,X14,"WATTS/UM STER",

SC 101 2811

X11,"WATTS/CM" /

SC 101 2811

);

SC 101 2811

LISPLOT(F7.3,E12.3,6E14.3),

SC 101 2811

MBAR("AFTER",IS," ITERATIONS, MBAR=",E10.3," WHERE N=KE=",E10.3))

SC 101 2811

0010 IS 0166 LONG, NEXT SEG 0002

DEFINE JO01FOR J=0 STEP 1 UNTIL 6 DO #;

SC 21 2811

JO01FOR J=1 STEP 1 UNTIL 6 DO #;

SC 21 2811

PROCEDURE CHOP\$ BEGIN

SC 21 2811

WR1ET(GE1,L,NHNU[L],NHNU[J],ABS(FNUONU),TKTN)

SC 21 2811

IF TKTN==" THICK" THEN TKTN==" THIN " ELSE TKTN==" THICK");

SC 21 4211

SUM=SUM+FNUONU)

SC 21 4713

FNUONU=0)

SC 21 4910

L=N+J;

SC 21 4913

END OF PROCEDURE CHOP\$;

SC 21 5012

PROCEDURE INTERP(DT,DELT)\$ REAL DT\$ ARRAY DELT[0]

SC 21 5210

BEGIN

SC 21 5210

LABEL JUMP\$

SC 21 5210

JO01

START OF SEGMENT \*\*\*\*\* 0011

SC 111 010

IF ZBAR<TEMP+Z[J] THEN BEGIN

SC 111 110

DT=DELT[J]=(DELT[J]-DELT[J-1])\*(TEMP-ZBAR)/

SC 111 310

(TEMP+Z[J-1]) J GO JUMP END;

SC 111 612

JUMP\$

SC 111 1113

END OF PROCEDURE INTERP\$

SC 111 1210

0011 IS 0013 LONG, NEXT SEG 0002

```

REAL SC 21 5210
PROCEDURE SIMPSUM(A,B,X,Y,N);
COMMENT N MUST BE EVEN;
VALUE A,B,X,Y;
REAL A,B,X,Y;
REGIN SC 21 5210
REAL DX,DX2,SUM2,SUM4,BB,SUM3 SC 21 5210
IF N MOD 2 = 0 THEN BEGIN SC 121 010
SUM2+SUM4+SUM+0;
DX=(B-A)/(N-1);
DX2=DX+DX; BB=B=DX+DX/3;
FOR X=A+DX STEP DX2 UNTIL BB DO SC 121 113
SUM2+SUM2+Y;
FOR X=A+BB DO SC 121 312
SUM+SUM+Y;
SIMPSDN=(SUM+2*SUM2+4*SUM4)*DX/3;
END ELSE WRITE(GETL,FORGDT);
END DF PROCEDURE SIMPSDN;
LABEL START,EXIT; SC 121 511
SC 121 813,
SC 121 1A1D
SC 121 1713
SC 121 2510
SC 121 2A13
SC 121 3113
SC 121 3312
SC 121 3711
SC 121 4013
0012 IS DD46 LDNG, NEXT SEG 0002
SC 21 5210

```

```

TIMEIT(GEIL);
FILL DELTE[*] WITH 0,,5816,,6833,,7849,,9225,1; SC 21 5210
SC 21 5310
START OF SEGMENT ***** 0013
0013 IS DD06 LDNG, NEXT SEG 0002
FILL DELTK[*] WITH 0,,223,,356,,513,,791,1; SC 21 5413
SC 21 5612
START OF SEGMENT ***** 0014
0014 IS DD06 LDNG, NEXT SEG 0002
FILL Z [*] WITH 0,1,2,4,16,100; SC 21 5811
SC 21 6110
FACT+1,1909=-12*(11605/1,438)*3;
VDIV*4; SC 21 6113
DV+1.5707963268/(VDIV-3);
V=-DV*.999999; SC 21 6310
FOR TEMP=0 STEP 1 UNTIL VDIV DO SC 21 4412
SINV[TEMP]=SINC(V+V+DV)*2;
READ(PASSKAPPA,*,,BT,DT,ET); SC 21 7110
SC 21 7612
NT=(ET-BT)/DT;
READ(PASSKAPPA,*,,NLAMBDA); SC 21 8912
READ(PASSKAPPA,NLAMBDA+1,HNU(*)); SC 21 9713
START;
READ(READER,TITLE)[EXIT]; WRITE(GEIL[PAGE]); WRITE(GEIL,TITLE);
READ(READER,/,D); SC 21 10113
SC 21 10210
SC 21 11211
d-3

```

```

        WRITE(GEIL,DESCRIPTION)
        NHNU=NLAGMBA
        FOR J=1 STEP 1 UNTIL NLAMBDA DO HNU(J)=1.2397/HNU(J)
        HNU(NLAMBDA+1)=0
        BEGIN
        ARRAY BNUS,KAPPAPRIME,FNUC(NHNU)
        SC   21 11913
        SC   21 12213
        SC   21 12312
        SC   21 12911
        SC   21 13110
        SC   21 13110
        START OF SEGMENT **** 0016
        IT=1
        FOR T=BT STEP DT UNTIL ET DO BEGIN
        WRITE(GEIL,WRITET,T)
        IT=IT+1
        READ(PASSKAPPA,NLAMBDA,KAPPA[IT+1])
        READ(PASSKAPPA,*,P))
        WRITE(GEIL,OP,D,P))
        WRITE(GEIL,[PAGE])
        FOR J=1 STEP 1 UNTIL NLAMBDA DO KAPPAPRIME[J]=KAPPA[IT,J]
        READ(PASSKAPPA,*,NE,NTDL))
        N=NTDL-NE
        M=NE/NJ
        THETA=T/180D0
        SQTHETA=SQRT(THETA))
        IF M>5 THEN ZBAR=1 ELSE
        ZBAR=M+.25/M
        SC   161 311
        SC   161 411
        SC   161 510
        SC   161 1211
        SC   161 1312
        SC   161 1711
        SC   161 2413
        SC   161 3411
        SC   161 3710
        SC   161 4310
        SC   161 5213
        SC   161 5410
        SC   161 5511
        SC   161 5612
        SC   161 5713
        SC   161 5913
        INTERP(DTK,DELTk))
        INTERP(DTK,DELTk))
        DENDM=ZBAR*.4342944819D3X      ( PRINT*      LN(2,4D1E20*THETA*3/
        (ZBAR*2*XN(X(1+ZBAR)*N)))))
        SIGMA=.286XSQTHETA*3*DTE/DENDM
        KK=.2465XSQTHETA*5*DTK/DENDM
        WRITE(GEIL, ))
        WRITE(GEIL,SIGMAK,PRINT,SIGMA,KK))
        FOR J=1 STEP 1 UNTIL NHNU DO BEGIN
        TAU=KAPPAPRIME[J]*D
        BNUE(J)=FACT*(TEMP1+HNU(J)) *3/[EXP(TEMP1/THETA )-1])
        UDIV=ENTIER(TAU*1.5)
        IF UDIV MOD 2#0 THEN UDIV=UDIV+1
        IF UDIV<2 THEN UDIV=2
        FNU(J)=     8066XBNUE(J)*(3.1415926536-4X
        TEMP+
        (
        IF UDIV>100 THEN 0 ELSE
        SIMPSON(0,1 ,U,SIMPSON(D,VDIV,V,EXP(-TAUXU/((U2+U*2)+(1-U2)*SINV(V))),.
        VDIV)*XU,UDIV).5707963268/VDIV
        )
        )
        END OF J LOOPS
        SC   161 6413
        SC   161 6611
        SC   161 6713
        SC   161 7012
        SC   161 7510
        SC   161 7811
        SC   161 8210
        SC   161 8413
        SC   161 9911
        SC   161 10010
        SC   161 10112
        SC   161 10710
        SC   161 10911
        SC   161 11211
        SC   161 11411
        SC   161 11611
        SC   161 11611
        SC   161 11811
        SC   161 13012
        SC   161 13113
        SC   161 13613
        SC   161 13910
    
```

```

        WRITE(GEIL,DBL));
        D3+3/D3;
        SUM=0;
        LOW=1;
        TEMP+SIGN(KAPPAPRIME[1]-D3);
        FNU0NU=FNU[1]*X(HNU[1]-HNU[2]);
        IF TEMP<0 THEN TKTN=" THIN " ELSE
        TKTN=" THICK";
        FOR J=2 STEP 1 UNTIL NHNU DO BEGIN
        IF TEMP> TEMP+SIGN(KAPPAPRIME[J]-D3)           THEN CMOP;
        DNU+HNU[JI]=HNU[J+1];
        FNU0NU=FNU0NU+TEMP1+FNU[JI]*DNU;
        END OF J LOOPS;
        CHOP;
        WRITE(GEIL,FINAL,SUM);
        WRITE(GEIL,EJ,TEMP+SORT(4*SUM/(SIGMAXDI),SIGMAXTEMP));
        WRITE(GEIL,DBL);
        WRITE(GEIL,TITLEPLOT,THETA,TEMP1+(1+M)*V,N,
              TEMP+11605*THETA,TEMP1*TEMP/(2.687*19*273));
        WRITE(GEIL,LISTPLOT,FOR J=1 STEP 1 UNTIL NHNU DO [TEMP1+HNU[J],
              1.2397/TEMP1, TEMP+KAPPAPRIME[ J], TEMP*D,
              EXPON=1-EXP(-TEMP*DI),BNU[J],EXPON*XNU[J],FNU[J]]);
        WRITE(GEIL,PAGE);

```

SC 161 14111  
SC 161 14410  
SC 161 14511  
SC 161 14610  
SC 161 14613  
SC 161 15010  
SC 161 15212  
SC 161 15412  
SC 161 15713  
SC 161 16010  
SC 161 16613  
SC 161 16710  
SC 161 16912  
SC 161 17113  
SC 161 17211  
SC 161 18011  
SC 161 19411  
SC 161 19710  
SC 161 20612  
SC 161 21911  
SC 161 22713  
SC 161 23711  
SC 161 25211

```

END OF THETA LOOPS;
TIMEIT(GEIL);
END DYNAMIC HNU;

```

SC 161 25510  
SC 161 25811  
SC 161 25911

```

EXIT: END.

```

0016 IS 0263 LONG, NEXT SEG 0002  
SC 21 13310

0002 IS 0136 LONG, NEXT SEG 0001

EXP	IS SEGMENT NUMBER 0017, PRT ADDRESS IS 0213	
LN	0018	0211
SIN	0019	0171
SORT	0020	0210
OUTPUT(W)	0021	0034
BLOCK CONTROL	0022	0005
INPUT(W)	0023	0173
GO TO SOLVER	0024	0176
ALGOL WRITE	0025	0014
ALGOL READ	0026	0015
ALGOL SELECT	0027	0016

NUMBER OF ERRORS DETECTED = 000

LAST CARD WITH ERROR HAS SEQ #

PRT SIZE=01473 TOTAL SEGMENT SIZE=00937 WORDS DISK STORAGE REQ.=01128 WORDS NO. SEGS.=0028.  
ESTIMATED CORE STORAGE REQUIREMENT = 04331 WORDS.

17141138 MONDAY, OCTOBER 25, 1965 PROCESSOR TIME = 15.18 SECONDS I/O TIME = 50.82 SECONDS

RUN DATE  
OCT. 25, 1965

RUN TIME  
5:41 PM

PROCESSOR TIME  
1 SEC.

I/O TIME  
11 SEC.

XENON  
CYLINDER  
 $T = 9000$  DEGREES  
 $D = 1.00$        $P = 760.00$  ATM

FOR HOMOGENEOUS TEMPERATURE, NEGLECTING THERMAL CONDUCTIVITY

LN LAMBDA = 7.068E+00  
 ELECTRICAL CONDUCTIVITY SIGMA = 3.702E+01 INVERSE OHMS INVERSE C  
 THERMAL CONDUCTIVITY K = 9.572E-03 WATTS/CM DEGREES

FROM NU=24.794 TO NU= 12.397 THE VALUE OF THE INTEGRAL OF FNU IS 3.412E+00 WATTS/CM<sup>2</sup>  
 FROM NU=11.807 TO NU= 0.025 THE VALUE OF THE INTEGRAL OF FNU IS 5.658E+01 WATTS/CM<sup>2</sup>  
 FROM NU= 0.012 TO NU= 0.012 THE VALUE OF THE INTEGRAL OF FNU IS 2.238E-02 WATTS/CM<sup>2</sup>

RADIANT EMITTANCE F = 6.001E+01 WATTS/CM<sup>2</sup>  
 ELECTRIC FIELD E = 2.546E+00 VOLTS/CM  
 CURRENT DENSITY J = 9.427E+01 AMP/CM<sup>2</sup>

THETA=0.78 EV      NTOTAL=8.155E+17      NDENSITY=7.677E+17 PARTICLES/CM<sup>3</sup>  
 T= 9000.0 DEGREES K,      P=1.001E+00 ATM

HNU	WAVELENGTH	KAPPA-PRIME	TAU	(-TAU)	RNU	INU	FNU
EV	MICRONS	1/CM		1-E	WATTS/CM STER	WATTS/CM	WATTS/CM
24.794	5.000E-02	7.544E+00	7.544E+00	9.995E-01	1.244E-10	1.244E-10	3.110E-06
22.540	5.500E-02	1.771E+01	1.771E+01	1.000E+00	1.710E-09	1.710E-09	4.323E-05
20.662	6.000E-02	2.617E+01	2.617E+01	1.000E+00	1.484E-08	1.484E-08	3.757E-04
19.072	6.500E-02	3.334E+01	3.334E+01	1.000E+00	9.063E-08	9.063E-08	2.995E-03
17.710	7.000E-02	3.948E+01	3.948E+01	1.000E+00	4.204E-07	4.204E-07	1.065E-02
16.529	7.500E-02	4.481E+01	4.481E+01	1.000E+00	1.566E-06	1.566E-06	3.968E-02
15.406	8.000E-02	4.946E+01	4.946E+01	1.000E+00	4.890E-06	4.890E-06	1.239E-01
13.774	9.000E-02	5.723E+01	5.723E+01	1.000E+00	3.163E-05	3.143E-05	8.013E-01
12.397	1.000E-01	6.344E+01	6.344E+01	1.000E+00	1.362E-04	1.362E-04	3.451E+00
11.807	1.050E-01	1.348E-04	1.348E-04	1.000E+00	2.519E-04	3.304E-08	9.556E-04
8.265	1.500E-01	2.759E-04	2.759E-04	1.000E+00	8.318E-03	2.025E-06	5.785E-02
6.199	2.000E-01	4.966E-04	4.966E-04	1.000E+00	5.040E-02	2.502E-05	6.307E-01
4.959	2.500E-01	7.908E-04	7.908E-04	1.000E+00	1.278E-01	1.010E-04	2.546E+00
4.132	3.000E-01	1.155E-03	1.155E-03	1.000E+00	2.153E-01	2.445E-04	6.264E+00
3.542	3.500E-01	1.582E-03	1.582E-03	1.000E+00	2.919E-01	4.616E-04	1.163E+01
3.099	4.000E-01	2.082E-03	2.082E-03	1.000E+00	3.490E-01	7.259E-04	1.829E+01
2.755	4.500E-01	2.636E-03	2.636E-03	1.000E+00	3.861E-01	1.018E-03	2.561E+01
2.479	5.000E-01	3.236E-03	3.236E-03	1.000E+00	4.067E-01	1.314E-03	3.311E+01
2.254	5.500E-01	2.368E-03	2.368E-03	1.000E+00	4.145E-01	9.803E-04	2.471E+01
2.066	6.000E-01	2.816E-03	2.816E-03	1.000E+00	4.134E-01	1.142E-03	2.929E+01
1.907	6.500E-01	9.768E-04	9.768E-04	1.000E+00	4.060E-01	3.944E-04	9.991E+00
1.771	7.000E-01	1.014E-03	1.014E-03	1.000E+00	3.946E-01	4.000E-04	1.008E+01
1.653	7.500E-01	1.194E-03	1.194E-03	1.000E+00	3.806E-01	4.541E-04	1.144E+01

1.550	8.000E-01	1.389E-03	1.389E-03	1.388E-03	3.653E-01	5.070E-04	1.278E+01
1.458	8.500E-01	1.600E-03	1.600E-03	1.599E-03	3.494E-01	5.546E-04	1.408E+01
1.377	9.000E-01	1.137E-03	1.137E-03	1.137E-03	3.334E-01	3.749E-04	9.550E+00
1.305	9.500E-01	1.275E-03	1.275E-03	1.275E-03	3.176E-01	4.048E-04	1.020E+01
1.240	1.000E+00	1.421E-03	1.421E-03	1.420E-03	3.022E-01	4.292E-04	1.092E+01
1.181	1.050E+00	1.575E-03	1.575E-03	1.573E-03	2.875E-01	4.524E-04	1.140E+01
1.127	1.100E+00	1.447E-03	1.447E-03	1.446E-03	2.734E-01	3.954E-04	9.967E+00
1.078	1.150E+00	1.041E-03	1.041E-03	1.040E-03	2.601E-01	2.705E-04	6.819E+00
1.033	1.200E+00	1.159E-03	1.159E-03	1.158E-03	2.475E-01	2.867E-04	7.225E+00
0.942	1.250E+00	6.422E-04	6.422E-04	6.420E-04	2.355E-01	1.512E-04	3.811E+00
0.954	1.300E+00	7.084E-04	7.084E-04	7.081E-04	2.243E-01	1.588E-04	4.003E+00
0.918	1.350E+00	7.780E-04	7.780E-04	7.777E-04	2.137E-01	1.662E-04	4.190E+00
0.886	1.400E+00	8.512E-04	8.512E-04	8.508E-04	2.038E-01	1.714E-04	4.371E+00
0.855	1.450E+00	9.279E-04	9.279E-04	9.275E-04	1.945E-01	1.804E-04	4.546E+00
0.826	1.500E+00	1.008E-03	1.008E-03	1.008E-03	1.857E-01	1.871E-04	4.716E+00
0.800	1.350E+00	9.844E-04	9.844E-04	9.839E-04	1.775E-01	1.746E-04	4.400E+00
0.775	1.600E+00	1.017E-03	1.017E-03	1.017E-03	1.697E-01	1.726E-04	4.340E+00
0.751	1.650E+00	1.055E-03	1.055E-03	1.055E-03	1.624E-01	1.713E-04	4.318E+00
0.729	1.700E+00	1.098E-03	1.098E-03	1.098E-03	1.555E-01	1.707E-04	4.302E+00
0.708	1.750E+00	1.145E-03	1.145E-03	1.145E-03	1.491E-01	1.706E-04	4.300E+00
0.689	1.800E+00	1.197E-03	1.197E-03	1.196E-03	1.430E-01	1.710E-04	4.309E+00
0.670	1.850E+00	1.252E-03	1.252E-03	1.251E-03	1.372E-01	1.717E-04	4.327E+00
0.652	1.900E+00	1.311E-03	1.311E-03	1.310E-03	1.318E-01	1.727E-04	4.352E+00
0.636	1.950E+00	1.374E-03	1.374E-03	1.373E-03	1.266E-01	1.739E-04	4.383E+00
0.620	2.000E+00	1.440E-03	1.440E-03	1.439E-03	1.218E-01	1.753E-04	4.418E+00
0.248	5.000E+00	1.039E-02	1.039E-02	1.034E-02	2.533E-02	2.615E-04	6.594E+00
0.124	1.000E+01	4.473E-02	4.473E-02	4.374E-02	6.880E-03	3.009E-04	7.562E+00
0.062	2.000E+01	1.849E-01	1.849E-01	1.688E-01	1.792E-03	3.025E-04	7.532E+00
0.025	5.000E+01	1.177E+00	1.177E+00	6.917E-01	2.937E-04	2.031E-04	4.010E+00
0.012	1.000E+02	4.734E+00	4.734E+00	9.912E-01	7.401E-05	7.336E-05	1.205E+00

T = 10000 DEGREES  
 P = 1.00 ATM

LN LAMBDA = 6.6538+00  
 ELECTRICAL CONDUCTIVITY SIGMA = 4.6050+01 INVERSE OHMS INVERSE CM  
 THERMAL CONDUCTIVITY K = 1.3230+02 WATTS/CM DEGREES

FROM NU=24.794 TO NU= 12.397 THE VALUE OF THE INTEGRAL OF FNU IS 1.8680+01 WATTS/CM<sup>2</sup> THICK  
 FROM NU=11.807 TO NU= 0.062 THE VALUE OF THE INTEGRAL OF FNU IS 2.3340+02 WATTS/CM<sup>2</sup> THIN  
 FROM NU= 0.025 TO NU= 0.012 THE VALUE OF THE INTEGRAL OF FNU IS 1.2360+01 WATTS/CM<sup>2</sup> THICK

RADIANT EMITTANCE F = 2.5220+02 WATTS/CM<sup>2</sup>  
 ELECTRIC FIELD E = 4.6810+00 VOLTS/CM  
 CURRENT DENSITY J = 2.1560+02 AMP/CM<sup>2</sup>

THETA=0.86 EV NTOTAL=7.3400+17 NDENSITY=6.3400+17 PARTICLES/CM<sup>3</sup>  
 T = 10000.0 DEGREES K. P=1.0010+00 ATM

HNU	WAVELENGTH	KAPPA-PRIME	TAU	(-TAU)	BNU	INU	FNU
EV	MICRONS	1/CM		1-E	WATTS/CM <sup>2</sup>	STER	WATTS/CM
24.794	5.0000E-02	5.6010E+00	5.6010E+00	9.9630E-01	3.0440E-09	3.0230E-09	7.5140E-05
22.540	5.5000E-02	1.3150E+01	1.3150E+01	1.0000E+00	3.1280E-08	3.1280E-08	7.8920E-04
20.662	6.0000E-02	1.9440E+01	1.9440E+01	1.0000E+00	2.1310E-07	2.1310E-07	5.3890E-03
19.072	6.5000E-02	2.4760E+01	2.4760E+01	1.0000E+00	1.0600E-06	1.0600E-06	2.6830E-02
17.710	7.0000E-02	2.9320E+01	2.9320E+01	1.0000E+00	4.1250E-06	4.1250E-06	1.0440E-01
16.529	7.5000E-02	3.3270E+01	3.3270E+01	1.0000E+00	1.3200E-05	1.3200E-05	3.3420E-01
15.496	8.0000E-02	3.6730E+01	3.6730E+01	1.0000E+00	3.6070E-05	3.6070E-05	9.1350E-01
13.774	9.0000E-02	4.2490E+01	4.2490E+01	1.0000E+00	1.8680E-04	1.8680E-04	4.7320E+00
12.397	1.0000E-01	4.7100E+01	4.7100E+01	1.0000E+00	4.7360E-04	4.7360E-04	1.7040E+01
11.807	1.0500E-01	3.6450E-04	3.6450E-04	3.6440E-04	1.1540E-03	4.2070E-07	1.0600E-02
8.265	1.5000E-01	7.4720E-04	7.4720E-04	7.4690E-04	2.4150E-02	1.8030E-05	4.5460E-01
6.199	2.0000E-01	1.3500E-03	1.3500E-03	1.3490E-03	1.1210E-01	1.5120E-04	3.8110E+00
4.959	2.5000E-01	2.1610E-03	2.1610E-03	2.1580E-03	2.4260E-01	5.2350E-04	1.3190E+01
4.132	3.0000E-01	3.1650E-03	3.1650E-03	3.1600E-03	3.6820E-01	1.1470E-03	2.9320E+01
3.542	3.5000E-01	4.3420E-03	4.3420E-03	4.3330E-03	4.6380E-01	2.0690E-03	5.0630E+01
3.099	4.0000E-01	5.7220E-03	5.7220E-03	5.7060E-03	5.2520E-01	2.9070E-03	7.5510E+01
2.755	4.5000E-01	7.2400E-03	7.2400E-03	7.2140E-03	5.5780E-01	4.0240E-03	1.0144E+02
2.479	5.0000E-01	8.8760E-03	8.8760E-03	8.8370E-03	5.6900E-01	5.0280E-03	1.2674E+02
2.254	5.5000E-01	6.7450E-03	6.7450E-03	6.7220E-03	5.6540E-01	3.8010E-03	9.5750E+01
2.066	6.0000E-01	8.0220E-03	8.0220E-03	7.9900E-03	5.5220E-01	4.4170E-03	1.1118E+02
1.907	6.5000E-01	3.2440E-03	3.2440E-03	3.2390E-03	5.3310E-01	1.7260E-03	4.3510E+01
1.771	7.0000E-01	3.3410E-03	3.3410E-03	3.3360E-03	5.1060E-01	1.7010E-03	4.2920E+01
1.653	7.5000E-01	3.9290E-03	3.9290E-03	3.9220E-03	4.8660E-01	1.9080E-03	4.8090E+01

1.350	8.000e-01	4.569e-03	4.569e-03	4.558e-03	4.622e-01	2.107e-03	5.304e+01
1.448	8.000e-01	5.240e-03	5.260e-03	5.247e-03	4.380e-01	2.205e-03	5.790e+01
1.377	9.000e-01	3.630e-03	3.630e-03	3.623e-03	4.146e-01	1.502e-03	3.785e+01
1.305	9.500e-01	4.069e-03	4.069e-03	4.061e-03	3.922e-01	1.503e-03	1.013e+01
1.240	1.000e+00	4.533e-03	4.533e-03	4.523e-03	3.709e-01	1.678e-03	4.228e+01
1.181	1.050e+00	5.022e-03	5.022e-03	5.010e-03	3.509e-01	1.758e-03	4.429e+01
1.127	1.100e+00	4.605e-03	4.605e-03	4.584e-03	3.321e-01	1.555e-03	3.919e+01
1.078	1.150e+00	3.545e-03	3.545e-03	3.539e-03	3.144e-01	1.113e-03	2.804e+01
1.033	1.200e+00	3.942e-03	3.942e-03	3.934e-03	2.979e-01	1.172e-03	2.953e+01
0.992	1.250e+00	2.180e-03	2.180e-03	2.178e-03	2.825e-01	1.154e-04	1.551e+01
0.954	1.300e+00	2.401e-03	2.401e-03	2.398e-03	2.682e-01	6.422e-04	1.421e+01
0.918	1.350e+00	2.634e-03	2.634e-03	2.630e-03	2.547e-01	6.700e-04	1.488e+01
0.886	1.400e+00	2.877e-03	2.877e-03	2.873e-03	2.422e-01	6.959e-04	1.754e+01
0.855	1.450e+00	3.133e-03	3.133e-03	3.128e-03	2.305e-01	7.209e-04	1.817e+01
0.826	1.500e+00	3.399e-03	3.399e-03	3.394e-03	2.196e-01	7.451e-04	1.979e+01
0.800	1.550e+00	3.344e-03	3.344e-03	3.339e-03	2.093e-01	6.948e-04	1.761e+01
0.775	1.600e+00	3.464e-03	3.464e-03	3.458e-03	1.998e-01	6.907e-04	1.740e+01
0.751	1.650e+00	3.600e-03	3.600e-03	3.594e-03	1.908e-01	6.856e-04	1.722e+01
0.729	1.700e+00	3.753e-03	3.753e-03	3.746e-03	1.824e-01	6.832e-04	1.722e+01
0.708	1.750e+00	3.921e-03	3.921e-03	3.913e-03	1.745e-01	6.828e-04	1.721e+01
0.689	1.800e+00	4.104e-03	4.104e-03	4.095e-03	1.671e-01	6.842e-04	1.724e+01
0.670	1.850e+00	4.300e-03	4.300e-03	4.291e-03	1.601e-01	6.870e-04	1.731e+01
0.652	1.900e+00	4.510e-03	4.510e-03	4.499e-03	1.536e-01	6.909e-04	1.741e+01
0.636	1.950e+00	4.732e-03	4.732e-03	4.721e-03	1.474e-01	6.957e-04	1.753e+01
0.620	2.000e+00	4.967e-03	4.967e-03	4.954e-03	1.416e-01	7.013e-04	1.767e+01
0.624	5.000e+00	3.686e-02	3.686e-02	3.618e-02	2.562e-02	1.035e-03	2.603e+01
0.124	1.000e+01	1.600e-01	1.600e-01	1.479e-01	7.707e-03	1.140e-03	2.842e+01
0.062	2.000e+01	6.643e-01	6.643e-01	4.854e-01	1.099e-03	9.701e-04	2.367e+01
0.025	5.000e+01	4.238e+00	4.238e+00	9.856e-01	3.268e-04	3.221e-04	7.894e+00
0.012	1.000e+02	1.706e+01	1.706e+01	1.000e+00	8.230e-05	9.230e-05	2.080e+00

Program e  
Symbol Table for Radiation Flux

R = radius of the cylinder (input)

KAPPA [ILAMBDA, IT] = effective absorption coefficient (including stimulated emission) at the ILAMDA<sup>th</sup> wavelength and IT<sup>th</sup> temperature (input from DOUBLE).

BT = minimum temperature at which the KAPPA's have been calculated (input from DOUBLE).

DT = temperature step size (input from DOUBLE).

ET = maximum temperature at which the KAPPA's have been calculated (input from DOUBLE).

NLAMBDA = number of wavelengths at which KAPPA has been calculated (input from DOUBLE).

ALAMBDA [ILAMBDA] = ILAMDA<sup>th</sup> wavelength (input from DOUBLE).

NR = number of equidistant radial distances (of the cylinder) at which the temperature will be input. These points will be at equal intervals from 0 to R along the radial direction (input).

T[IR] = temperature at point  $\frac{IR}{NR} R$  along the radius (input).

$G[x] = \int_0^{\pi/2} e^{-\frac{x}{\sin\theta}} \sin\theta d\theta$  (tabulated at intervals of .1 from x = 0 to x = 30)

NPHI = number of  $\phi$  values at which intergrand will be evaluated during numerical integration (input)

DPHI =  $\phi$  step size

DLAMBDA [ILAMBDA] = ALAMBDA [ILAMBDA] - ALAMBDA [ILAMBDA - 1]

ARI [I] = I<sup>th</sup> value of  $R_i$  at which flux is to be found (input).

NRI = number of  $R_i$ 's at which flux is to be found.

## REFERENCES

1. Yu. P. Raizer, "A Simple Method of Calculating the Degree of Ionization and Thermodynamic Functions of a Multiply Ionized Ideal Gas," Sov. Phys.-J.E.T.P. 9, 1124-1125 (1959).
2. Yu. R. Raizer, "Simple Method for Computing the Mean Range of Radiation in Ionized Gases at High Temperatures," Sov. Phys.-J.E.T.P. 10, 769 (1960).
3. R. A. Pappert and S. S. Penner, "Approximate Opacity Calculations for Polyelectronic Atoms at High Temperatures," J. Quant. Spectr. Rad. Transfer 1, 259-268, (1961).
4. S. S. Penner and M. Thomas, "Approximate Theoretical Calculation of Continuum Opacities", A.I.A.A. Journ. 2, 1572-1575 (1964).
5. K. Drelliskak, C. Knopp, and A. B. Cambel, "Partition Functions and Thermodynamic Properties of Argon Plasmas", Phys. Fluids 6, 1280-1288 (1963).
6. L. Biberman and G. Norman, "Plasma Radiation due to Recombination and Bremsstrahlung Processes", J. Quant. Spectr. Rad. Transfer 3, 221-245 (1963) General Atomics-San Diego Translation GA tr 4943.
7. R. S. Cohen, L. Spitzer, Jr. and P. Routly, "The Electrical Conductivity of an Ionized Gas," Phys. Rev. 80, 230-238 (1950).
8. L. Spitzer, Jr. and R. Harm, "Transport Phenomena in a Completely Ionized Gas", Phys. Rev. 89, 977-981 (1953).

09119159 TUESDAY, NOVEMBER 9, 1965

```

BEGIN
COMMENT FLUXI
COMMENT GEIL,BRUCE SWANSON,220,F04371
FILE IN PASSG DISK SERIAL(1, 330)
FILE IN PASSKAPPA DISK SERIAL(2, 60, 1200)
FILE IN READER(2, 10)
FILE OUT GEIL 4(2, 15)
COMMENT DOLLAR OR DOUBLE DOLLAR CARD GOES HERE *****+*****+*****+*****+*****+
ARRAY ARI[0:20]
INTEGER JJ
REAL I, NRJ
REAL R, RI, NPHI, NTHTETA, DS, NLAMBDA, NLAMRDA, HT, DT,
ET, NT, IN, IT, NR, COSPHI, SUMF, PROPS, THETA, TANPHI, INLAMRDA,
INS, INTHTETA, INNPHI, COUNTS, DPHI, TI, ILAMBDA, LAMBDA, LPHI, MPHT,
TAN2PHI, SINPHI, COSALPH, SINALPH, PHI, Z, LENGTH, PROP, NDS,
APPROXDS, LS, WS, VM, S, RGHXY, TM, IBM, ZM, KLM, IBB, TEMP, YMT,
EPS, SUMJ
REAL XJ
ARRAY SAVEWR(D112, D15, D114)
ARRAY GID1300J
ARRAY TI0140J, ALAMBDA, EXPARG10150, KAPPAD150, D135, ALAMBDAE01
20J
FORMAT
INPUT("R=",E15.8,X5,"RI=",E15.8,X5,"NPHI=",E15.8,X5,"APPROXDS=",E15.8,X5,"NLAMBDA="E15.8,X5,"NLAMRDA="E15.8,X5,"HT=",E15.8,X5,"EPS=",E15.8),
LAMBOAALONE(/"ALAMBDA"/(6E16.8)),
TIMES("TOTAL TIME IN LAMBDA=",F9.3," SECONDS"),
"TOTAL TIME IN S     =",F9.3," SECONDS",
"TOTAL NUMBER OF S VALUES=",I9,"TOTAL TIME IN THETA =",F9.3,
" SECONDS"/"TOTAL TIME IN PHI   =",F9.3," SECONDS",
"TOTAL PROCESSOR TIME=",F9.3," SECONDS"/"TOTAL I/O      TIME=",F9.3," SECONDS"),
RR1("NR=",E15,8*X10,"/IIR) ARRAY FOLLOWS"/(6E16.8)),
TT("BT=",E15.8,X5,"DT=",E15.8,X5,"ET=",E15.8),
TITLEKAPPAD150, PRINTKAPPAD150, DCLCKITIME FOR 300 INTEGRATIONS USING ROMBERG OF ORDER 6 IS"FR
3),
OUT1("P=",F9.3,"")="E20.11),
IN1UT1("R=",E15.8,X5,"I1=",E15.8,X5,"NPHI=",E15.8,X5),
INDLT2("APPROXDS0=",E15.8,X5,"NLAMBDA="E15.8,X5,"N=",E15.8,X5,
"EP=",E15.8),
TIME("TOTAL TIME IN LAMBDA=",F9.3," SECONDS"),
TIMEPI("TOTAL PROCESSOR TIME=",F9.3," SECONDS"),
TIMEI("TOTAL I/O TIME=",F9.3," SECONDS"),
RESULT("P=",E15.8," WATTS/CM2"))
LABEL NEXTARY
LABEL EXIT, NEXTARY
REAL PROCEDURE LAG(X, X0, OX, Y, NJ)
COMMENT ORDER 3 LAGRANGE INTERPOLATION. EQUAL INDEPENDENT STEP.
SINGLE DEPENDENT, INDEPENDENT VARIABLE. EXTRAPOLATE IF NOT X0<X<X0+N*OX.
X - DESIRED INDEPENDENT VALUE
X0 - FIRST INDEPENDENT VALUE OF Y TABLE (FOR Y(I))
OX - TABLE STEP FOR INDEPENDENT
Y - NAME,DEPENDENT VARIABLE VALUE TABLE (MUST BE SINGLE SUBSCRIPT)
N - MAX INDEX OF Y TABLE ( 2 4 ) J
VALUE X, X0, OX, NJ
REAL X, X0, OX
INTEGER NJ
ARRAY Y(I0)
BEGIN
INTEGER IJ
REAL SJ
I= ENTIER(S+(X-X0)/OX)
IF S>I THEN
LAG+ Y(I)
ELSE
LAG+(Y(I+1)-Y(I))*(S-I)+Y(I)
END LAG
COMMENT DOLLAR OR DOUBLE DOLLAR CARD GOES HERE *****+*****+*****+*****+*****+
TIMEIT(GEIL))
READ(READER,, RI)
READ(READER,, NPHI, APPROXDS)
READ(READER,, NJ)
READ(READER,, EPS)
READ(PASSKAPPA,, BT, DT, ET)
COMMENT                                     TEMPS AT WHICH KAPPALT IS GIVEN
READ(PASSKAPPA,, NLAMBDA)
READ(PASSKAPPA,, NLAMBDA+1, ALAMBDA+1))
READ(READER,, NR, FOR IR=0 STEP 1 UNTIL NR DO TI(R))
WRITE(GEIL, RR1, NR, FOR IR=0 STEP 1 UNTIL NR DO TI(R))
FOR ILAMBDA=1 STEP 1 UNTIL NLAMRDA DO
ALAMBDA(ILAMBDA)= ALAMBDA(ILAMBDA)*R=4
NT=(ET-BT)/DT)
FOR IT=0 STEP 1 UNTIL NT DO
BEGIN
READ(PASSKAPPA,, FOR ILAMBDA+1 STEP 1 UNTIL NLAMRDA DO KAPPA
NLAMRDA, IT)

```

```

READ(PASSKAPPA,*, X, X)
END OF IT LOOPJ
READ(PASSG, 301, GE(*)))
IF FALSE THEN
  BEGIN
    INLAMBDAA+ TIME(2)
    FOR IT= 0 STEP 1 UNTIL 300 DO
      BEGIN
        X= IT/10J
        G[IT]= ROMBERG(.000000001, 1.5/0.7963268, 6, THETA, EXP(-
          X/(CTEMP+ SIN(THETA)))*TEMP)
      END OF IT LOOPJ
    INLAMBDAA+ TIME(2)=INLAMBDAA
    WRITE(GE(L, OCLDCK, IT/LAMBDAA/60))
    WRITE(PASSG, 301, (*+))
    WRITE(GEIL, OUTG, FOR IT= 0 STEP 1 UNTIL 300 DUCIT, G(IT)))
  ENDJ
  OPHI= 3.1415926536/NPMI
  IF FALSE THEN
    BEGIN
      WRITE(GEIL, TITLEKAPPA)
      FOR ILAMBDA= C STEP 1 UNTIL NLAMBDAA DO
        WRITE(GEIL, PRINTKAPPA, ALAMBDA(ILAMBDA)), FOR (T= 0 STEP 1
          UNTIL NT DO KAPPALAMBDA(T, IT)))
      WRITE(GEIL, LAMBDAALONE, FOR LAMBDA= 1 STEP 1 UNTIL NLAMBDAA DO
        ALAMBDA(ILAMBDA)))
      WRITE(GEIL, TT, BT, DT, ET))
    ENDJ
  WRITE(GEIL(DBL))
  FOR ILAMBDA= 2 STEP 1 UNTIL NLAMBDAA DO
    DLAMBDA(ILAMBDA)= ALAMBDA(ILAMBDA)-ALAMBDA(ILAMBDA-1)
  DLAMBDA(1)= DLAMBDA(2)
  READ(READER,/, FOR I= 0 STEP 1 UNTIL 21 DO ARI(I))(NEXTRI))
NEXTRI:
CLOSE(READER, RELEASE)
NRI= I-1
FOR I= 0 STEP 1 UNTIL NRI DO
  BEGIN
    RI= ARI(I)
    COUNTS+ DJ
    INLAHDDA+ INS+ INTMETA+ INPHI+ 0J
    WRITE(SAVEWR(1, 1,*), INOUT1, R, RI, NPHI))
    WRITE(SAVEWR(1, 2,*), INOUT2, APPROXDS, NLAMBDAA, ND, EFD))
    SUMH+ 0J
    IF RI=1 THEN
      LPHI= 1.5707963268+OPHI/2
    ELSE
      LPHI= OPHI/2J
    HPMI= 3.1415926536-OPMI*4J
    INPHI= INPHI-TIME(2)
    FOR PHI= LPHI STEP OPHI UNTIL HPMI DO
      BEGIN
        TAN2PHI=(TANPHI+(SINPHI+ SIN(PHI))/COSPHI+ COS(PHI))*2
        SUH+ 0J
        COSALPHI=(RI/R*TAN2PHI)=SQRT((1+TAN2PHI*(I-(RI/R)*2))/(I+
          TAN2PHI))
        SINALPHI= SQRT(1-COSALPHI*2)
        IF ABS(SINALPHI/(COSALPHI*RI/R)-TAN2PHI)>.0000000C TMEN
          BEGIN
            COSALPHI=(RI/R*TAN2PHI)+SQRT((+TAN2PHI*(I-(RI/R)*2))
              -)/((+TAN2PHI))
            SINALPHI= SQRT((+COSALPHI*2))
          ENDJ
        INTMETA+ INTMETA-TIME(2)
        LENGTH+ SIWALPHM*R/SINP*IJ
        FOR ILAMBDA= C STEP 1 UNTIL NLAMBDAA DO
          EXPARG(ILAMBDA)= 0J
        IF NOS+ ENTIER(LENGTH/APPROXDS)+I<N THEN
          DS+ LENGTH/NDS
        ELSE
          DS+ LENGTH/NJ
        LS+ DS/2J
        HS+ LENGTH=LS*.8J
        VM+ DJ
        INS+ INS-TIME(2)
        FOR S= LS STEP DS UNTIL MS DO
          BEGIN
            COUNTS+ COUNTS+()
            RSMXY= SQRT((RI*S*COSPHI)*2+(S*SINPHI)*2)
            TM= LAG(RSMXY, 0, R/NR, T, NR)
            IBM= (.44022/TM)
            ZH+ DJ
            INLAMBDAA= INLAMBDAA-T(WE(2))
            FOR ILAMBDA= C STEP 1 UNTIL NLAMBDAA DO
              BEGIN
                LAMBDA= ALAMBDA(ILAMBDA)
                KLH= LAG(TM, BT, DT, KAPPA(ILAMBDA, +), NT)
                IBB= (.1925*-12/(LAMBDA*5*EXP(TM/LAMBDA)-1
                  ))
                EXPARG(ILAMBDA)= TM*KLH*IBB*EXP(ARG(ILAMBDA))
              ENDJ
            ENDJ
          ENDJ
        ENDJ
      ENDJ
    ENDJ
  ENDJ
  WRITE(GEIL, OUTG, FOR IT= 0 STEP 1 UNTIL 300 DUCIT, G(IT)))
  ENDJ

```

```

    IF TEMP>30 THEN
      BEGIN
        YMT+ KLMX(ABLAG(TEMP, 0, ,1, G, 300))
        ZM+ ZH+YMT*OLAMBDA(ILAMRDA)
      END TEMP30
    END OF LAMBDA LOOP
    INLAMBOA+ INLAMBOA+TIME(2)
    VM+ VM+ZM
  END OF S LOOP

NEXTRAY1
  INS+ INS+TIME(2)
  SUM+ SUM+VM*DS
  INTMETA+ INTMETA+TIME(2)
  SUMF+ SUMF+SUMX*COSPHI
END OF PHI LOOP
INPHI+ INPHI+TIME(2)
SUMF+SUMFX*ADPHI
WRITE(SAVEWR(I, 0,*), RESULT, SUMF)
WRITE(SAVEWR(I, 3,*), TIMEI, INLAMBOA/60)
WRITE(SAVEWR(I, 4,*), TIMEP, TIME(2)/60)
WRITE(SAVEWR(I, 5,*), TIMEID, TIME(3)/60)
END OF RI LOOP
FOR I= 0 STEP 1 UNTIL NR1 00
BEGIN
  WRITE(GEIL(PAGE)))
  FOR J= 0 STEP 1 UNTIL 5 DO
    WRITE(GEIL, 15, SAVEWR(I, J,*)))
END OF I LOOP
EXIT
ENO,

```

09120115 TUESDAY, NOVEMBER 9, 1965 PROCESSOR TIME = 5.83 SECONDS I/O TIME = 22.57 SECONDS